MOLAR HEAT CAPACITIES AND HEATS OF MIXING OF AQUEOUS SOLUTIONS OF 2-(PROPYLAMINO)ETHANOL, 2-(BUTYLAMINO)ETHANOL, 1-(2-HYDROXYETHYL)PIPERIDINE, BIS(2-METHOXYETHYL)AMINE AND OTHER ALKANOLAMINES OF IMPORTANCE TO CARBON DIOXIDE CAPTURE

A Thesis

Submitted to the Faculty of Graduate Studies and Research

In Partial Fulfillment of the Requirements

For the Degree of

Master of Applied Science

In

Process Systems Engineering

University of Regina

By

Irfan Wahid Noor Shaikh

Regina, Saskatchewan

December, 2012

UNIVERSITY OF REGINA

FACULTY OF GRADUATE STUDIES AND RESEARCH

SUPERVISORY AND EXAMINING COMMITTEE

Irfan Wahid Noor Shaikh, candidate for the degree of Master of Applied Science in Process Systems Engineering**,** has presented a thesis titled, ***Molar Heat Capacities and Heats of Mixing of Aqueous Solutions of 2-(Propylamino)Ethanol, 2-(Butylamino)Ethanol, 1-(2Hydroxyethyl)Piperidine, BIS (2-Methoxyethyl)Amine and Other Alkanolamines of Importance to Carbon Dioxide Capture,*** in an oral examination held on November 23, 2012. The following committee members have found the thesis acceptable in form and content, and that the candidate demonstrated satisfactory knowledge of the subject material.

External Examiner:	Dr. Ezeddin Shirif, Petroleum Systems Engineering
Supervisor:	Dr. Amr Henni, Process Systems Engineering
Committee Member:	Dr. Mohamed Ismail, Industrial Systems Engineering
Committee Member:	Dr. David deMontigny, Process Systems Engineering
Chair of Defense:	Dr. Malek Mouhoub, Department of Computer Science

*Not present at defense

ABSTRACT

This study is concerned with the determination of the molar heat capacity, Cp, and molar heat of mixing ,H^E, of aqueous 2-(Propylamino)ethanol (PAE), 2-(Butylamino)ethanol (BAE), 1-(2-Hydroxyethyl)piperidine (HEP), and Bis(2-methoxyethyl)amine (BMOEA) solutions, as well as the Cp of 2-(Ethylamino)ethanol (EAE) and H^E of aqueous Diglycolamine (DGA) using a C80 heat flow calorimeter over a full range of mole fractions (x_1). Cp measurements were performed in a temperature range of 303.15K to 353.15K, while H^E measurements were performed at three temperatures (298.15, 313.15, and 333.15 K).

Of the five alkanolamines studied, BMOEA and BAE exhibited the highest values of heat capacity, whereas EAE had the lowest values. Cp increased with an increase in the size of the alkyl group. Primary amines had the highest contribution, followed by secondary and tertiary amines. Straight chains showed higher Cp values than the cyclic alkyl groups. Hydroxyl groups led to lower Cp than ether groups. The Cp^E data, partial molar excess quantities and the reduced molar excess heat capacity functions, $Cp^E/(x_1x_2)$, were calculated at several temperatures and correlated as a function of x_1 employing the Redlich-Kister expression (RK). Percentages of relative deviation (% RD) from all the predicted heat capacity data for the Group Additivity Analysis and Molecular Connectivity Analysis were found to be within 1.83 and 2.64 %, respectively.

Hydrogen bonding plays a major role within the interactions present in aqueous solutions of alkanolamines; stronger bases reacted more with water. Excess enthalpies

increased with an increase in the size of the carbon chain. Cyclic alkyl groups had lower H^E than straight chains. Tertiary amines had the lowest values, followed by secondary and primary amines. Ether groups exhibited stronger H-bonding with water than the hydroxyl groups.

Excess enthalpies of amines and water at infinite dilution were calculated from the coefficients of the Redlick Kister equations. The modified UNIFAC model regressed the data with the lowest Percentage Relative Deviations (≤1%).

ACKNOWLEDGEMENTS

Alhamdulillah (thanks to God) for granting me the opportunity to study at the University of Regina, and pursue my M.A.Sc. in an exceptional environment of research in engineering and technology. It has been a great mercy and maximum blessings from Him to have the right combination of everything. I would like to express my sincere appreciation to everyone who made this work possible, both directly and indirectly through their assistance and support.

My deepest gratitude goes to my supervisor and professor, Dr. Amr Henni, for allowing me the opportunity to conduct this interesting research. His trustworthy advice and support throughout all phases of the research was most welcome and appreciated.

I would like to extend a special thank you to my beloved parents, Wahid Noor Shaikh and Jamila Khatoon, older brother, Arshad, and all my siblings for their care, encouragement, loving kindness, compassion and moral support.

TABLE OF CONTENT

LIST OF TABLES

LIST OF FIGURES

LIST OF SYMBOLS

a	NRTL and UNIQUAC energy interaction parameter
a_i	Redlich-Kister equation parameters
a_{nm}	UNIFAC group interaction parameter between groups n and m, K
b	NRTL and UNIQUAC energy interaction parameter, K
b_{nm}	UNIFAC group interaction parameter between groups n and m
c_{nm}	UNIFAC group interaction parameter between groups n and m, K^{-1}
C_p	molar heat capacity, $J{\cdot}mol^{-1}{\cdot}K^{-1}$
C_{pi}	heat capacity of individual structural groups
$C_p(T)$	molar heat capacity of the subs. at the desired temp. T, $J{\cdot}mol^{-1}{\cdot}K^{-1}$
$C_{p,reference}(T)$	molar heat capacity of the reference substance (sapphire) at the desired temperature T, $J{\cdot}mol^{-1}{\cdot}K^{-1}$
C_p^E	molar excess heat capacity, $J{\cdot}mol^{-1}{\cdot}K^{-1}$
G	parameter in NRTL model
g^E	excess Gibbs free energy, $J{\cdot}mol^{-1}$
H	molar enthalpy ($J{\cdot}mol^{-1}$)
H-bond	Hydrogen bond (...)
ΔH^E	change in molar excess enthalpy, $J{\cdot}mol^{-1}$
ΔH or ΔH_{mixing}	Heat of mixing or actual heat of mixing, kJ/mol
ΔH^{id}	Ideal heat of mixing, kJ/mol
H_{final}	Enthalpy of final substances
$H_{initial}$	Enthalpy of initial substances
ΔH_1^{∞}	molar enthalpy of amine at infinite dilution, kJ/mol
ΔH_2^{∞}	molar enthalpy of water at infinite dilution, kJ/mol
H^{E}	molar excess enthalpy ($J{\cdot}mol^{-1}$)
H_{blank}^F	heat flow of the blank cells ($J{\cdot}mol^{-1}$)
$H_{reference}^F$	heat flow of the reference material (sapphire), $J{\cdot}mol^{-1}$
H_{sample}^F	heat flow of the sample, $J{\cdot}mol^{-1}$
$m_{reference}$	mass of the reference (sapphire), g
$\mathrm{m_{sample}}$	mass of the sample, g
$M_{Solvent}$	mass of amine, g

M_{Water}	mass of water, g
$MW_{Solvent}$	molecular weight of amine, g/mol
MW_{Water}	molecular weight of water, g/mol
N	number of moles
n_i	Number of individual structural groups
$q, \acute{q}$	surface area parameter
Q	objective function to be minimized by data regression in eq. (3.26)
$\mathcal{Q}$	heat transfer, J/mol
Q_k	relative van der Waals surface area of subgroup k
r	volume parameter
R	universal gas constant, 8.314472(15) J/K/mol
ΔT	difference between the final (T_f) and initial (T_i) temperatures, K
T_f	final temperature, K
T_i	initial temperature, K
x_1	mole fraction of amine
x_2	mole fraction of water
X_m	group mole fraction of group m in the liquid phase
z	coordination number
Z	variables in equation (3.26)

Acronyms

1,2-HEPZ	1-(2-hydroxyethyl)piperzine
1, 3-Bis-DMA-2P	1,3-bis(dimethylamino)-2-propanol
1,4-DMPZ	1,4-dimethyl piperazine
1-MPZ	1-methyl piperazine
2-PE	2-piperidineethanolamine
1DMAP	1-Dimethylamino-2-propanol
3DMA-1,2PD	3-(dimethylamino)-1,2-propanediol
3DEA-1,2PD	3-(diethylamino)-1,2-propanediol
3DMAP	3-Dimethylamino-1-propanol
3-MOPA	3-morpholinopropyl amine
4,2-HEMO	4-(2-hydroxyethyl)morpholine
AAD	Average absolute deviation

AEEA	2-((2-aminoethyl)amino)ethanol
AMP	2-amino-2-methyl-1-propanol
AP	3-amino-1-propanol
BAE	2-(Butylamino)ethanol
BMOEA	Bis(2-methoxyethyl)amine
CO_2	Carbon dioxide
DEA	diethanolamine
DEEA	Diethylethanolamine
DGA	diglycolamine
DIPA	di-2-propanolamine
DiEtA	diethylamine
DMEA	n-n-dimethylethanolamine or dimethyl-2-aminoethanol
DETA	Diethylenetriamine
EAE	2-(Ethylamino)ethanol
EDA	Ethylenediamine
EtOH	Ethanol
H_2O	Water
H_2S	Hydrogen sulfide
HEP	1-(2-Hydroxyethyl)piperidine
IPAE	2-(Isopropylamino)ethanol
MAE or MMEA	Methylethanolamine or N-methyl-2-aminoethanol
MDEA	Methyldiethanolamine
MEA	Monoethanolamine or 2-aminoethanol
MIPA	1-amino-2-propanol
NRTL	Non random two liquid
PAE	2-(Propylamino)ethanol
RD	Relative deviation
RK	Redlich–Kister
TMEDA	tetramethylethylenediamine
TMEDA-EO	2-{[2-(dimethylamino)ethyl]methylamino}ethanol
TEA	Triethanolamine
UNIFAC	universal quasi chemical functional group activity coefficients

UNIQUAC	universal quasi chemical

Greek Letters

α	randomness factor in NRTL model
Γ_k	group activity coefficient of group k in the mixture
$\Gamma_k^{(i)}$	group activity coefficient of group k in the pure substance
Γ	activity coefficient
Θ	area fraction in UNIQUAC model
θ_m	surface fraction of group m in the liquid phase
$\nu_k^{(i)}$	number of structural groups of type k in molecule i
σ_z	standard deviation of the indicated data in equation (3.26)
Σ	standard deviation
T	energy interaction parameters in NRTL and UNIQUAC models
Φ^*	segment fraction in UNIQUAC model
Ψ_{nm}	UNIFAC group interaction parameter between groups n and m

Superscripts

C	combinatorial
Cal	calculated value
E	excess property
Exp	experimental value
R	residual

Subscripts

1	amine
12	interactions between amine and water
2	water
21	interactions between water and amine
E	estimated data in equation (3.26)
I	number of variables in equation (3.26)
i and j	species
i, j	interactions between i and j component
J	number of data points in equation (3.26)
j, i	interactions between j and i component
K	number of sets in equation (3.26)
M	measured data in equation (3.26)
Nm	groups n and m

"It is not allowable [i.e., possible] for the sun to reach the moon, nor does the night overtake the day, but each, in an orbit, is swimming".

(Qur'an: 33:40)

1. INTRODUCTION

The processing of natural gas is required to eliminate impurities and to prevent corrosion, environmental risks, and address the safety concerns associated with the transport of natural gas.[1] Pipeline regulations make it compulsory for natural gas be purified before it is sent to transportation pipelines. A typical natural gas stream contains a mixture of methane, ethane, propane, butane, other hydrocarbons, oil, water vapour, condensates, carbon dioxide, hydrogen sulfide, nitrogen, in addition to other gases and solid particles.[2] The free water and its vapors are corrosive to transportation equipment, especially if CO_2 and H_2S are also present. Hydrates can plug gas line accessories, generating various flow problems. Carbon dioxide and hydrogen sulfide also lower the heating value of natural gas, and as a result, reduce its overall fuel efficiency.[3]

The absorption of CO_2 in aqueous solutions of alkanolamine-based absorbent is a common practice for the removal of CO_2 in the natural gas industry, fossil-fuel-fired power plants, and petroleum industries.[4] Among all solvents, aqueous solutions of alkanolamines such as monoethanolamine (MEA), diethanolamine (DEA), diglycolamine (DGA), di-2-propanolamine (DIPA), n-methyldiethanolamine (MDEA), and triethanolamine (TEA) are the most common in gas sweetening processes.[5] These

absorption practices require technological enhancements to minimize the high capital cost (columns, pumps, exchangers, and solvent) and energy requirements. The cost of steam needed in the amine regeneration column is roughly half the running cost of the plant,[6] which relies mainly on the unit operations design. The use of better solvents or process design improvement can minimize the capital and energy costs, significantly.

Energy consumption for amine regeneration is a vital parameter and is generally known as the "reboiler heat duty" because the total energy required for amine regeneration is supplied by steam passing through a reboiler at the bottom of the stripper column.[7] Reboiler steam generally has three purposes:[8, 9] (1) to provide enough energy to reverse the exothermic alkanolamine acid gas reaction (i.e., breaking the chemical bonds between CO_2 and amine); (2) to dilute and establish a working CO_2 partial pressure as required for CO_2 stripping; and (3) to provide enough sensible heat to heat the liquid feed of the rich amine to the boiling point.

1.1. Importance of heat capacity and excess enthalpy

Molar heat capacity, C_p, has a direct relation (with temperature derivatives) to fundamental thermodynamic properties such as enthalpy, entropy and Gibbs energy. It is also used to measure the effect of temperature on phase and reaction equilibria.[10] The data for heat capacities of amine solutions are widely used in heat duty calculation in heat exchangers, condensers, reboilers, absorbers and regenerators in gas-treating processes. Furthermore, it also serves as a good indicator of phase transition and aids in understanding any alteration in the structure of a liquid solution.[11, 12]

In contrast, molar excess enthalpy, H^E, is an important thermodynamic property of the amine solution. Information with respect to molar excess enthalpy values of amine solutions is important in several applications of chemical engineering (for example, distillation and heat exchanger design).[12] Data regarding H^E for amine solution is able to provide information regarding the macroscopic behaviour of fluid mixtures and molecular interactions. Moreover, it is a requirement in order to develop new solution theories and to analyse the feasibility of existing theories, as it is an indication of the intermolecular force alteration caused by the mixing process. Also, molar excess enthalpy is needed to model multistage, multi-component equilibria in both absorption, and stripping columns.[4] The coefficients of the correlation, obtained from measured experimental data, can be used to model the solubility of gases in aqueous amine solutions.[4]

1.2. Calorimeter

All physical and chemical processes involve energy exchange. The study of measuring the amounts of heat released and absorbed during a physical or chemical process is called a "calorimetric measurement" and the equipment associated with this measurement is known as a "calorimeter". It is well-insulated, and thus ideal as it does not allow heat exchanges with the surroundings. The most reliable method with which to achieve precise and accurate data of the heat capacity and heat of mixing is to measure it directly using different types of calorimeters.

1.2.1. Adiabatic calorimeter

The adiabatic batch calorimeter, initially designed by McGlashan, one of the most successful calorimeters with which to determine the heat effects of a solid and/or liquid system over a wide range of temperatures, which include heat capacity, heat of formation, latent heat of phase changes, heat of mixing, and heat of chemical reaction.[13-16] It contains a calorimetric vessel that is thermally isolated from its surroundings. Thus any heat produced by the sample material under study causes the sample to rise in temperature. The major drawbacks of these calorimeters are they have comparatively large thermal inertia and the temperature of the calorimeter changes during a run. Hence, they are less desirable for kinetic studies of biological or chemical transformations.[17] Furthermore, at a higher temperature, as a result of large heat outflow amounts, the calorimeter becomes more difficult to operate.

1.2.2. Isothermal calorimeter

An isothermal calorimeter, originally developed by Mrazek and Van Ness in 1961, is a calorimeter where no temperature change takes place throughout the experiment. It has two advantages over the previous calorimeter: first, no corrections are required due any change in heat content of the mixing vessel, and second, no compensation if requuired any heat losses from the mixing vessel to its surroundings. It is widely used for heat of mixing measurements because of its capability to generate very precise and accurate results for various types of heat effects.[18, 19]

There are two approaches to achieve a constant temperature. The first approach is based upon the phase change and the main drawback of this technique is the observation can only be carried out at the temperature of the phase change of the calorimeter fluid.[20] In order to maintain a constant temperature, electrical cooling or a heating system is used in the second technique to balance the addition or removal of heat, respectively.[21, 22] The main advantages of this technique are, the independence of results from the heat capacity of the calorimeter while its temperature does not vary, and easier control of heat leakage.[23]

1.2.3. Isothermal dilution calorimeter

The isothermal dilution calorimeter offers an alternative method of measuring the isothermal heat of mixing. In this technique, one fluid is introduced slowly into a stirred vessel wherein the other fluid has been placed. To keep the isothermal state within the calorimeter, electrical energy is provided to the electrical cooling or heating of the system at a suitable rate and is used to balance the heat.[24, 25] The injection of the second fluid may be discontinued at any desired point for a suitable composition. The heat of mixing may be determined by measuring the amount of the first fluid in the vessel, as well as the amount of the second fluid injected and the amount of electrical energy added. A further addition of the second fluid permits the determination of the heat of mixing at other compositions. The precision of the observations are approximately 0.2% of the highest value of H^E. A more detailed description of the different types of isothermal dilution calorimeters was published by Marsh.[20]

1.2.4. Flow calorimeter

The dilution calorimeter has one fluid being injected into the mixing vessel of another. On the other hand, the flow calorimeter has both fluids introduced into a mixing vessel at a steady and known flow rate. The isothermal process is achieved in a similar manner through the dilution calorimeter. The flow rates can be changed in an uninterrupted, known manner so that a full composition range of heat of mixing curve can be produced rapidly with a precision of approximately 1%. [26] A flow calorimeter is used for the measurement of the heat capacity of fluids or fluid mixtures, or in the determination of heat effects which take place in mixing processes.[17] The major drawback of this calorimeter lies in producing a non-pulsed, steady, but promptly variable flow rate. Moreover, this type of calorimeter is undesirable for those liquids with large differences in density, or for viscous fluids.

Flow calorimeters have the benefit of being easily flexible to measurements over a large range of pressures and temperatures, and having the ability to cover the entire range of concentration in only a few hours. The choice of a suitable calorimeter depends upon the research necessities. A batch-type calorimeter is generally desirable for processes such as phase change, chemical reaction, and bio-processes, in contrast a flow calorimeter is much more effective in determining the heat of mixing of liquid systems, mainly when the experiments involve a multi component system. A flow calorimeter is one of the best choices to pinpoint the heat of mixing for most liquid systems.

1.3. Experimental apparatus

Experiments that measure the molar heats of mixing and molar heat capacity were performed with the "C80 calorimeter" manufactured by SETARAM Instrumentation (France). It is a robust, high performance calorimeter, and adapted to isothermal calorimetry. It works on the Tian-Calvet heat flow principles, discussed in depth by Calvet et al.[27] The C80 calorimeter was designed to investigate material transformation, such as fusion, phase transition etc., with respect to studies on thermal stability, mixing, etc. A multitask program, provided by SETARAM, enabling other modules of the calorimeter are used to acquire and compute the experimental data. The working range of the instrument is 25 to 300°C. It uses high precision Calvet detectors with a temperature accuracy and precision of ±0.1°C and ±0.05°C, respectively. The sensitivity of the calorimeter is 30μV/mW at 30°C (using Joule effect technique).[28]

The C80 calorimeter determines the heat flow rate as a function of temperature. The heat flow rate is defined as the rate at which the heat flows into a sample. It is equal to the power needed to maintain the temperature of the sample rising, at a specified scanning rate or set-heating rate. The difference in power provided to the cells and the calorimetric block is considered to be the true measurement. The measured signal is the power needed by the sample heater to maintain the isothermal state in both the reference and the sample cells. This signal reflects either the heat of mixing or the heat capacity of the sample.[28]

1.3.1. Overview of the C80 calorimeter

Figures 1.1 and 1.2 present a sectional view and schematic sketch of the C80 calorimeter, respectively. A massive aluminum block, used as a calorimetric thermostat, is placed at the middle of the cylindrical calorimeter shell. Two identically designed experimental cells (C_1 and C_2) are positioned separately into two identical vertical chambers placed in a symmetrical manner from the centerline of the calorimeter. The first cell operates as a measurement or sample cell and the second as a reference cell. The purpose of the reference cell is to correct the thermal effect as a result of the samples.[29]

Both standard cells are fabricated of stainless-steel cylinders having threaded-top caps. “Standard” and “Membrane Mixing” cells were used for the determination of the heat capacity and heat mixing, respectively.

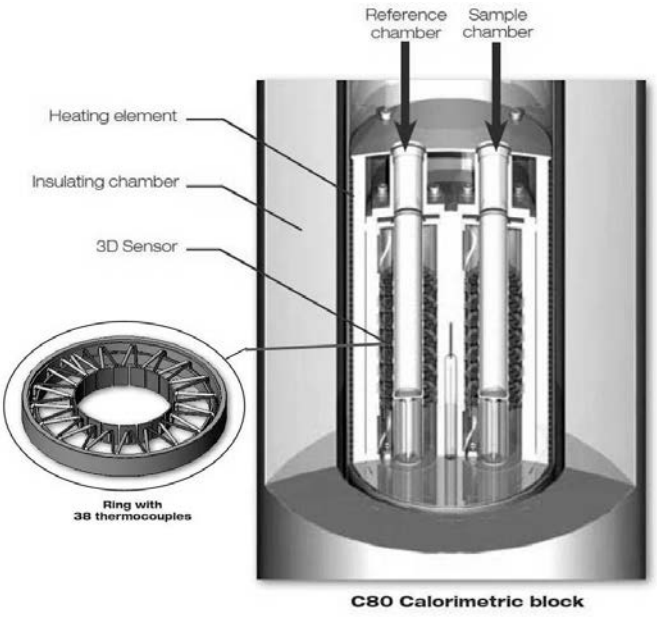

Figure 1.1. Sectional view of the C80 calorimeter and thermopile (courtesy of SETARAM Co.)

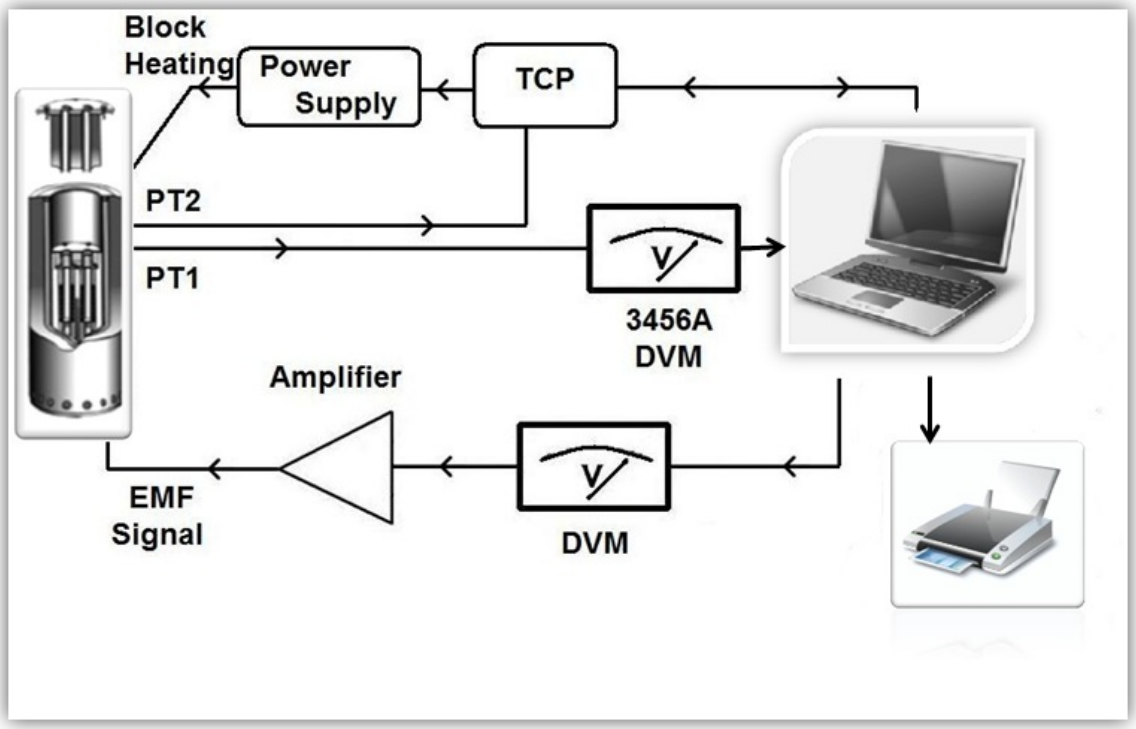

Figure 1.2. Schematic sketch of the C80 heat flow calorimeter (courtesy of SETARAM Co.)

Each cell is enclosed by a separate thermopile or fluxmeter. Both fluxmeters are identical in design and are connected in such a manner as to produce a differential fluxmeter output signal. This special arrangement eliminates interfering signal disturbances caused by the temperature programming or the presence of residual temperature instability.

Each fluxmeter thermally connects the cell to the calorimetric thermostat. So, any thermal exchange between the cell and the calorimetric thermostat signals the fluxmeter to output a signal, which is channelled to a DVM (digital voltmeter). The calorimeter is connected to a data acquisition system and control unit system, and finally to a computer provided with the SETSOFT-2000 program, which is used for the data collection, processing and integration.[28]

Two different platinum resistance probes (labelled PT_1 and PT_2) are located inside the calorimeter to measure and regulate the temperatures of the sample and reference cells. The probe PT_1, known as the "measuring probe", measures the temperature of the cells inside the calorimeter. It has approximately 100Ω of resistance at 0˚C is located between the cells and is connected to the temperature safety unit (SETARAM TS_1). It converts the measured voltage across PT_1 into a temperature. If the temperature rises above the set safety temperature, the power supply to the calorimeter would be disconnected automatically. The probe PT_2, known as the "controlling probe", is used to regulate the temperature of the calorimetric thermostat. It has approximately 20Ω of

resistance at 0˚C and is connected to the temperature controller unit (TCU). The aluminum block heater is also connected with TCU, to regulate the set experimental temperature of the calorimeter. The block is surrounded by an insulating air gap and a layer of insulating material is used outside the air gap. Finally, air cooling is used when the calorimeter requires a reduced temperature.

1.4. Systems studies

The thermodynamic properties of six aqueous alkanolamine solutions were studied. One was primary, four were secondary, and there was one tertiary cyclic amine. To the author's knowledge, no literature is available with regard to the molar heat capacity of the five selected alkanolamines [2-(Butylamino)ethanol (BAE), 1-(2-Hydroxyethyl)piperidine (HEP) and Bis(2-methoxyethyl)amine (BMOEA)], except for 2-(Ethylamino)ethanol (EAE), and 2-(Propylamino)ethanol (PAE) (except the data measured by Rayer et al.).[30] Also, there is no published data available with respect to the molar excess enthalpy for the five selected binary (alkanolamine + water) systems [Diglycolamine (DGA), BAE, HEP and BMOEA] except for PAE at 298.15 K as measured by Mathonat et al.[31] The molecular structures of the six amines discussed are presented in Table 1.1 (showing their structural similarities or differences).

Table 1.1. Illustration and brief information of the selected alkanolamines

	Chemical Information	Molecular Structure	3D Structure
1	2-(Ethylamino)ethanol [$C_4H_{11}NO$] CAS Number: 110-73-6 Purity: ≥98 % Molecular Mass: 89.14	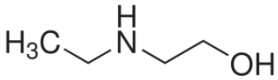	
2	2-(Propylamino)ethanol [$C_5H_{13}NO$] CAS Number: 16369-21-4 Purity: ≥99 % Molecular Mass: 103.16	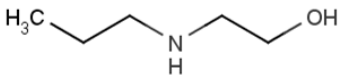	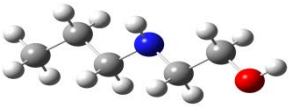
3	2-(Butylamino)ethanol [$C_6H_{15}NO$] CAS Number: 111-75-1 Purity: ≥98 % Molecular Mass: 117.19	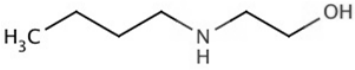	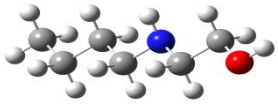
4	1-(2-Hydroxyethyl) piperidine [$C_7H_{15}NO$] CAS Number: 3040-44-6 Purity: 99 % Molecular Mass: 129.20	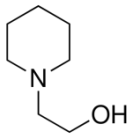	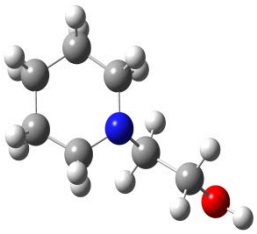
5	Diglycolamine [$C_4H_{11}NO_2$] CAS Number: 929-06-6 Purity: 98 % Molecular Mass: 105.14	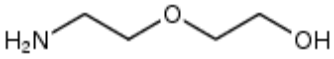	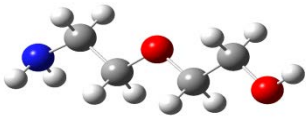
6	Bis(2-methoxyethyl)amine [$C_6H_{15}NO_2$] CAS Number: 111-95-5 Purity: 98 % Molecular Mass: 133.19	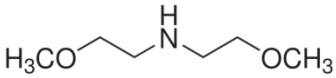	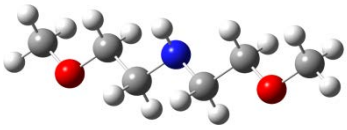

1.5. Research objectives

The purpose of this research is to experimentally measure the molar heat capacity (C_p) and molar excess enthalpy (H^E) of five aqueous alkanolamine binary systems. The objectives of this investigation include:

- Experimental measurement of the molar heat capacity (C_p) of aqueous solutions of 2-(Ethylamino)ethanol (EAE), 2-(Propylamino)ethanol (PAE), 2-(Butylamino)ethanol (BAE), 1-(2-Hydroxyethyl)piperidine (HEP) and Bis(2-methoxyethyl)amine (BMOEA) from 303.15 to 353.15K at atmospheric pressure, and for the entire range of mole fractions. Molar excess heat capacity will be calculated based on the measured molar heat capacity and will be correlated as a function of mole fractions using the Redlich-Kister relation.[32] Reduced excess heat capacity will be derived from excess properties on a point-to-point basis, and the partial molar excess heat capacity will also be derived. A group additivity and molecular connectivity analysis will be used to predict the values of the molar heat capacities of the alkanolamines.
- Measurement of molar heats of mixing or molar excess enthalpy (H^E) for the binary mixtures of the five aqueous alkanolamines systems including Diglycolamine (DGA), 2-(Propylamino) ethanol (PAE), 2-(Butylamino)ethanol (BAE), 1-(2-Hydroxyethyl)piperidine (HEP) and Bis(2-methoxyethyl)amine (BMOEA) at three temperatures (298.15, 313.15 and 333.15K), and for the whole range of mole fraction. Experimental data of molar excess enthalpy will be correlated as a function of mole fractions using the Redlich-Kister relation[32] and

the partial molar excess enthalpy at infinite dilution will also be derived. In addition, the experimental data will be correlated as a function of mole fractions employing the NRTL (Non Random Two Liquid), UNIQUAC (Universal Quasi Chemical) and the modified UNIFAC (Universal Quasi Chemical Functional Groups Activity Coefficient, Dortmund) models. The aforementioned models are the most widely used to interpret this type of measurements.

1.6. Overview of content

Chapter 2 presents a review of published literature for the heat capacity of alkanolamines. Chapter 2 also discusses the different techniques for representing the experimental heat capacity data. In addition, this chapter deals with the estimation of molar heat capacity using Group Additivity Analysis and Molecular Connectivity Analysis. Heat capacity measurement methods, calibration and verification of the C80 calorimeter are also discussed. The experimental results and discussion and fittings of the calculated molar excess heat capacity, partial molar excess heat capacity by the Redlich-Kister relation and reduced heat capacity are also presented. Chapter 3 presents a literature review regarding the different studies dealing with the heats of mixing of aqueous alkanolamine solutions, and an evaluation of various existing methods for correlating the experimental molar excess enthalpy data. The heat of mixing measurement method, the calibration and verification of the C80 calorimeter are also reported. In addition, experimental data are correlated and represented by a variety of methods such as empirical, solution theory and group contribution methods. Several simulation models such as NRTL, UNIQUAC and Modified UNIFAC-Dortmund are therefore presented.

Experimental excess enthalpies, represented by means of various VLE models, are also included in this chapter. Chapter 4 summarizes the conclusions from all chapters and offers some recommendations for future work.

"And it is He who created the night and the day and the sun and the moon; all [heavenly bodies] in an orbit are swimming".

(Qur'an: 21:33)

2. HEAT CAPACITY

Heat capacity is an essential material property. It is a fundamental quantity for the determination of other thermodynamic quantities, such as enthalpy (H), entropy (S), and Gibbs free energy (G). As mentioned earlier, it can be used in several applications of chemical engineering such as heat exchanger, distillation absorption, and stripping columns design.[12]

2.1. Literature review

Hayden et al.[33] reported the heat capacities of 23wt% and 50wt% aqueous MDEA solutions at 298.15, 323.15, and 248.15K. The data for MEA, DEA and TEA, taken from the Dow Chemical Co. (1954) and Mehl (1934) at 303.15K, were reported by Riddick et al.[34] In an annual report by Lee[35], the values for MEA, DEA, TEA, and MDEA, in the temperature range of 303.15 to 423.15K were presented. Lide[36] reported the values of Cp for MEA, TEA at 298.15K, and DEA at 303.15K.

Maham et al.[37] measured the molar heat capacities of fourteen pure alkanolamines and suggested their results could be predicted by the molecular structure. They introduced the Group Additivity Analysis and limited the study to only four structural groups such as $-CH_2$, -NH, -N and -OH. They pointed out that the structural group contributions in the molar heat capacities are governed by $-CH_2$ and -OH groups

although the -NH group exhibited a maximum dependence on temperature and these contributions increased with rising temperature, whereas the contribution of the -N group is very minute, almost zero at all temperatures. Furthermore, they applied Molecular Connectivity Modelling to the molar heat capacity data of several alkanolamines.

Chiu et al.[38] measured the heat capacity of eight alkanolamines such as MEA, DGA, DEA, DIPA, TEA, MDEA, AMP, 2-PE, at different temperatures from 303.15 to 353.15K with a differential scanning calorimeter. They also measured the heat capacities of aqueous solutions of the aforementioned eight amines for temperatures ranging from 303.15 to 353.15K and mole fractions of amine of 0.2, 0.4, 0.6, and 0.8.[39]

The molar Cp of the aqueous solutions of AEEA, AP, DMEA MAE, and MIPA at several temperatures from 303.15 to 353.15K, and over the entire range of mole fractions were reported by Mundhwa and Henni.[40] They found that AEEA had the highest values and MAE had the lowest values. They also found that the partial molar quantities for alkanolamines increased with elevated temperatures and similar behaviour was noted with regard to the partial molar quantities of water, except the MIPA and DMEA system. Their values decreased at elevated temperatures. Finally, the molar excess heat capacity curves for all temperatures are positive except the MAE solution at 303.15K for $x1 = 0.9$, wherein a slightly negative result was exhibited. Poozesh reported that the contributions of the $–CH_2$, –N, –OH, –O, $–NH_2$ groups increased with rising temperatures and the contributions of the –NH and $–CH_3$ groups decreased with rising temperatures

for cyclic amines. In addition, the molar C_P of aqueous (1, 4-DMPZ), (1, 2-HEPZ), (1-MPZ), (3-MOPA) and (4, 2-HEMO) solutions were measured at various temperatures from 298.15 to 353.15K, and over the whole range of mole fractions, and all molar excess Cp were found to be positive.[41]

Uddin found in the group additivity analysis that the contributions of the $–CH_3$, $–CH_2$, –OH groups rose with an increasing temperature although the contributions of –N and –CH groups decreased with a rising temperature for the investigated tertiary amines.[42] Molar heat capacities of aqueous TMEDA, TMEDA-EO, (3DMA-1, 2PD), (3DEA-1, 2PD), and (1,3-Bis-DMA-2P) solutions were measured at several temperatures ranging from 303.15 to 353.15 K, and over the full range of mole fractions and all molar excess Cp were found to be positive. Narayanaswamy[43] concluded that heat capacity increases with the addition of extra functional groups in the following order: NH_2 and OH > CH_2. Primary alcohol appeared to have a greater heat capacity than secondary alcohol and this may be attributed to the position of the –OH group in the secondary alcohol due to its steric hindrance effect. Moreover, molar heat capacities of aqueous 1DMAP, 3DMAP, DEEA, DETA and EDA solutions were measured at several temperatures from 303.15 to 353.15K, and over the entire range of mole fractions.

Finally, Rayer et al. measured the molar heat capacities of 38 pure solvents at atmospheric pressure in a temperature range of 303.15 to 393.15K.[30] They improved the Group Additivity Analysis by extending it to the thirteen structural groups such as

CH_3, CH_2, CH, C, =CH, =C, NH_2, NH, N, =N, OH, O and =O and also enhanced the Molecular Connectivity Analysis.

2.2. Heat capacity

Thermodynamically, the relationship between heat transfer (Q) and the change in temperature (ΔT) during a process at constant pressure is given by:

$$Q = C_P \Delta T = C_P(T_2 - T_1) \quad (2.1)$$

where Cp, the proportionality constant, is the molar heat capacity of a substance, which is described as the amount of heat required to raise the temperature of the substance by one degree. Also, T_2 and T_1 are the final and initial temperatures of a process respectively.

2.2.1. Excess molar heat capacity

Heat capacity data are generally expressed in terms of the excess heat capacity of the system. With regard to a binary mixture, an excess molar heat capacity, Cp^E, suggested by Lide and Kehiaian[44] is as follows:

$$C_p^E = C_p - \{x_1 C_{p,1} + x_2 C_{p,2}\} \quad (2.2)$$

where Cp, $Cp,_1$ and $Cp,_2$ are the molar heat capacity of the mixture, pure alkanolamine and water, respectively. The molar heat capacity data for water is taken from Osborne et al.[45] x_1 and x_2 are the mole fractions of amine solvent and water, respectively. Usually, the value of excess molar heat capacity of a binary mixture shows the degrees

of non-ideality. The smaller the value indicated, the nearer the system approaches an ideal solution.

Small negative Cp^E is obtained for mixtures where no special interactions occur, and can be described as the change in free volume upon mixing, e.g., for mixtures of two short n-alkanes. If there is destruction during the mixing of the molecular structure in either or both of the pure species, larger negative Cp^E values are found. Destruction of dipolar order in one or both species should also yield negative Cp^E. In contrast, positive Cp^E has been associated with the development of structure or arrangement in the solution such as the dispersion of solute or a complex formation between the constituents. In these systems, the structure in the solution is given by the formation of different hydrogen-bonded substances. All previously discussed situations Cp^E curves are skewed or nearly parabolic, i.e., the higher or lower is found roughly at equimolar concentration.[46]

2.2.2. Reduced excess heat capacity

Frequently, excess molar property plots are unable to explain all the important characteristics of their composition dependence. This methodology can be deceiving in some situations and hide strong interactions at low concentrations.[47] To project some of the more subtle characteristics, several different approaches are available in the literature, such as apparent molar and reduced excess molar properties. A key feature of the apparent and reduced properties is that they are derived from excess properties on a point-to-point basis, and there is no requirement of any type of curve fitting or local smoothing of the data. As a comparison with excess apparent molar properties, the

reduced excess molar properties are more informative with respect the composition dependence at higher water concentrations.[48] The reduced excess heat capacity function works as a sensitive indicator of phase transitions and is also used to interpret the modifications in the structure formation of liquid solutions.[40] As far as a binary mixture, a reduced excess molar heat capacity is calculated as follows:

$$C_{p(red.)}^{E} = \frac{C_p^E}{x_1 x_2} = \frac{C_p - \{x_1 C_{p,1} + x_2 C_{p,2}\}}{x_1 x_2} \quad (2.3)$$

where Cp^E is the excess molar heat capacity of the mixture and x_1 and x_2 are the mole fractions of amine solvent and water, respectively. This function provides a better representation of the origin of non-ideality in the mixtures.[47]

2.2.3. Partial molar excess heat capacity

A partial molar property is a thermodynamic quantity which points out how an extensive property of a mixture or solution varies with changes in the molar composition of the mixture or solution at a constant pressure and temperature. They are especially beneficial when considering specific properties of pure chemical substances (that is, properties of one mole of pure chemical substance) and properties of mixing. As for a binary mixture, the partial molar excess heat capacities of the alkanolamines at infinite dilution in water (x_1 = 0), and of water in alkanolamines at infinite dilution (x_2 = 0 or x_1 = 1) are proposed by Maham et al.[49, 50] are as follows:

- for alkanolamines @ x_1 = 1

$$C_1^0 - C_1^* = \sum_{i=0}^{n} a_i (-1)^{i-1} \quad (2.4)$$

- for water @ $x_1 = 0$

$$C_2^0 - C_2^* = \sum_{i=0}^{n} a_i \quad (2.5)$$

where a_i are the polynomial coefficients of the Redlich-Kister equation[32] obtained from the least squares regression method of the dependence of excess heat capacity on x_1 or x_2.

2.3. Calibration of the C80 calorimeter

To obtain a precise and accurate measurement of the molar heat capacity and the molar heat of mixing of a sample, the temperature scale and the sensitivity of the instrument must first be calibrated. Calibration gives a mechanism with which quantifying uncertainties. Moreover, it confirms the validity of the instrument with the help of well-defined and tested standard operating procedures. The International Confederation for Thermal Analysis and Calorimetry (ICTAC)[51] has recommended standard operating procedures for the temperature as well as the sensitivity calibration of this instrument.

2.3.1. Sensitivity calibration

With respect to the Tian-Calvet heat flow calorimeter, the sensitivity calibration was carried out using the Joule Effect method. According to the SETARAM recommendation, the calibration was executed for a wide range of temperatures (from 30 to 300˚C) at the scanning rate of 0.1K.min^{-1}. A calibration or Joule Effect unit (EJ3) and two specially designed cells for the Joule Effect calibration were provided by the SETARAM, and all the required accessories were used for the calibration. Both cells are identical in design and

are made up of a metallic cylinder adjusted to fit and surrounded by a heat flux transducer.

A sample cell was connected to the calibration unit (EJ3) via the Joule Effect cable. The main target of this calibration procedure was to supply stable and constant power to the calibration resistance heater for an identified period of time. The standard values for calibration that were used for power (P), the time of the Joule Effect (TEJ) and the total time (T_{total}) are 10mW, 2100sec and 4500sec respectively. After a sufficient period of time (roughly 3hours), the calorimeter reaches thermal equilibrium at the specified temperature. Subsequently, the calibration was started by pressing the impulsion start switch on the EJ3 unit. The set power in the calibration unit (EJ3) was automatically provided to the resistance of the cell heater. The power supply setting of 10mW was checked by measuring the current and voltage, and was found to be 9.998mW. Following the start of the experiment, the differential fluxmeter signal rose and ultimately levelled off with time. The sensitivity constants, listed in Table 2.1, were taken from the results of the sensitivity calibration experiment, and provided the values to the SETSOFT 2000 software. Figure 2.1 presents the sensitivity curve and the calculated sensitivity constants.

Table 2.1. Sensitivity constants for C80 heat flow calorimeter.

Sensivity Constants	Values (µV/mW)
a(0)	3.13E+01
a(1)	-1.77E-04
a(2)	-1.81E-04
a(3)	3.91E-07
a(4)	-3.37E-10

2.3.2. Temperature calibration

In order to obtain better results, the temperature scale of the Tian-Calvet heat flow calorimeter must be corrected. The purpose of temperature calibration is to compensate the sample's lag of real temperature with that of the exhibited temperature. This lag occurs as a result of the time needed to transfer heat from the heater into the sample. The heat flow calorimeter was calibrated in accordance with the American Society for Testing and Materials standard ASTM E 967-08 “Standard Practice for the Temperature Calibration of Differential Scanning Calorimeters and Differential Thermal Analyzers”.

The temperature calibration is carried out by measuring the exhibit temperature of a phase change of a standard substance, which has a well-documented exact transition temperature. The melting point was obtained by measuring the rate of heat flow into the sample as a function of temperature at the time of melting. The difference between

the observed and the real transition temperature determines the amount of adjustment required to determine an unidentified temperature accurately.

The temperature calibration, the melting points of pure Tin and Indium were used for the purpose of temperature calibration. Both sample and reference cells were filled to precisely one third of their height with calcined aluminum oxide (Al_2O_3). A sample of the standard substance, either Tin or Indium, was covered with aluminum foil and placed inside the sample cell. Aluminum oxide does not have any phase transition in the temperature range of the standard substances. The purpose of aluminum oxide is simply to raise the thermal mass of the cells and thereby increase the total specific heat of the loaded sample. The total quantity of heat absorbed by the sample during melting is estimated by measuring the area under the peak, as presented in Figure 2.2. The melting point is the temperature at area under the peak, as presented in Figure 2.2. The melting point is the temperature at which the extrapolated baseline under the peak and the line expressing the initial rise in heat flow for the duration of melting, cross each other. When this temperature is described in terms of the exhibited temperature on the calorimeter during melting, the temperature is known as the "apparent melting temperature".

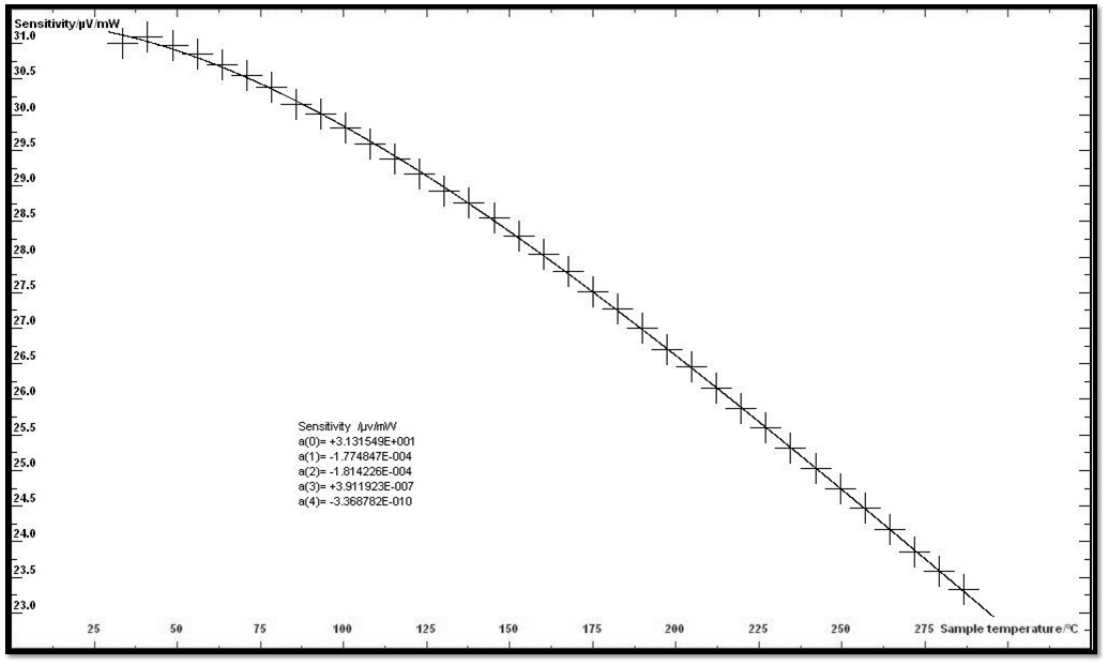

Figure 2.1. Sensitivity calibration curve using SETSOFT-2000 software

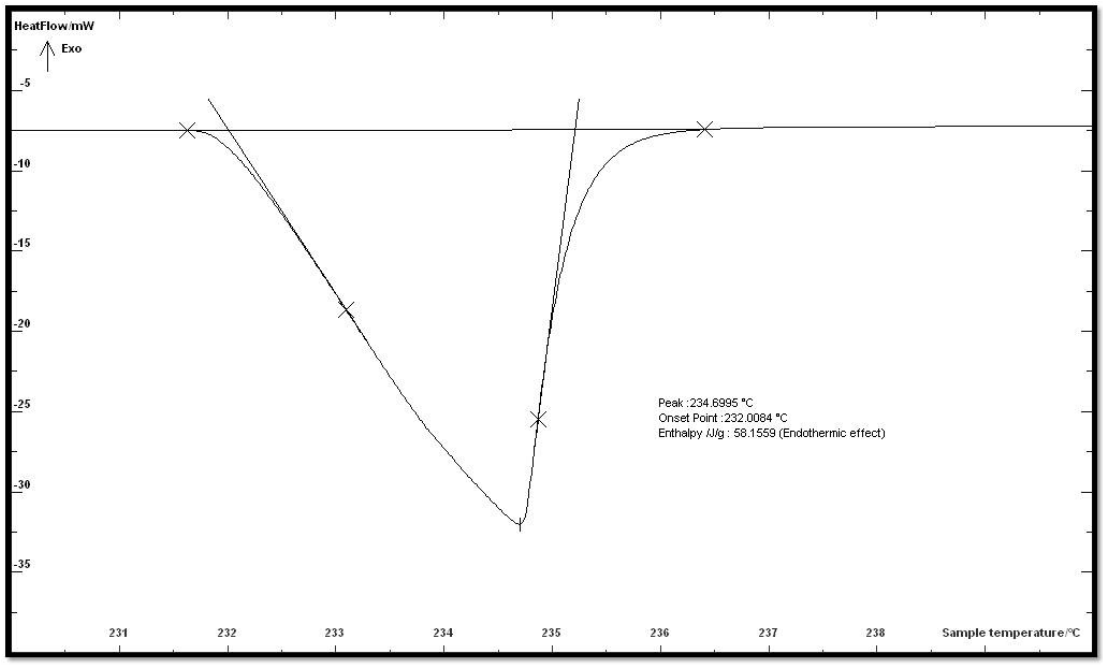

Figure 2.2. Temperature calibration with tin at the scanning rate of 0.1 K.min-1 using SETSOFT-2000 software

Table 2.2. Melting points of indium and tin at different scanning rates and temperature correction coefficients

Sample	Scanning rate ($K \cdot min^{-1}$)	Temperature (°C)		
		Theoretical	Experimental	Calculated
Indium	0.1	156.598	156.571	156.661
Indium	0.2	156.598	157.147	156.653
Indium	0.4	156.598	158.554	156.541
Indium	0.6	156.598	159.612	156.671
Indium	0.8	156.598	160.650	156.712
Tin	0.1	231.928	232.008	231.936
Tin	0.2	231.928	232.552	231.941
Tin	0.4	231.928	233.582	231.938
Tin	0.6	231.928	234.562	231.956
Tin	0.8	231.928	235.640	231.951
Temp. Correction Coefficients	-1.12E+00	1.27E-02	1.23E+01	-2.04E+00

The value achieved for the apparent melting temperature depends upon the heating or scanning rate. This temperature is measured for various scanning rates such as 0.4, 0.8, and $1 K \cdot min^{-1}$ for both Indium and Tin. The SETSOFT 2000 software is used to reconcile the temperature difference between the apparent and the real temperature to the scanning rate, and to provide the values of temperature correction coefficients such as b_0, b_1, b_2, and b_3. Temperature calibration values, along with the temperature correction coefficients, are documented in Table 2.2.

2.4. Molar heat capacity (Cp) measurements

The C-80 calorimeter is proficient in measuring heat capacities over a wide range of temperatures (from ambient to 300°C). Molar heat capacity experiments were conducted in a temperature range from 30 to 80°C, using standard cells.

The standard or regular batch cells used for the molar heat capacity measurements, as illustrated in Figure 2.3, consist of concentric stainless steel cylinders. The diameter, height and volume of the cells are 17mm, 80mm and 12.5cm^3, respectively. The top section of the cells is firmly closed by a lid with a tapered bearing surface, which is supported by a "U" shaped O-ring.

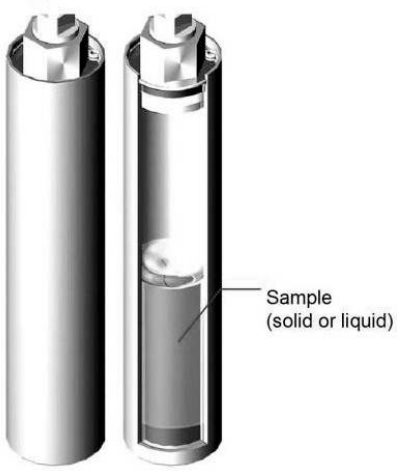

Figure 2.3. Regular batch cell for a Cp measurement (courtesy of SETARAM Co.)

2.4.1. Methods of measuring molar heat capacity

In the C80 calorimeter, there are generally two recognized ways to measure molar heat capacity at a specific temperature.

2.4.1.1. Continuous two step method

In this technique, it is necessary to perform a reference run with both empty cells before measuring the molar heat capacity of the sample. The main objective of this run is to correct the minor asymmetry between the fluxmeters and also between the reference and the measurement cells. To measure the molar heat capacity, a liquid sample weight of approximately 5 to 6g was placed within the sample cell. The sample and empty cells were placed in the measurement chamber (C_1) and reference chamber (C_2) of the calorimeter, respectively. A significant thermal unbalance takes place when the cells are introduced into the calorimeter. To re-gain the steadiness of the calorimetric signal, both the sample and the reference cells are given enough time (3 to 4hours) to form an isothermal condition before proceeding with the experiment. The scanning rate was set at $0.1K \cdot min^{-1}$ for all sample experiments. After holding the cells at the suitable initial temperature of 25°C (or 298.15K) for a sufficient period of time to achieve the isothermal condition, both cells were heated at a scanning rate of $0.1K \cdot min^{-1}$. The calorimetric signal raises as a function of time for the duration. When it reached the higher set temperature, the calorimeter automatically returned to an isothermal state, causing the calorimetric signal to revert to the baseline. The heat capacity of the substance is determined by measuring the difference between the reference and measurement signal at any suitable temperature.

2.4.1.2. Continuous three step method

The most reliable and accurate data with respect to heat capacity can be obtained using the continuous three step method.[40] The key difference in this technique, compared to

the two step method, is the addition of one extra run for the reference material such as Sapphire. Thus, the measurements of the heat capacity were executed with a sample, blank and reference (as a third step) runs, respectively. Figure 2.4 presents the thermal analysis curves for the baseline (or blank), standard reference, and sample profiles. There is a difference between the isothermal signals at the start and end of the experiments as a result of temperature dependence of the coefficients for heat transfer.

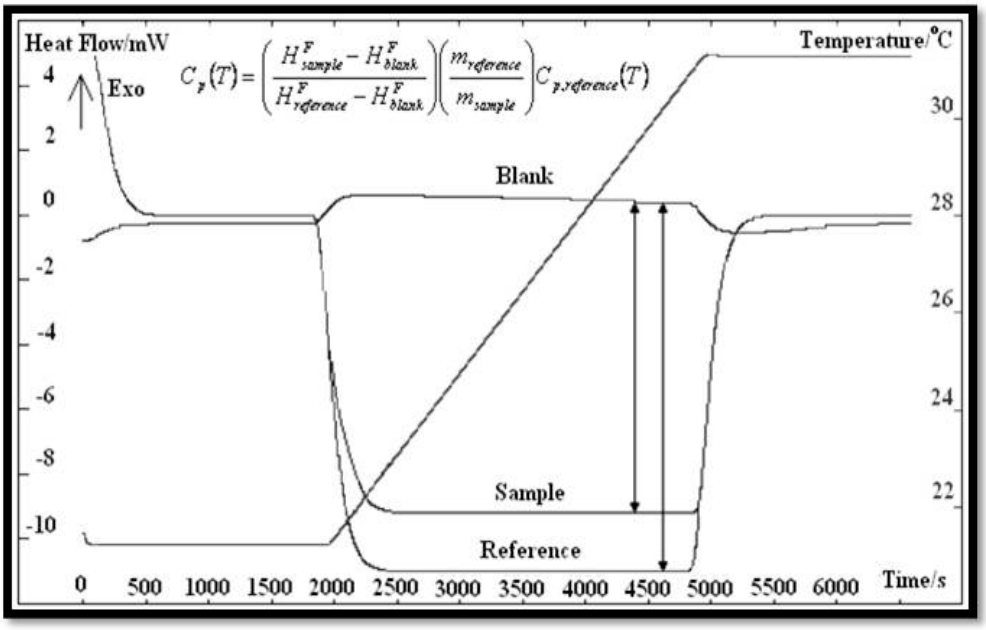

Figure 2.4. Heat flow profile for the three step method of different runs

This technique is widely used for the measurement of the liquid molar heat capacity. Becker et al.[52] and Becker and Gmehling[53] have investigated the measurements of the Cp for nine and twelve organic substances, respectively, using this technique. The scanning rate for the temperature was generally set at 0.1K·min^{-1}.

In this technique, the rest of the method is identical to the two step method. All three runs were carried out under the same experimental conditions. The heat flow data were measured in a temperature range of 303.15 to 353.15K. The following expression was used to estimate the molar heat capacity values: [29, 54]

$$C_p(T) = C_{p,reference}(T) \times \left\{\frac{H^F_{sample} - H^F_{blank}}{H^F_{reference} - H^F_{blank}}\right\}\left\{\frac{m_{reference}}{m_{sample}}\right\} \qquad (2.6)$$

where Cp(T) and $Cp_{,\ reference}(T)$ are the molar heat capacity of the substance and reference material (Sapphire) at temperature T, respectively. The data of $Cp_{,\ reference}$ (T) for reference material Sapphire, in Equation 2.6, were taken from the National Bureau of Standards.[55] Whereas, m_{sample} and $m_{reference}$ are the mass of the sample and reference material (Sapphire) and H^F_{sample}, $H^F_{reference}$ and H^F_{blank} are the heat flow for the sample, reference material (Sapphire) and blank cells, respectively.

2.5. Verification of the C80 heat flow calorimeter

2.5.1. Molar heat capacity measurements:

The reason the calorimeter is checked prior to using it is to determine its reliability. In this investigational study, in order to confirm the reliability of the C80 calorimeter in the molar heat capacity measurement, two "standard" alkanolamines: monoethanolamine (99wt.% pure) and methyldiethanolamine (99+wt.% pure) were used. The two solvents were purchased from Sigma Aldrich Canada Ltd. and were used without additional purification. The heat capacities of the aforementioned solvents were observed in a

temperature range of 303.15 to 353.15K, at a scanning rate of 0.1K·min^{-1}, and are compared to the results available in the literature.

Table 2.3. Comparison data of the molar heat capacity of MEA and MDEA

T/K	MEA		MDEA	
	Cp/ J·mol·$^{-1}$·K^{-1}		Cp/ J·mol·$^{-1}$·K^{-1}	
	Chiu et al.	This Study	Chen et al.	This Study
303.15	167	171	272	269
308.15	169	172	275	275
313.15	170	173	278	278
318.15	172	174	281	280
323.15	173	175	285	283
328.15	175	176	288	286
333.15	176	177	291	289
338.15	178	178	295	291
343.15	179	179	298	294
348.15	180	180	301	296
353.15	182	181	304	299

The molar C_P of MEA and MDEA, measured with the C80 calorimeter, are in good agreement with those reported by Chiu et al.[38] and Chen et al.[56] using a differential scanning calorimeter (DSC), respectively. A comparison of the molar heat capacity data of MEA and MDEA is listed in Table 2.3, and presented in Figures 2.5 and 2.6.

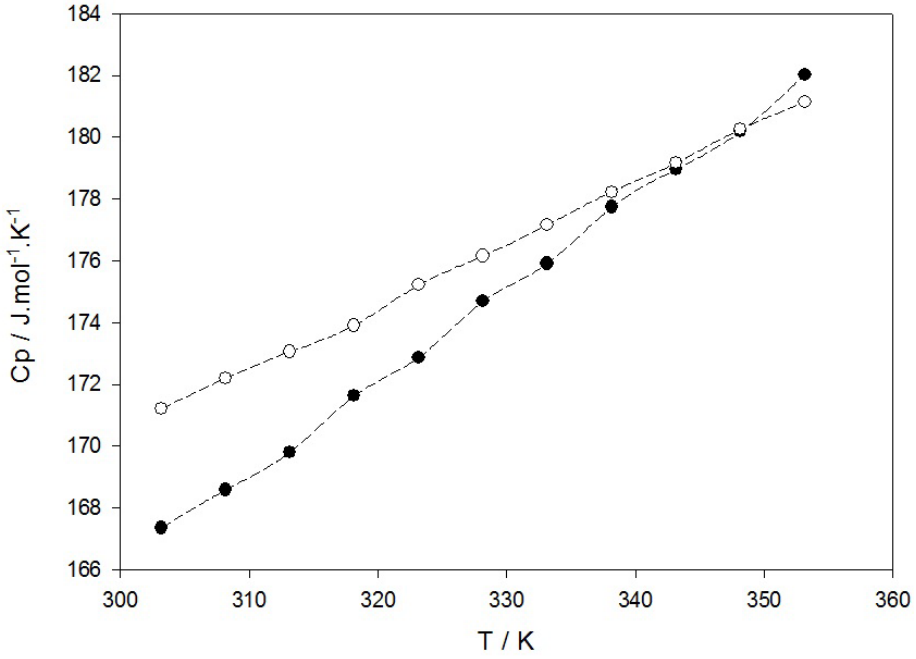

Figure 2.5. Comparison of the molar heat capacity data for pure MEA: ●-, Chui et al.[38] and ○-, This study

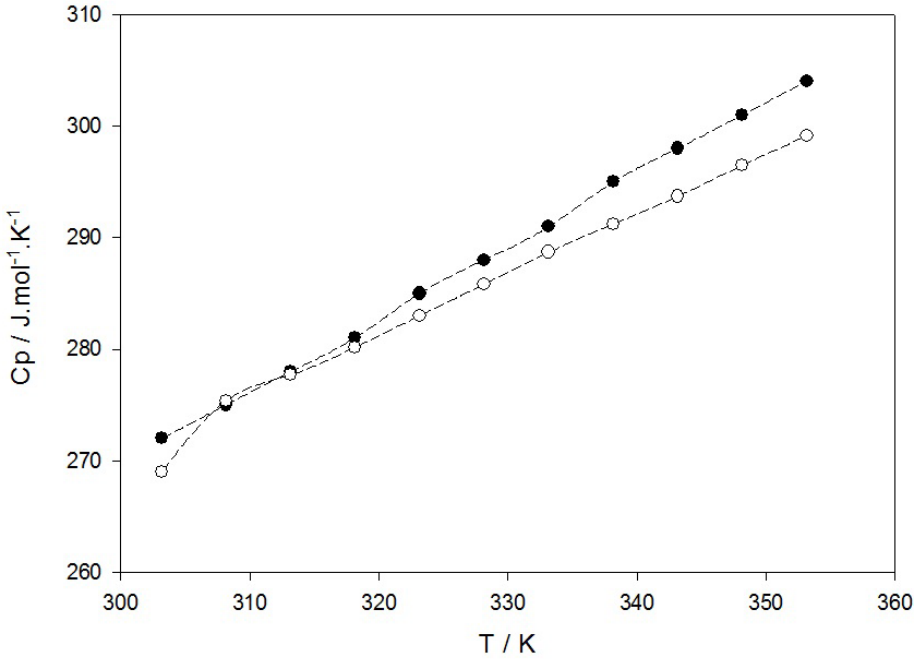

Figure 2.6. Comparison of the molar heat capacity data for pure MDEA: ●-, Chen et al.[56] and ○-, This study

Percentages of relative deviation (%RD) or average absolute deviation (%AAD)[57] for the molar heat capacity data of MEA and MDEA, as measured in this study, were 1.05, and 0.88% when compared to the data published by Chiu et al.[38] and Chen et al.[56], respectively.

2.6. Correlation and prediction approaches

The key objective of the correlation is to provide a convenient and optimum usage of the experimental data. Due to the complexities involved in experimental measurement and the additional time required for each component of a multi-component mixture, it is highly suitable to develop realistic approaches capable of predicting the physical and chemical properties of multi-component systems.[58]

2.6.1. Empirical expressions

Empirical expressions are very helpful and suitable when dealing with data correlation and prediction. The parameters in the formulas are fitted to the measured experimental data and a number of parameters can be determined according to the required accuracy.

2.6.1.1. Redlich-Kister equation

In this study, excess molar heat capacity data were regressed using the Redlich-Kister expression[32]. It is a mixing rule form which is similar to a convergent series with a finite number of terms. With regard to the binary system, this expression has the following polynomial form:

$$C_P^E / J \cdot mole^{-1} \cdot K^{-1} = x_1 x_2 \sum_{i=0}^{n} a_i (x_1 - x_2)^i \qquad (2.7)$$

where C_P^E is the excess molar heat capacity, x_1 and x_2 are the mole fractions of alkanolamine and water, respectively and a_i are the polynomial coefficients obtained from the least squares fitting of the dependence of C_P^E on x_1 or x_2, and n is determined using the F-Test.[59, 60]

2.6.2. Group additivity analysis (GAA)

This technique assumes each dissimilar structural group in a molecule contributes definite values of the Cp to the whole molecular heat capacity. The compounds under investigation were divided into structural component groups to maximize the number of degrees of freedom in order to represent the molar heat capacities over the full experimental temperature range. Rayer et al.[30] suggested that each molecule can be broken into 13 structural groups such as CH_3, CH_2, CH, C, =CH, =C, NH_2, NH, N, =N, OH, O and =O. Contributions of each structural group to the molar heat capacity were estimated, and the sum of several structural group contributions may be considered as the molar heat capacity of the molecule:[30]

$$C_P = n_1 C_{P(-CH_3)} + n_2 C_{P(>CH_2)} + n_3 C_{P(>CH-)} + n_4 C_{P(>C<)} + n_5 C_{P(=CH-)}$$
$$+ n_6 C_{P(=C<)} + n_7 C_{P(-NH_2)} + n_8 C_{P(>NH)} + n_9 C_{P(>N-)} + n_{10} C_{P(=N-)}$$
$$+ n_{11} C_{P(-OH)} + n_{12} C_{P(-O-)} + n_{13} C_{P(=O)} \quad (2.8)$$

This can be represented in the following simple form:

$$C_P = \sum_{i=1}^{13} n_i C_{Pi} \quad (2.9)$$

where Cp is the heat capacity of the alkanolamine and n_i and Cp_i are the number and heat capacities of the individual structural groups, respectively. This technique is based upon the molecular structural group and not on a molecular functional group. This represents one of its major disadvantages. For example, this technique cannot distinguish among primary, secondary and tertiary alcohols. Rayer et al.[30] used the following basic approach of analysis:

$$\beta = KC^{-1} \qquad (2.10)$$

Table 2.4. Estimated group contributions to the molar heat capacities[30]

Structural groups	Temperature /K									
	303.15	313.15	323.15	333.15	343.35	353.15	363.15	373.15	383.15	393.15
	Heat Capacity /J·mol^{-1}·K^{-1}									
CH_3	41.03	43.56	45.13	47.20	49.53	50.82	56.13	62.35	59.53	58.02
CH_2	30.80	31.40	31.57	31.41	33.02	33.50	35.26	32.50	31.94	30.10
CH	47.95	48.19	45.98	37.55	39.57	41.11	22.03	13.99	23.65	22.93
C	-0.81	10.04	7.92	4.03	2.76	2.48	-5.47	-19.51	10.84	6.66
=CH	22.17	21.24	21.25	21.84	22.08	24.47	31.16	39.40	34.54	38.17
=C	8.16	-0.81	-4.79	-7.94	-14.44	-13.29	-2.74	6.05	0.06	-0.17
NH_2	56.47	58.40	59.16	61.02	59.79	59.30	58.10	63.08	63.98	68.48
NH	41.05	42.27	42.74	42.85	41.15	45.45	42.28	43.33	54.83	57.87
N	4.77	2.00	2.56	4.71	0.02	2.15	-3.41	-7.75	0.73	9.68
=N	24.07	34.81	39.22	42.10	48.97	47.01	27.46	7.68	7.08	13.04
OH	55.37	57.51	58.57	60.11	60.31	59.74	59.27	67.13	67.76	70.33
O	22.96	22.50	22.59	22.33	20.44	20.19	15.83	32.78	30.15	30.57
=O	19.66	29.03	32.38	35.81	41.82	37.82	35.52	28.73	35.68	36.65

where K represents the matrix of the experimental molar heat capacities of the alkanolamines and C represents the matrix formed from breaking the molecular structures into thirteen structural group component contributions (Table 2.4). The percentage relative deviations [57] of the predicted heat capacity, with respect to the experimental heat capacity, are listed in Table 2.14.

2.6.3. Molecular connectivity analysis (MCA)

A single expression that models the molar heat capacity data of the alkanolamines over a wide range of temperatures can be developed using molecular connectivity indexes. This technique encodes simple structural information into a range of simple indexes which may then be used to model a wide range of properties of structurally similar compounds. It utilizes an algorithm to encode chemical bond contributions to a molecular branching index, as suggested by Randic[61]and this branching algorithm was used as a basis for a structural description example by Kier and Hall.[62]

A set of six molecular connectivity indexes, for the analysis of alkanolamines, which are described using two cardinal numbers, δ_i (delta index) and δ^v_i (delta valence index),are listed in Table 2.5, and are identified as the summation of the delta index, D, the summation of the delta valence index, D^v, the zeroth-order simple molecular connectivity index, ^0X, the zeroth-order valence molecular connectivity index, $^0X^v$, the first-order simple molecular connectivity index, ^1X, and the first-order valence molecular connectivity index, $^1X^v$. The following expressions are used to estimate the indexes for each molecule representing the alkanolamine.

$$D = \sum \delta_i \quad (2.11)$$

$$D^v = \sum \delta_i^v \quad (2.12)$$

$${}^0X = \sum(\delta_i)^{-0.5} \quad (2.13)$$

$${}^0X^v = \sum(\delta_i^v)^{-0.5} \quad (2.14)$$

$${}^1X = \sum\left(\delta_i\delta_j\right)^{-0.5} \quad (2.15)$$

$${}^1X^v = \sum\left(\delta_i^v\delta_j^v\right)^{-0.5} \quad (2.16)$$

where i and j represent the adjacent non-hydrogen atoms forming a sigma bond. Rayer et al.[30] modified the molecular connectivity equation proposed by Maham et al.[37] to fit the heat capacity data:

$$C_P = b_0D + b_1D^v + b_2\ {}^0X + b_3\ {}^0X^v + b_4\ {}^1X(T/K) + b_5\ {}^1X^v(T/K) + \frac{b_6}{(T/K)^2} \quad (2.17)$$

where b_0 to b_6 are the regression coefficients as analyzed by Rayer et al.[30] and are listed in Table 2.6. With respect to the experimental heat capacity, the percentage of relative deviations [57] of the predicted heat capacity, are listed in Table 2.15.

Table 2.5. The values of two cardinal numbers, δ (delta index) and δ^v (delta valence index).[30]

Group	δ	δ^v	Group	δ	δ^v	Group	δ	δ^v
$-CH_3$	1	1	**=C<**	3	4	**-OH**	1	5
$-CH_2-$	2	2	**$-NH_2$**	1	3	**-O-**	2	6
>CH-	3	3	**-NH-**	2	4	**=O**	1	6
>C<	4	4	**>N-**	3	5			
=CH-	2	3	**=N-**	2	5			

Table 2.6. Calculated values of b_i parameters for molecular connectivity analysis[30]

Parameters	Coefficients	Parameters	Coefficients
$\mathbf{b_0}$	-9.58	$\mathbf{b_4}$	-0.02
$\mathbf{b_1}$	-1.76	$\mathbf{b_5}$	0.17
$\mathbf{b_2}$	105.27	$\mathbf{b_6}$	0.09
$\mathbf{b_3}$	-61.04		

2.7. Results and discussion of molar heat capacity measurements

The experimental molar heat capacities of the aqueous 2-(Ethylamino)ethanol (EAE), 2-(Propylamino)ethanol (PAE), 2-(Butylamino)ethanol (BAE), 1-(2-Hydroxyethyl)piperidine (HEP), and Bis(2-methoxyethyl)amine (BMOEA) solutions were measured at eleven temperatures (303.15, 308.15, 313.15, 318.15, 323.15, 328.15, 333.15, 338.15, 343.15, 348.15, and 353.15K) for the complete range of mole fractions are given in Tables 6.1, 6.2, 6.3, 6.4, and 6.5 of the Appendix 6.1, respectively.

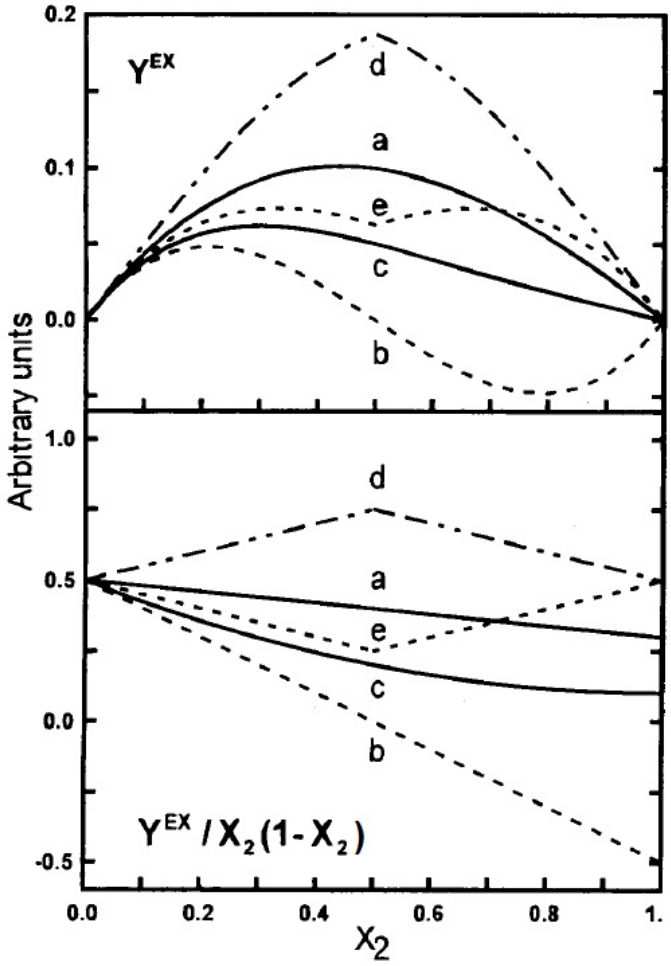

Figure 2.7. Typical trends for excess and reduced molar thermodynamic quantities of liquid mixtures[47]

a: similar size and polarity of mixtures of liquids

b: $(C_2^0 - C_2^*)$ has the opposite sign from $(C_1^0 - C_1^*)$

c: different size and polarity of mixtures of liquids

d: Complex formed between the two components

e: both $(C_2^0 - C_2^*)$ and $(C_1^0 - C_1^*)$ are positive

2.7.1. 2-(Ethylamino)ethanol (EAE)

The molar heat capacities of 2-(Ethylamino)ethanol (EAE) increased with increasing temperature, as presented in Figure 2.8. Data regarding pure EAE is shown in Table 2.12, and can be represented as a linear function of temperature ranging from 303.15 to 353.15K using Equation 2.18 as follows:

$$C_{P,EAE}/(J.mol^{-1}.K^{-1}) = 0.4425 \times T/(K) + 97.443 \qquad (2.18)$$

where $Cp_{,EAE}$ represents the molar heat capacity of pure 2-(Ethylamino)ethanol. The percentage of relative deviation (%RD)[57] between the experimental and calculated values was found to be 0.16%.

The molar excess heat capacity, Cp^E, was calculated from the measured molar heat capacity data using Equation 2.2 and correlated as a function of the mole fractions employing the Redlich-Kister expression[32]. The coefficients of this expression and percentages of relative deviation for 2-(Ethylamino)ethanol (1) + water (2) binary system are presented in Table 2.7 and the calculated molar excess heat capacity data are listed in Table 6.6 of the Appendix 6.1. Figure 2.9 represents how the molar excess heat capacities vary with EAE concentration in aqueous solution at several temperatures. The molar excess heat capacity curves were positive for the entire range of mole fractions with the maximum varying between x_1 = 0.1 and x_1 = 0.3. Furthermore, Cp^E values increased with increasing temperature for the whole range of mole fractions. The rapid variation in molar excess heat capacity was found in the water-rich region and not in the 2-(Ethylamino)ethanol -rich region. The shape of the curves resembles the shape of Case

c, as presented in Figure 2.7 which is the common situation observed with mixtures of liquids of different sizes and polarity, as described by Desnoyers and Perron.[47] The extrapolated excess partial molar quantities for EAE ($C_1^0 - C_1^*$) and water ($C_2^0 - C_2^*$) are given in Table 2.13.

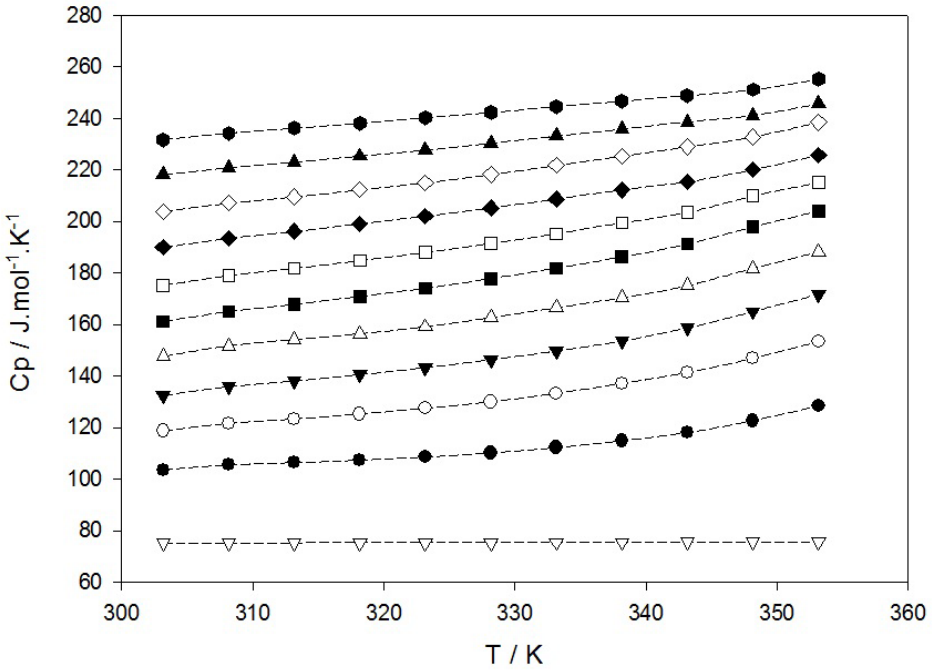

Figure 2.8. Molar heat capacity of aqueous 2-(Ethylamino)ethanol solutions at several mole fractions: ▽-,water; ●-, 0.1; O-, 0.2; ▼-, 0.3; △-, 0.4; ■-, 0.5; □-, 0.6; ◆-, 0.7; ◇-,0.8; ▲-, 0.9; ⬢-, EAE.

The reduced molar excess heat capacity of aqueous (Ethylamino)ethanol solutions at nine temperatures were also calculated, and plotted against the mole fractions which show the non-ideal behaviour, as presented in Figure 2.10. It is apparent that it decreases with an increase in the mole fraction of EAE, and increases with increasing temperature. It shows a sharp change in the region of lower mole fractions of amine and the minimum value occurs at x_1 = 0.9.

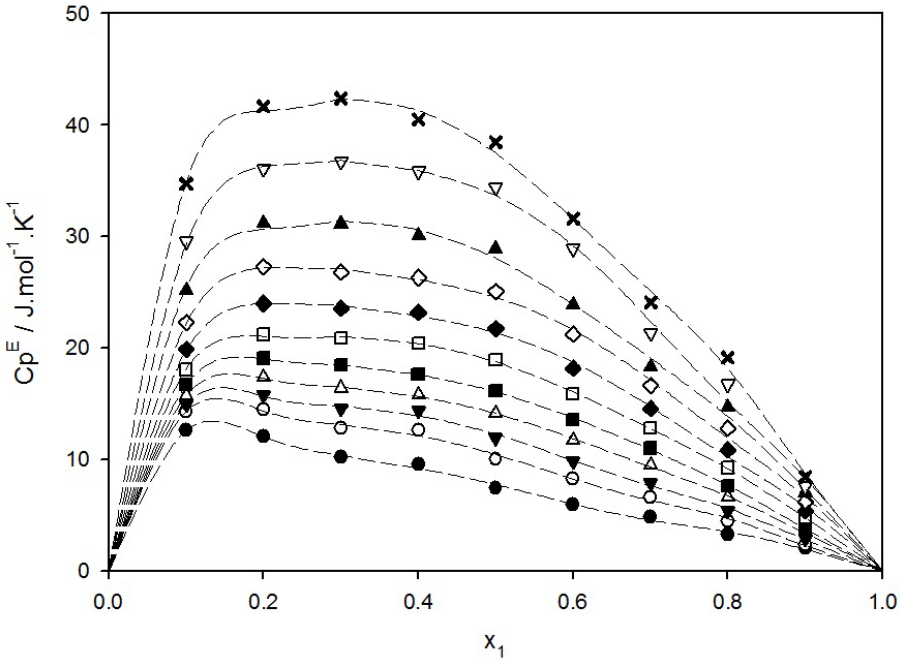

Figure 2.9. Molar excess heat capacity of aqueous 2-(Ethylamino)ethanol solutions at several temperatures: ●,303.15K; O, 308.15K; ▼, 313.15K; △, 318.15K; ■, 323.15K; □, 328.15K; ◆, 333.15K; ◇, 338.15K; ▲, 343.15K; ▽, 348.15K; ×, 353.15K and --, RK

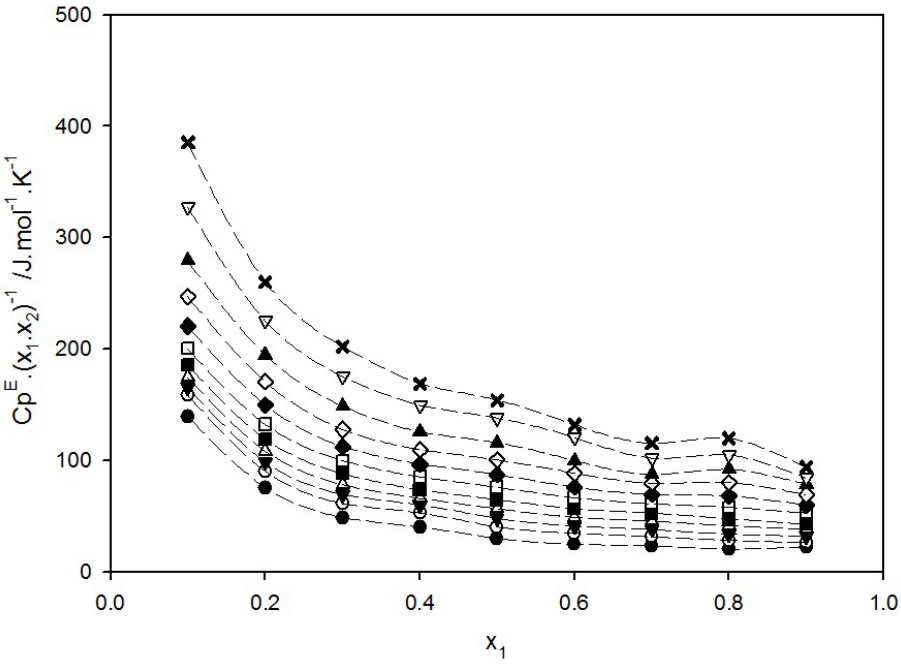

Figure 2.10. Reduced molar excess heat capacity of aqueous EAE solutions at several temperatures: ●-,303.15K; O-, 308.15K; ▼-, 313.15K; △-, 318.15K; ■-, 323.15K; □-, 328.15K; ◆-, 333.15K; ◇-, 338.15K; ▲-, 343.15K; ▽-, 348.15K and ×-, 353.15K

Table 2.7. Redlich-Kister coefficients for the molar excess heat capacity of aqueous solution of 2-(Ethylamino)ethanol at a temperature range of 303.15 to 353.15K

T /K	Redlich-Kister Coefficients						%RD
	a_0	a_1	a_2	a_3	a_4	a_5	
303.15	30.96	-33.77	12.65	12.47	101.17	-117.37	3.37
308.15	41.77	-41.22	12.40	27.51	103.22	-146.18	2.62
313.15	49.00	-42.53	11.74	21.26	102.67	-135.31	2.14
318.15	56.51	-38.74	16.75	-8.32	95.34	-101.50	0.96
323.15	64.29	-39.10	21.95	-25.18	86.92	-83.82	0.58
328.15	75.02	-44.44	19.32	-13.32	96.58	-96.21	0.53
333.15	85.58	-39.61	24.42	-89.28	98.46	---	2.45
338.15	98.26	-43.04	28.59	-101.03	106.95	---	2.59
343.15	112.32	-68.97	31.27	-4.54	121.51	-129.56	2.52
348.15	134.88	-64.92	16.20	-125.08	156.08	---	3.36
353.15	150.13	-102.88	41.95	46.40	161.25	-263.24	2.18

The shape of the curves resembles the shape of Case c, as shown in Figure 2.7. A case observed wherein mixtures of liquids of different sizes and polarity are mixed, as described by Desnoyers and Perron.[47]

2.7.2. 2-(Propylamino)ethanol (PAE)

The molar heat capacities of 2-(Propylamino)ethanol (PAE) increased with increasing temperature, as shown in Figure 2.11. Data of pure PAE, as shown in Table 2.12, can be represented as a linear function of temperature ranging from 303.15 to 353.15K using Equation 2.19 as follows:

$$C_{P,PAE}/(J \cdot mol^{-1} \cdot K^{-1}) = 0.4533 \times T/(K) + 127.08 \qquad (2.19)$$

where $Cp_{,PAE}$ represents the molar heat capacity of pure 2-(Propylamino)ethanol. The percentage of relative deviation (%RD)[57] between the experimental and calculated values is found to be 0.17%.

The molar excess heat capacity, Cp^E, was calculated from the measured molar heat capacity data using Equation 2.2 and correlated as a function of the mole fractions employing the Redlich-Kister expression.[32] The coefficients of this expression and percentages of relative deviation for 2-(Propylamino)ethanol (1) + water (2) binary system are listed in Table 2.8 and the calculated molar excess heat capacity data are listed in Table 6.7 of the Appendix 6.1. Figure 2.12 represents how the molar excess heat capacities vary with the concentration of 2-(Propylamino)ethanol in aqueous solution at several temperatures. Molar excess heat capacity curves were positive for the entire range of mole fractions with the maximum varying between x_1 = 0.2 and x_1 = 0.4. In addition, Cp^E values increased with increasing temperature for the whole range of mole fractions. The rapid variation in molar excess heat capacity was found in the water-rich region rather than in the 2-(Propylamino)ethanol-rich region and the shape

of the curves resembles the shape of Case c in Figure 2.7, a case of observed mixtures of liquids of different sizes and polarity, as described by Desnoyers and Perron.[47] The extrapolated excess partial molar quantities for PAE ($C_1^0 - C_1^*$) and water ($C_2^0 - C_2^*$) are given in Table 2.13.

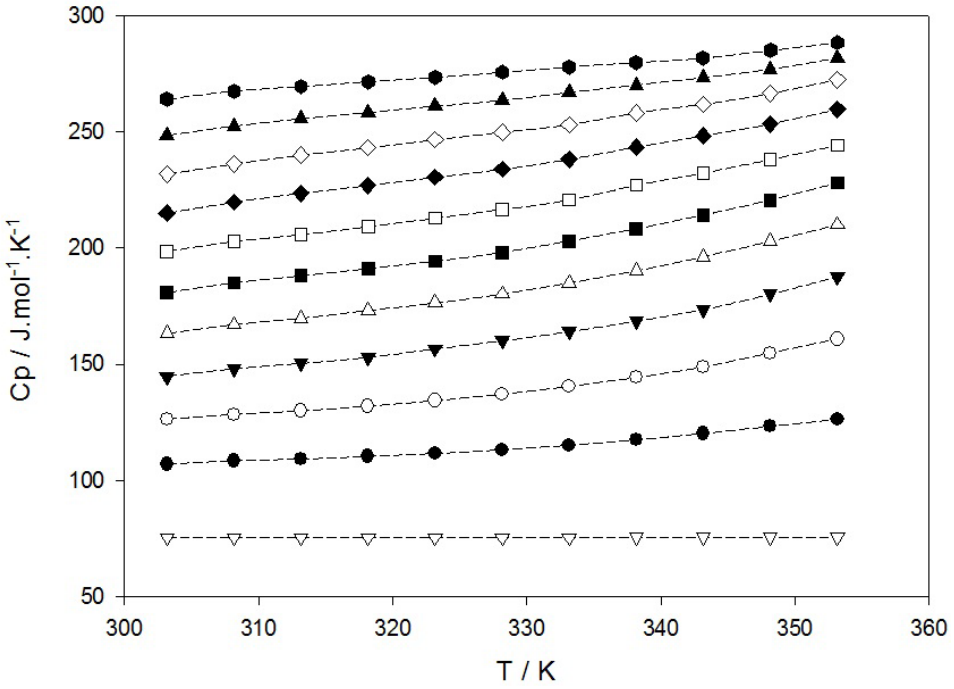

Figure 2.11. Molar heat capacity of aqueous 2-(Propylamino)ethanol solutions at several mole fractions: ▽-,water; ●-, 0.1; O-, 0.2; ▼-, 0.3; △-, 0.4; ■-, 0.5; □-, 0.6; ◆-, 0.7; ◇-,0.8; ▲-, 0.9; ⬢-, PAE.

Reduced molar excess heat capacity of aqueous PAE solutions at several temperatures were also calculated, and plotted against the mole fractions showing non-ideal behaviour as presented in Figure 2.13. It also shows a sharp change in the water-rich region and the minimum value occurring at x_1 = 0.9. The shape of the curves resembles that of Case c, as shown in Figure 2.7. It is the case observed with mixtures of liquids of different sizes and polarity, as described by Desnoyers and Perron.[47]

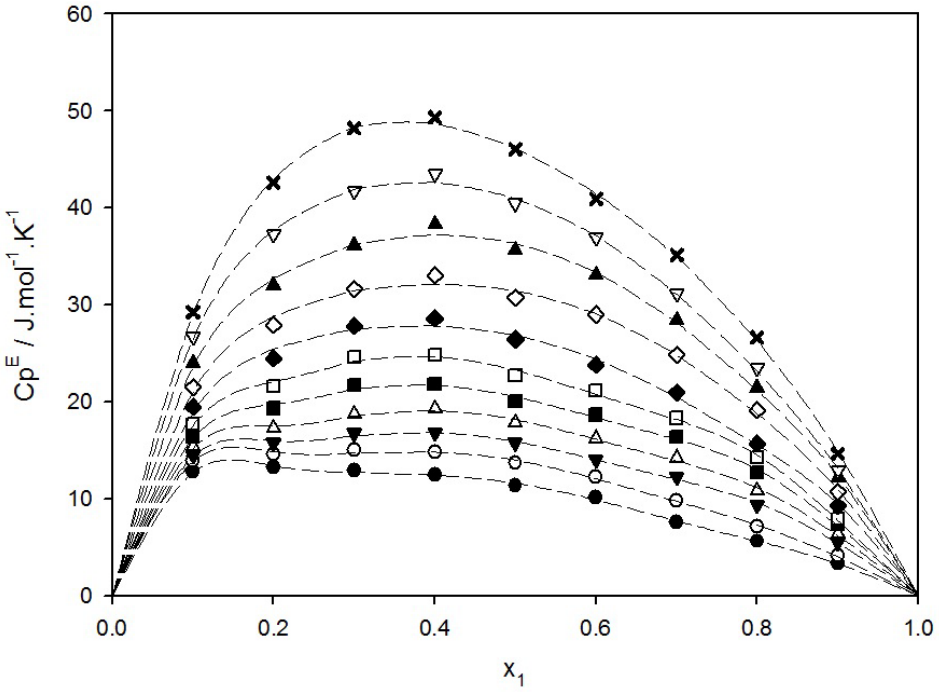

Figure 2.12. Molar excess heat capacity of aqueous PAE solutions at several temperatures: ●,303.15K; O, 308.15K; ▼, 313.15K; △, 318.15K; ■, 323.15K; □, 328.15K; ◆, 333.15K; ◇, 338.15K; ▲, 343.15K; ▽, 348.15K; ×, 353.15K and --, RK

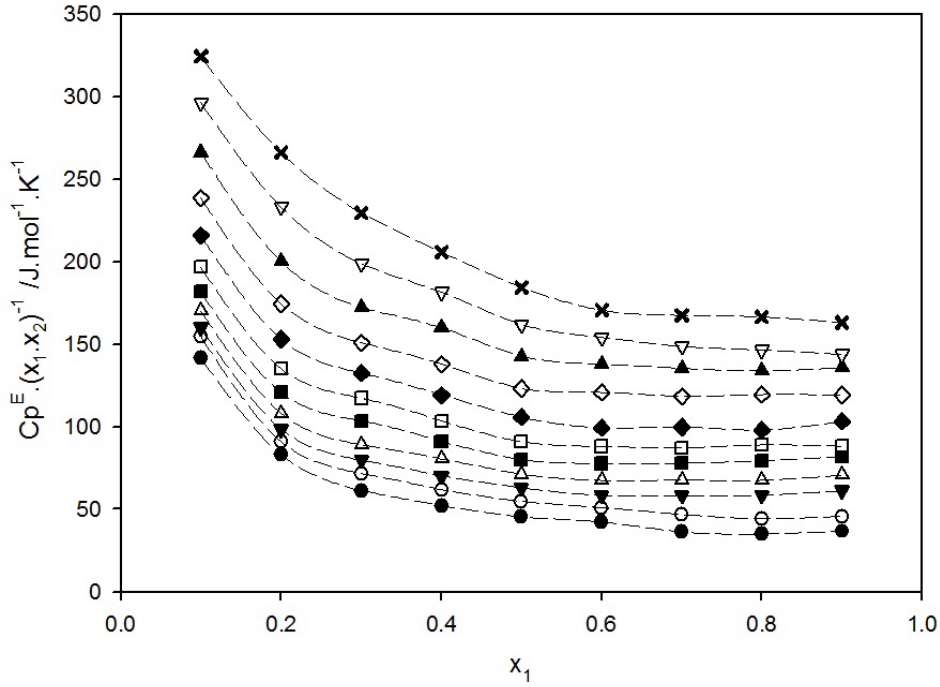

Figure 2.13. Reduced molar excess heat capacity of aqueous PAE solutions at several temperatures: ●-,303.15K; O-, 308.15K; ▼-, 313.15K; △-, 318.15K; ■-, 323.15K; □-, 328.15K; ◆-, 333.15K; ◇-, 338.15K; ▲-, 343.15K; ▽-, 348.15K and ×-, 353.15K

Table 2.8. Redlich-Kister coefficients for the molar excess heat capacity of aqueous solution of 2-(Propylamino)ethanol at a temperature range of 303.15 to 353.15K

T /K	Redlich Kister Coefficients						%RD
	a_0	a_1	a_2	a_3	a_4	a_5	
303.15	46.35	-25.97	-2.26	-13.47	107.39	-75.46	1.11
308.15	55.85	-28.98	-2.37	12.05	109.36	-114.02	1.60
313.15	63.61	-30.60	11.26	46.56	94.82	-149.09	1.25
318.15	72.63	-32.71	14.02	56.44	91.66	-160.99	1.53
323.15	82.08	-36.89	33.45	63.38	64.73	-161.01	1.80
328.15	92.99	-43.24	40.13	74.00	53.76	-174.86	1.57
333.15	107.39	-34.35	30.57	-47.71	74.74	---	2.22
338.15	125.84	-30.06	40.97	-60.88	62.08	---	1.77
343.15	145.39	-38.57	37.53	-59.55	73.78	---	1.54
348.15	163.89	-55.36	54.60	-56.62	50.65	---	1.10
353.15	184.54	-74.16	84.37	-35.30	12.25	---	0.98

2.7.3.2-(Butylamino)ethanol (BAE)

Molar heat capacities of 2-(Butylamino)ethanol (BAE) increased with increasing temperature, as given in Figure 2.14. The data for pure BAE is shown in Table 2.12, and can be represented as a linear function of temperature ranging from 303.15 to 353.15K using Equation 2.20 as follows:

$$C_{P,BAE}/(J \cdot mol^{-1} \cdot K^{-1}) = 0.5916 \times T/(K) + 112.13 \qquad (2.20)$$

where $Cp_{,BAE}$ represents the molar heat capacity of pure 2-(Butylamino)ethanol. The percentage of relative deviation (%RD)[57] between the experimental and calculated values is found to be 0.47%.

The molar excess heat capacity, Cp^E, was calculated from the measured molar heat capacity data using Equation 2.2 and correlated as a function of the mole fractions employing the Redlich-Kister expression.[32] The coefficients of this expression and percentages of relative deviation for 2-(Butylamino)ethanol (1) + water (2) binary system are given in Table 2.9 and the calculated molar excess heat capacity data are listed in Table 6.8 of the Appendix 6.1. Figure 2.15 represents how the molar excess heat capacities vary with a concentration of BAE in aqueous solution at several temperatures. The molar excess heat capacity curves were positive for the entire range of mole fractions with a maximum of around x_1 = 0.3. Moreover, Cp^E values increased with increasing temperature for the whole range of mole fractions. The rapid variation in molar excess heat capacity is found in the water-rich region rather than in the 2-(Butylamino)ethanol-rich region. The shape of the curves resembles Case c, as

presented in Figure 2.7. The case is observed with mixtures of liquids of different sizes and polarity, as described by Desnoyers and Perron[47] The extrapolated excess partial molar quantities for BAE ($C_1^0 - C_1^*$) and water ($C_2^0 - C_2^*$) are given in Table 2.13.

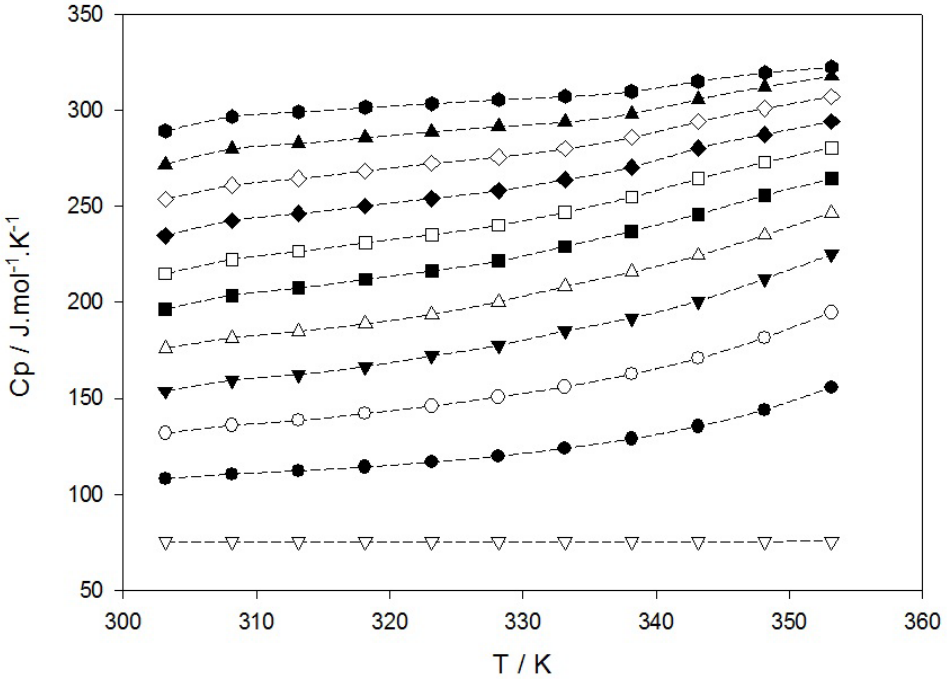

Figure 2.14. Molar heat capacity of aqueous 2-(Butylamino)ethanol solutions at several mole fractions: ▽-,water; ●-, 0.1; O-, 0.2; ▼-, 0.3; △-, 0.4; ■-, 0.5; □-, 0.6; ◆-, 0.7; ◇-,0.8; ▲-, 0.9; ⬢-, BAE.

Reduced molar excess heat capacity of aqueous solutions of 2-(Butylamino)ethanol and water, at nine temperatures, were also calculated, and plotted against its mole fractions which show the non-ideal behaviour, as presented in Figure 2.16. It shows a sharp change in the region of lower mole fractions of amine and a minimum value occurring at x_1 = 0.9. The shape of the curves resembles the shape of Case c, as shown in Figure 2.7, as observed with mixtures of liquids of different sizes and polarity, and described by Desnoyers and Perron.[47]

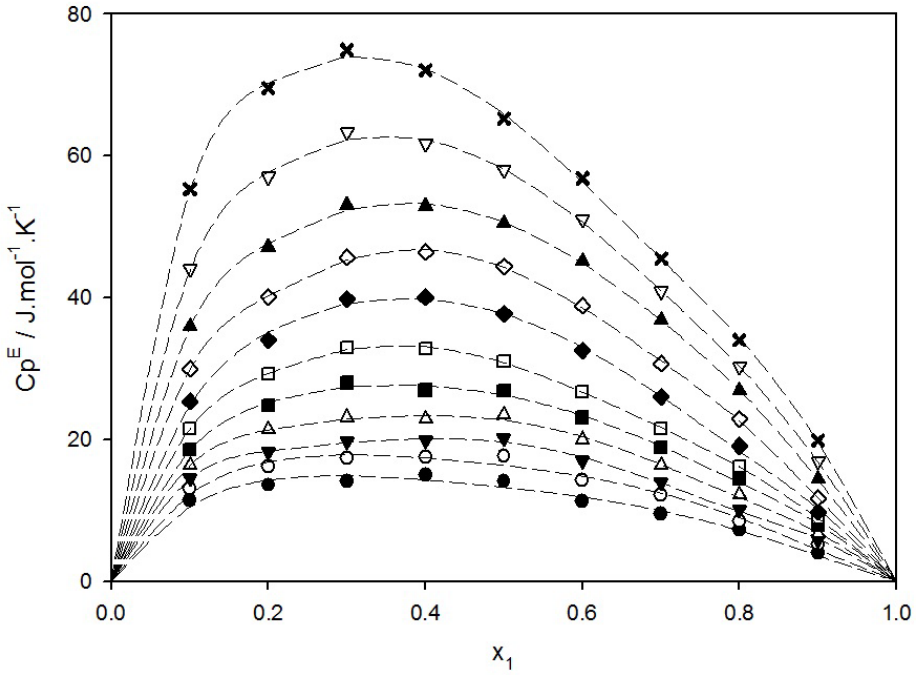

Figure 2.15. Molar excess heat capacity of aqueous 2-(Butylamino)ethanol solutions at several temperatures: ●,303.15K; O, 308.15K; ▼, 313.15K; △, 318.15K; ■, 323.15K; □, 328.15K; ◆, 333.15K; ◇, 338.15K; ▲, 343.15K; ▽, 348.15K; ×, 353.15K and --, RK

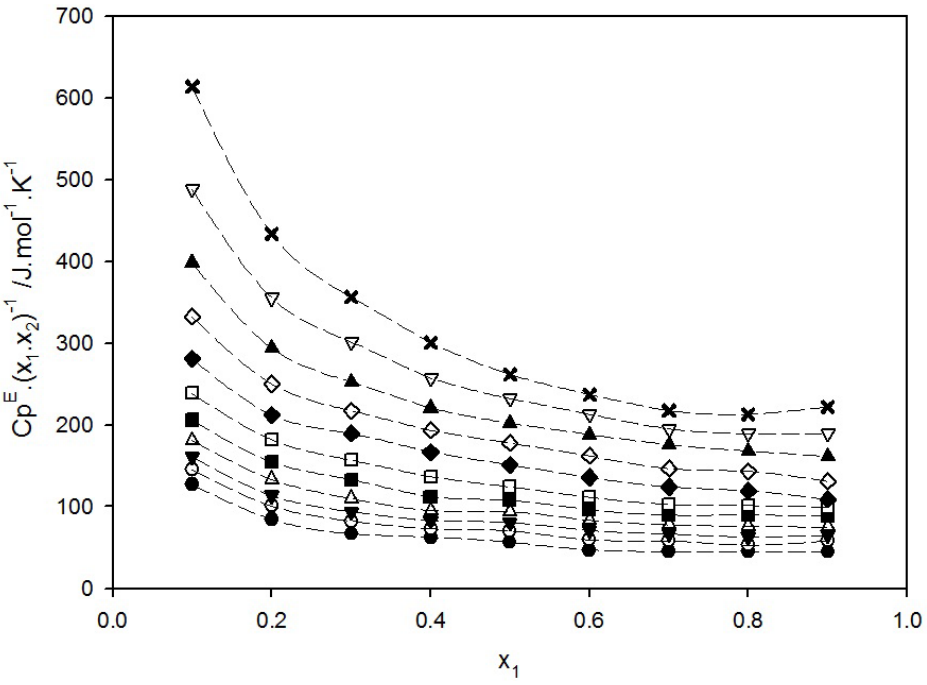

Figure 2.16. Reduced molar excess heat capacity of aqueous 2-(Butylamino)ethanol solutions at several temperatures: ●-,303.15K; O-, 308.15K; ▼-, 313.15K; △-, 318.15K; ■-, 323.15K; □-, 328.15K; ◆-, 333.15K; ◇-, 338.15K; ▲-, 343.15K; ▽-, 348.15K and ×-, 353.15K

Table 2.9. Redlich-Kister coefficients for the molar excess heat capacity of aqueous solution of 2-(Butylamino)ethanol at a temperature range of 303.15 to 353.15K

T /K	Redlich Kister Coefficients						%RD
	a_0	a_1	a_2	a_3	a_4	a_5	
303.15	52.97	-23.75	39.11	-36.47	---	---	1.42
308.15	65.36	-25.52	42.08	-43.13	---	---	1.89
313.15	78.55	-25.69	-8.54	-51.13	98.45	---	1.54
318.15	90.92	-29.12	4.19	-56.50	86.35	---	1.59
323.15	105.02	-42.14	25.26	-45.01	63.43	---	1.96
328.15	123.38	-68.05	26.57	34.98	69.46	-100.32	0.50
333.15	150.95	-69.56	16.05	-47.76	80.14	---	1.98
338.15	177.20	-88.01	12.34	51.68	114.50	-171.12	0.71
343.15	202.71	-87.75	41.80	-3.91	119.96	-139.74	0.66
348.15	232.73	-121.70	59.10	-2.65	162.84	-152.70	0.72
353.15	263.79	-168.26	96.95	33.30	218.47	-237.65	0.76

2.7.4. 1-(2-Hydroxyethyl)piperidine (HEP)

Molar heat capacity 1-(2-Hydroxyethyl)piperidine (HEP) values increase with increasing temperature, as shown in Figure 2.17. Data of pure HEP is presented in Table 2.12, and can be represented as a linear function of temperature ranging from 303.15 to 353.15K using Equation 2.21 as follows:

$$C_{P,HEP}/(J \cdot mol^{-1} \cdot K^{-1}) = 0.6127 \times T/(K) + 88.005 \qquad (2.21)$$

where $Cp_{,HEP}$ represents the molar heat capacity of pure 1-(2-Hydroxyethyl)piperidine. The percentage of relative deviation (%RD)[57] between the experimental and calculated values is found to be 0.30%.

Molar excess heat capacity, Cp^E, was calculated from the measured molar heat capacity data using Equation 2.2 and correlated as a function of the mole fractions employing the Redlich-Kister expression.[32] The coefficients of this expression and percentages of relative deviation for 1-(2-Hydroxyethyl)piperidine (1) + water (2) binary system are presented in Table 2.10 and the calculated molar excess heat capacity data are presented in Table 6.9 of the Appendix 6.1. Figure 2.17 represents how the molar excess heat capacities vary with HEP concentration at several temperatures. The molar excess heat capacity curves were positive for the entire range of mole fractions with the maximum varying between x_1 = 0.3 and x_1 = 0.5. In addition, Cp^E values increased with increasing temperature for the whole range of mole fractions. The rapid variation in molar excess heat capacity was found in the water-rich region rather than in the 1-(2-Hydroxyethyl)piperidine-rich region and the shape of the curves resemble the shape of

Case c is presented in Figure 2.7 which is the common situation observed with mixtures of liquids of different sizes and polarity, a is described by Desnoyers and Perron.[47] The extrapolated excess partial molar quantities for HEP ($C_1^0 - C_1^*$) and water ($C_2^0 - C_2^*$) are given in Table 2.13.

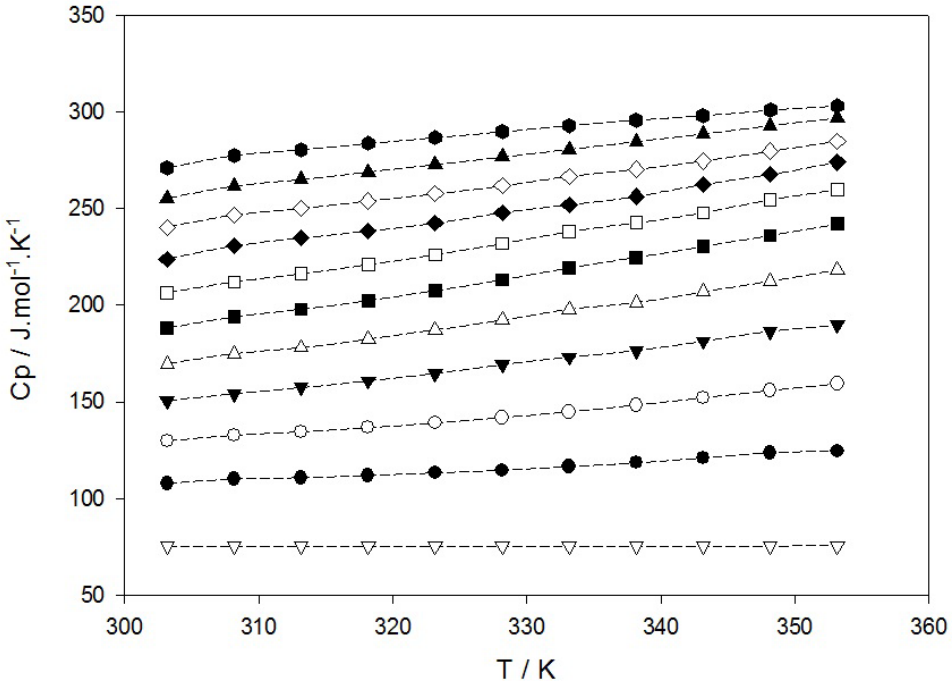

Figure 2.17. Molar heat capacity of aqueous 1-(2-Hydroxyethyl)piperidine solutions at several mole fractions: ▽-,water; ●-, 0.1; O-, 0.2; ▼-, 0.3; △-, 0.4; ■-, 0.5; □-, 0.6; ◆-, 0.7; ◇-,0.8; ▲-, 0.9; ⬢-, HEP

The reduced molar excess heat capacity of aqueous mixtures of 1-(2-Hydroxyethyl)piperidine and water, at several temperatures ranging from 303.15 to 353.15K, were also calculated, and plotted against the mole fractions which show the non-ideal behaviour, as presented in Figure 2.19. It shows the sharp change in the water-rich region and the lower value occurring at x_1 = 0.9. The shape of the curves resemble the shape of Case c is shown in Figure 2.7 which is the common situation.

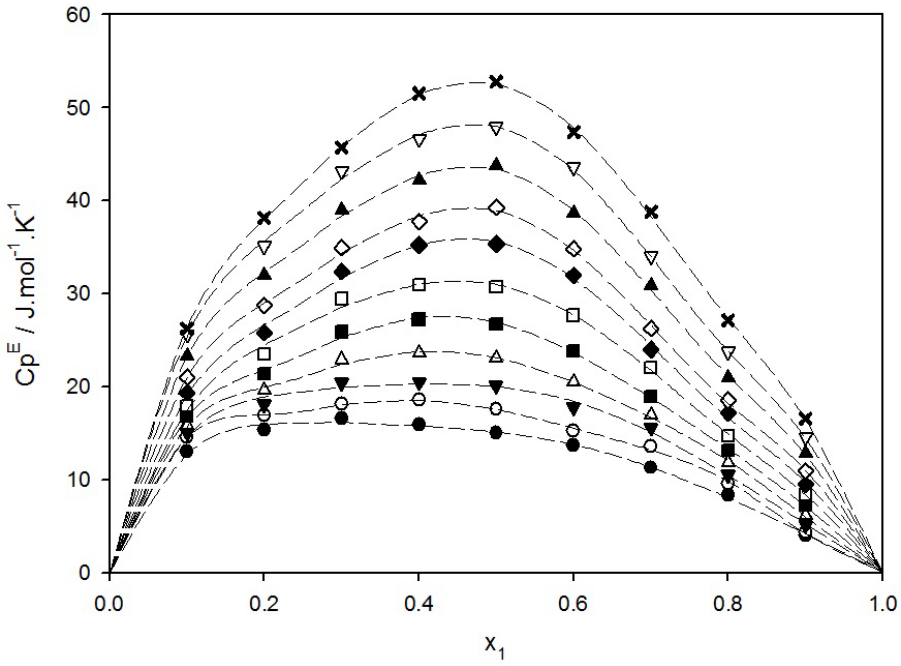

Figure 2.18. Molar excess heat capacity of aqueous 1-(2-Hydroxyethyl)piperidine solutions at several temperatures: ●,303.15K; O, 308.15K; ▼, 313.15K; △, 318.15K; ■, 323.15K; □, 328.15K; ◆, 333.15K; ◇, 338.15K; ▲, 343.15K; ▽, 348.15K; ×, 353.15K and --, Redlish Kister

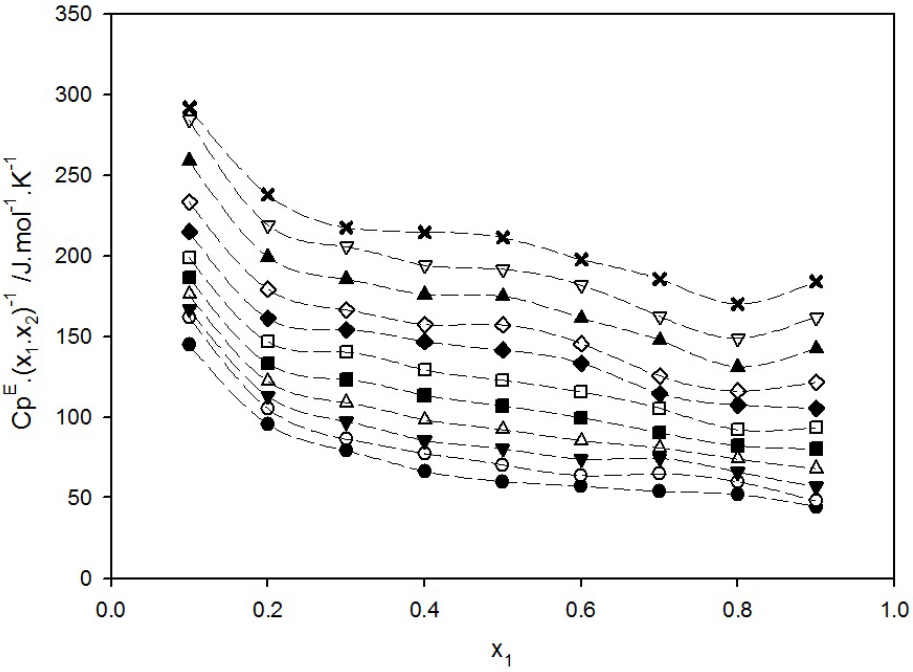

Figure 2.19. Reduced molar excess heat capacity of aqueous HEP solutions at several temperatures: ●-, 303.15K; O-, 308.15K; ▼-, 313.15K; △-, 318.15K; ■-, 323.15K; □-, 328.15K; ◆-, 333.15K; ◇-, 338.15K; ▲-, 343.15K; ▽-, 348.15K and ×-, 353.15K

Table 2.10. Redlich-Kister coefficients for the molar excess heat capacity of aqueous solution of 1-(2-Hydroxyethyl)piperidine at a temperature range of 303.15 to 353.15K

T /K	Redlich Kister Coefficients						%RD
	a_0	a_1	a_2	a_3	a_4	a_5	
303.15	60.48	-18.34	25.56	-63.40	41.21	---	2.30
308.15	70.15	-32.42	18.63	49.80	53.77	-173.16	1.27
313.15	80.04	-16.63	14.18	-75.06	51.53	---	2.39
318.15	92.41	-34.99	-7.98	27.76	80.99	-122.17	1.29
323.15	107.73	-39.67	-34.67	26.61	112.78	-105.66	1.31
328.15	124.06	-32.29	-44.74	-47.96	117.23	---	1.63
333.15	142.49	-35.22	-79.88	-44.99	166.10	---	1.84
338.15	155.80	-35.88	-95.54	-59.22	202.36	12.42	1.10
343.15	173.63	-35.91	-91.39	-64.00	205.39	10.53	1.07
348.15	191.96	-35.76	-96.00	-82.30	221.98	31.69	0.84
353.15	210.32	-33.64	-91.78	-64.95	209.96	17.43	0.55

observed with mixtures of liquids of different sizes and polarity, as described by Desnoyers and Perron.[47]

2.7.5. Bis(2-methoxyethyl)amine (BMOEA)

The molar heat capacities of Bis(2-methoxyethyl)amine (BMOEA) increased with increasing temperature, as shown in Figure 2.20. Data of pure BMOEA is presented in Table 2.12, and can be represented as a linear function of the temperature ranging from 303.15 to 353.15K, using Equation 2.22 as follows:

$$C_{P,BMOEA}/(J \cdot mol^{-1} \cdot K^{-1}) = 0.5133 \times T/(K) + 138.22 \qquad (2.22)$$

where $Cp_{,BMOEA}$ represents the molar heat capacity of pure Bis(2-methoxyethyl)amine. The percentage of relative deviation (%RD)[57] between the experimental and calculated values was found to be 0.60%.

The molar excess heat capacity, Cp^E, was calculated from the measured molar heat capacity data using Equation 2.2 and correlated as a function of the mole fractions employing the Redlich-Kister expression.[32] The coefficients of this expression and percentages of relative deviation for the BMOEA (1) + water (2) binary system are listed in Table 2.11 and the calculated molar excess heat capacity data are given in Table 6.10 of the Appendix 6.1. Figure 2.21 represents how the molar excess heat capacities vary with the concentration of Bis(2-methoxyethyl)amine at several temperatures. The molar excess heat capacity curves were positive for the entire range of mole fractions with the maximum occurring around x_1 = 0.4. Cp^E values increased with increasing temperature for the whole range of mole fractions. The rapid variation in molar excess heat capacity was found in the water-rich region rather than in the Bis(2-methoxyethyl)amine-rich region. The shape of the curves resembles the shape of Case c, as represented in Figure

2.7, which is the common situation observed with mixtures of liquids of different sizes and polarity (Desnoyers and Perron[47]) . The extrapolated excess partial molar quantities for BMOEA ($C_1^0 - C_1^*$) and water ($C_2^0 - C_2^*$) are given in Table 2.13.

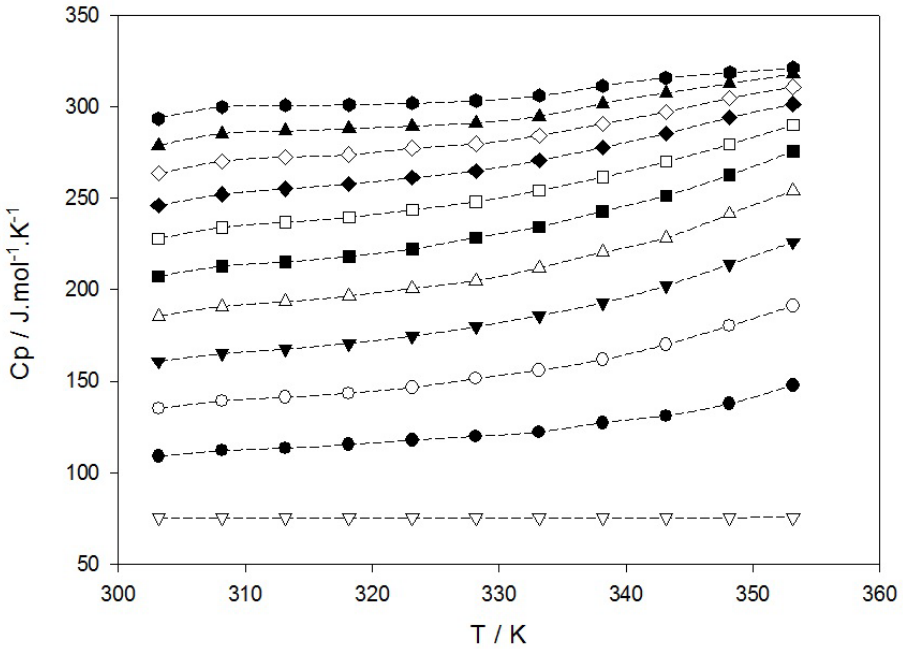

Figure 2.20. Molar heat capacity of aqueous Bis(2-methoxyethyl)amine solutions at several mole fractions: ▽-,water; ●-, 0.1; O-, 0.2; ▼-, 0.3; △-, 0.4; ■-, 0.5; □-, 0.6; ◆-, 0.7; ◇-,0.8; ▲-, 0.9; ⬢-, BMOEA

The reduced molar excess heat capacity of aqueous solution of Bis(2-methoxyethyl)amine at nine temperatures was also calculated and plotted against their mole fractions showing the non-ideal behaviour, as presented in Figure 2.22. Reduced molar excess heat capacity increases with increasing temperature and decreases with each increment in mole fraction of BMOEA. Moreover, the figure shows the sharp change in the water-rich region and the minimum value occurring at x_1 = 0.9.

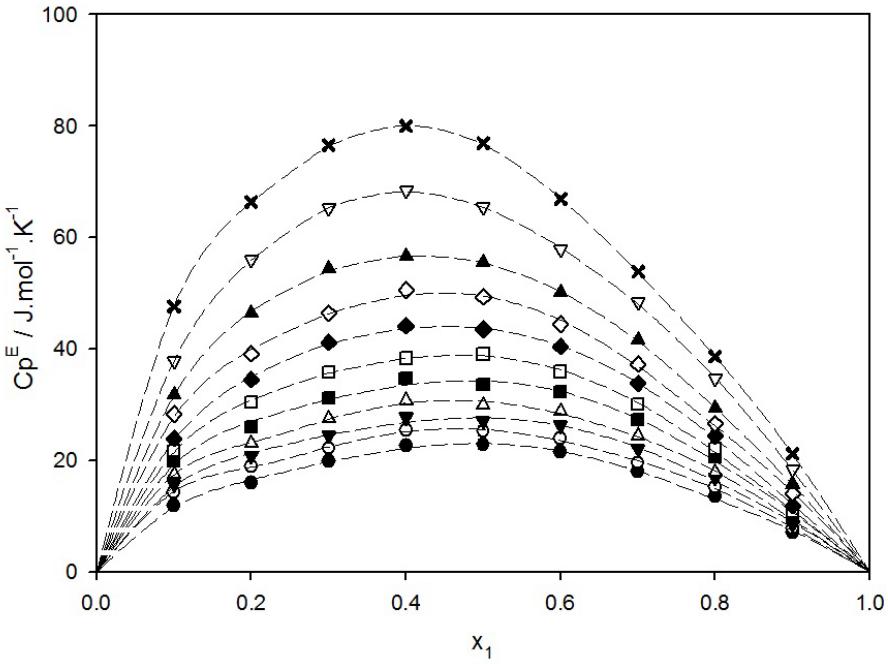

Figure 2.21. Molar excess heat capacity of aqueous Bis(2-methoxyethyl)amine solutions at several temperatures: ●,303.15K; O, 308.15K; ▼, 313.15K; △, 318.15K; ■, 323.15K; □, 328.15K; ◆, 333.15K; ◇, 338.15K; ▲, 343.15K; ▽, 348.15K; ×, 353.15K and --, Redlish Kister

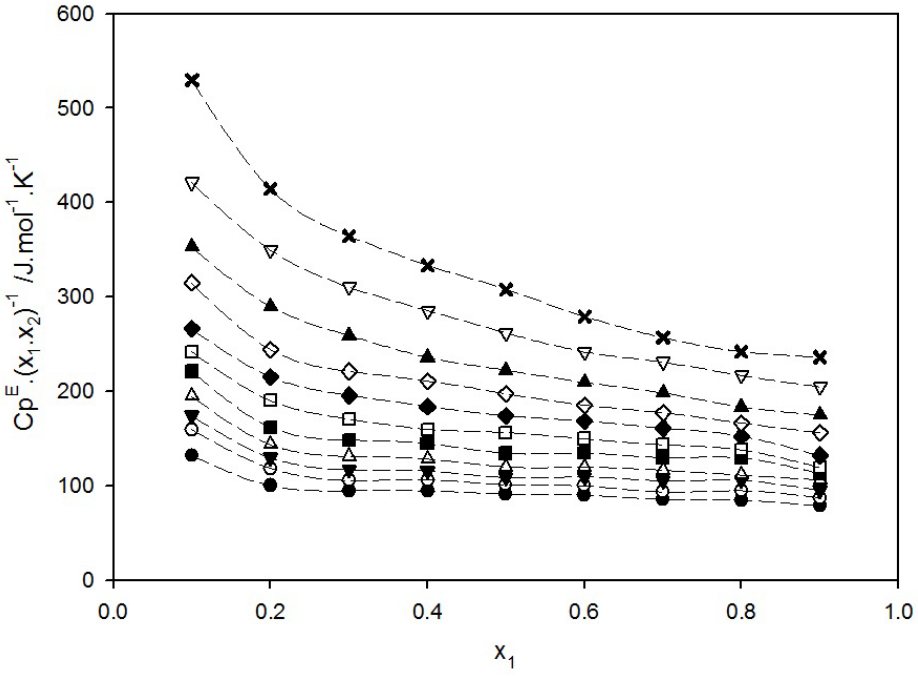

Figure 2.22. Reduced molar excess heat capacity of aqueous BMOEA solutions at several temperatures: ●-,303.15K; O-, 308.15K; ▼-, 313.15K; △-, 318.15K; ■-, 323.15K; □-, 328.15K; ◆-, 333.15K; ◇-, 338.15K; ▲-, 343.15K; ▽-, 348.15K and ×-, 353.15K

Table 2.11. Redlich-Kister coefficients for the molar excess heat capacity of aqueous solution of Bis(2-methoxyethyl)amine at a temperature range of 303.15 to 353.15K

T /K	Redlich Kister Coefficients						%RD
	a_0	a_1	a_2	a_3	a_4	a_5	
303.15	92.17	-3.71	-24.05	-39.24	68.84	---	2.09
308.15	102.24	-18.35	-23.82	42.92	90.20	-131.67	1.19
313.15	110.67	-3.29	-3.99	-63.17	64.07	---	2.25
318.15	122.58	-21.11	-11.41	34.63	81.81	-138.14	1.26
323.15	137.21	-8.45	1.16	-78.60	68.54	---	2.67
328.15	155.11	-18.02	1.93	-84.76	59.81	---	1.24
333.15	175.03	-29.19	13.02	-78.43	36.86	---	1.09
338.15	198.33	-44.05	-19.90	-75.80	118.88	---	1.47
343.15	222.15	-63.36	20.65	-73.64	66.55	---	0.43
348.15	262.02	-105.68	39.12	37.63	61.22	-132.44	0.37
353.15	307.22	-138.01	-15.61	53.52	208.19	-194.31	0.16

The shape of the curves resembles the shape of Case c, as shown in Figure 2.7, which corresponds to the common situation observed with mixtures of liquids of different sizes and polarity, as described by Desnoyers and Perron.[47]

2.8.Comparison of the heat capacity data of alkanolamines

The changes in the measured heat capacities of the five studied alkanolamines, as a function of temperature, are shown in Figure 2.23. Among the five alkanolamines, BMOEA and BAE, both being very close to each other, exhibited the maximum values of the heat capacity, whereas EAE had the minimum values of Cp. The experimental data of the heat capacity of the selected alkanolamines, in the temperature range of 303.15 to 353.15K, are listed in Table 5.9.

A comparison is made of the heat capacity data of alkylaminoethanol such as EAE, PAE and BAE, which share same aminoethanol group. Heat capacities of alkylaminoethanol increased with an increase in the size of the carbon chain. In addition to this contribution, alkyl- group increased with increasing temperature. Figure 2.24 shows the manner in which the alkyl- group is attached to the aminoethanol which influences the heat capacity of the resulting alkylaminoethanol. The order of the heat capacity of alkylaminoethanol is:

BAE>PAE>EAE>MAE>MEA

or Butyl>Proply>Ethyl>Methyl (2.23)

Figure 2.23 represents the heat capacities, showing that HEP is lower than BAE but higher than those of PAE and EAE. Note, all have an aminoethanol group. HEP is a cyclic alkylaminoethanol with a tertiary amine; whereas, BAE is a straight-alkylaminoethanol with a secondary amine. 2,3-Dimethyl aminoethanol (DMAE)[40] and 2-Ethylaminoethanol (EAE) have the same molecular formula ($C_4H_{11}NO$) although DMAE

has a lower heat capacity than EAE. The reason for this is DMAE is a tertiary amine; whereas, EAE is a secondary amine, as shown in Figure 2.25. Methylaminoethanol (MAE)[40] and 3-Amino-1-Propanol (AP)[40] are both isomers and their molecular formula is C_3H_9NO. MAE (secondary amine) has a lower molar heat capacity than AP (primary amine), as shown in Figure 2.25. The order of the Cp of amine is therefore:

$$1^{o} \text{ amine} > 2^{o} \text{ amine} > 3^{o} \text{ amine} \qquad (2.24)$$

Considering the molecular structures of Diethanolamine (DEA)[30], Methyldiethanolamine (MDEA)[30], Ethyldiethanolamine (EDEA)[30] and N-Butyldiethanolamine (N-BDEA),[30] are alkanolamines which are tertiary amines except DEA (secondary amine). In all tertiary amines, the heat capacity increased as the size of the alkyl chain increased. N-BDEA (butyl group) had the highest heat capacity; whereas, the MDEA (methyl group) had the lowest Cp values, as confirmed by Equation 2.23. Similarly, if the last hydrogen of an amine group of DEA is substituted by a methyl group to form MDEA, a small increase in the value of the molar heat capacity occurs. When amine changed its condition from secondary amine to tertiary amine, Cp values decreased and the addition of one methyl group to the amine group increased the Cp values. Thus, the net result is a small increase in Cp values occurs, as shown in Figure 2.26 which is confirmed by Equations 2.23 and 2.24. To obtain further details regarding the contribution of each group, please refer to the different groups' contributions in the Group Additivity Analysis, as presented in Table 2.4.

When taking into consideration the molecular structures of Diethanolamine (DEA) and Bis(2-methoxyethyl)amine (BMOEA), if each hydrogen of the hydroxyl (–OH) group of DEA was substituted with a methyl ($–CH_3$) group, the result of this substitution would be that the heat capacities of BMOEA would increase due to an addition of the two methyl groups, as represented in Figure 2.25.

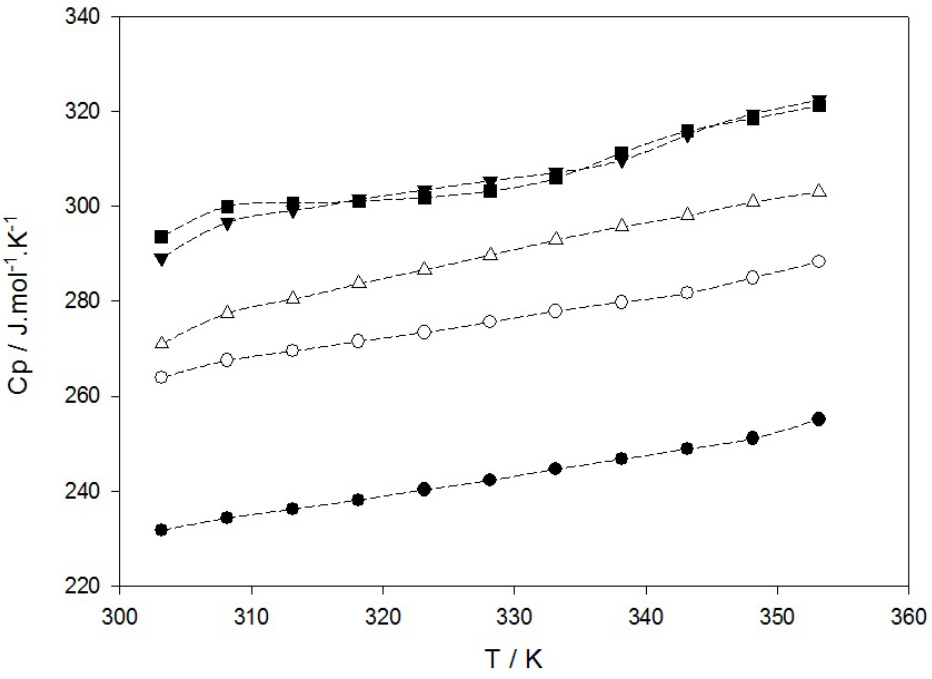

Figure 2.23. Comparison of measured heat capacities of the five selected pure alkanolamines as a function of temperature: ●-, EAE; O-, PAE; ▼-, BAE; △-, HEP; ■-, BMOEA

In general, $(C_1^0 - C_1^*)$ values increased with increasing temperature for all the studied amines, as listed in Table 2.13. In conducting a comparison of EAE, PAE and BAE, large positive values of $(C_2^0 - C_2^*)$ show there is a strengthening in the normal hydrophobic hydration of the alkyl chain. The increase in the positive values, with respect to temperature shows there is a stronger tendency for the structural entities to collapse.[47]

Table 2.12. Experimental heat capacities of the five selected pure alkanolamines

T /K	Heat Capacity Cp / J·mol^{-1}·K^{-1}				
	EAE	**PAE**	**BAE**	**HEP**	**BMOEA**
303.15	231.7	263.9	289.2	271.0	293.6
308.15	234.3	267.5	296.6	277.5	300.0
313.15	236.2	269.5	299.1	280.5	300.7
318.15	238.1	271.5	301.5	283.7	301.1
323.15	240.3	273.4	303.5	286.6	301.9
328.15	242.2	275.6	305.4	289.7	303.2
333.15	244.6	277.9	307.1	292.9	305.9
338.15	246.7	279.8	309.7	295.7	311.3
343.15	248.9	281.7	315.0	298.0	315.8
348.15	251.1	285.0	319.4	300.9	318.5
353.15	255.1	288.3	322.4	303.0	321.2

The experimental and predicted data of the heat capacity of pure alkanolamines and their percentages of relative deviation (%RD) for the Group Additivity Analysis (GAA), and the Molecular Connectivity Analysis (MCA) are listed in Tables 2.14 and 2.15, respectively. Percentages of relative deviations, for all predicted heat capacity data with the GAA method, were found to be within 0.6%, except HEP (1.83%), due to its cyclic nature. This method could not distinguish between straight -CH_2- and cyclic -CH_2-. On the other hand, percentages of relative deviation of all predicted heat capacity data for MCA were found to be around 2.64%.

Table 2.13. Extrapolated excess partial molar quantities for alkanolamines ($C_1^0 - C_1^*$) and water ($C_2^0 - C_2^*$)

T /K	EAE + H_2O		PAE+ H_2O		BAE+ H_2O		HEP + H_2O		BMOEA+H_2O	
	C_1-C_1^*	C_2-C_2^*	C_1-C_1^*	C_2-C_2^*	C_1-C_1^*	C_2-C_2^*	C_1-C_1^*	C_2-C_2^*	C_1-C_1^*	C_2-C_2^*
303.15	283.5	6.1	266.4	36.6	245.4	25.7	209.0	45.5	179.9	94.0
308.15	317.3	-2.5	293.8	31.9	223.2	85.7	298.3	-13.2	275.7	61.5
313.15	320.0	6.8	302.8	36.6	245.3	91.6	237.4	54.1	237.2	104.3
318.15	317.2	20.0	315.6	41.1	267.1	95.8	294.8	36.0	317.6	68.4
323.15	321.3	25.1	314.8	45.7	280.9	106.6	304.6	67.1	294.0	119.9
328.15	344.9	37.0	331.0	42.8	352.8	86.0	276.8	116.3	319.6	114.1
333.15	337.4	79.6	294.8	130.6	364.5	129.8	308.9	148.5	332.5	117.3
338.15	377.9	89.7	319.8	137.9	511.5	96.6	345.3	179.9	417.2	177.5
343.15	468.2	62.0	354.8	158.6	595.9	133.1	377.0	198.3	446.3	172.3
348.15	497.2	117.2	381.1	157.2	731.7	177.6	404.3	231.6	562.9	161.9
353.15	673.1	33.6	390.6	171.7	951.8	206.6	409.7	247.3	778.6	221.0

Table 2.14. Group additivity analysis of the studied alkanolamines

T /K	Heat Capacity Cp / J·mol^{-1}·K^{-1}									
	EAE		PAE		BAE		HEP		BMOEA	
	Exp.	Calc.	Exp.	Calc.	Exp.	Calc.	Exp.	Calc.	Exp.	Calc.
303.15	231.7	229.9	263.9	260.7	289.2	291.5	271.0	275.7	293.6	292.2
313.15	236.2	237.5	269.5	268.9	299.1	300.3	280.5	279.3	300.7	300.0
323.15	240.3	241.2	273.4	272.7	303.5	304.3	286.6	282.1	301.9	304.5
333.15	244.6	244.4	277.9	275.8	307.1	307.2	292.9	284.7	305.9	307.6
343.15	248.9	250.1	281.7	283.1	315.0	316.1	298.0	291.5	315.8	313.2
353.15	255.1	256.5	288.3	290.0	322.4	323.5	303.0	296.4	321.2	321.5
% RD	0.48		0.59		0.36		1.83		0.50	

Table 2.15. Molecular connectivity analysis of the studied alkanolamines

T /K	Heat Capacity Cp / J·mol^{-1}·K^{-1}									
	EAE		PAE		BAE		HEP		BMOEA	
	Exp.	Calc.	Exp.	Calc.	Exp.	Calc.	Exp.	Calc.	Exp.	Calc.
303.15	231.7	233.3	263.9	264.6	289.2	295.9	271.0	282.9	293.6	290.5
308.15	234.3	234.9	267.5	266.6	296.6	298.3	277.5	285.6	300.0	292.7
313.15	236.2	236.5	269.5	268.6	299.1	300.6	280.5	288.4	300.7	294.9
318.15	238.1	238.1	271.5	270.5	301.5	303.0	283.7	291.1	301.1	297.1
323.15	240.3	239.7	273.4	272.5	303.5	305.3	286.6	293.9	301.9	299.3
328.15	242.2	241.3	275.6	274.5	305.4	307.7	289.7	296.6	303.2	301.5
333.15	244.6	242.9	277.9	276.5	307.1	310.1	292.9	299.4	305.9	303.7
338.15	246.7	244.5	279.8	278.5	309.7	312.4	295.7	302.2	311.3	305.9
343.15	248.9	246.1	281.7	280.4	315.0	314.8	298.0	304.9	315.8	308.1
348.15	251.1	247.7	285.0	282.4	319.4	317.1	300.9	307.7	318.5	310.3
353.15	255.1	249.3	288.3	284.4	322.4	319.5	303.0	310.4	321.2	312.5
% RD	0.73		0.52		0.80		2.64		1.67	

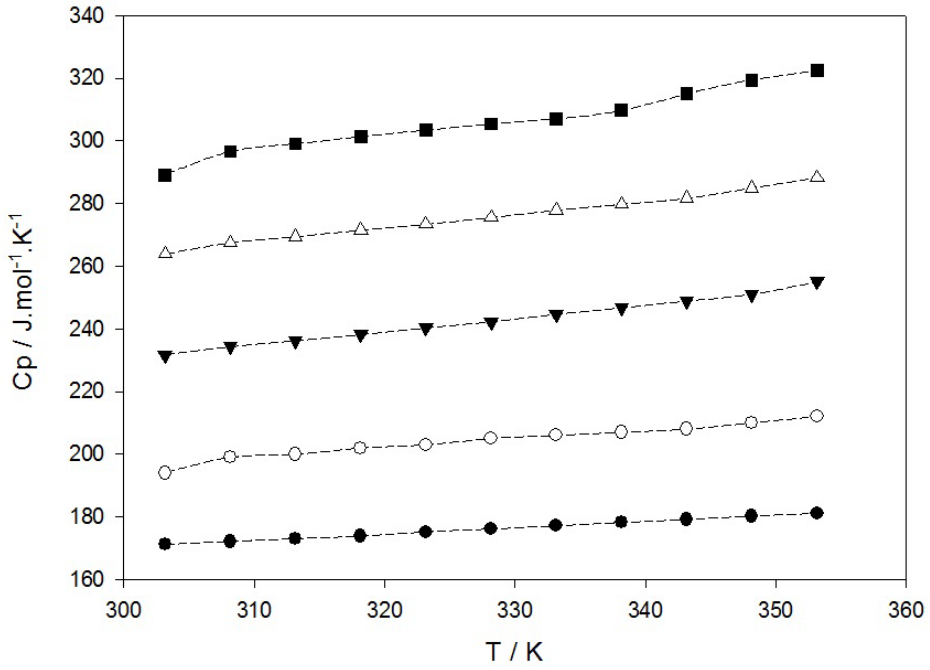

Figure 2.24. Comparison of heat capacities of the five pure alkylaminoethanols as a function of temperature: ●-, MEA; O-, MAE[40]; ▼-, EAE; △-, PAE; ■-, BAE

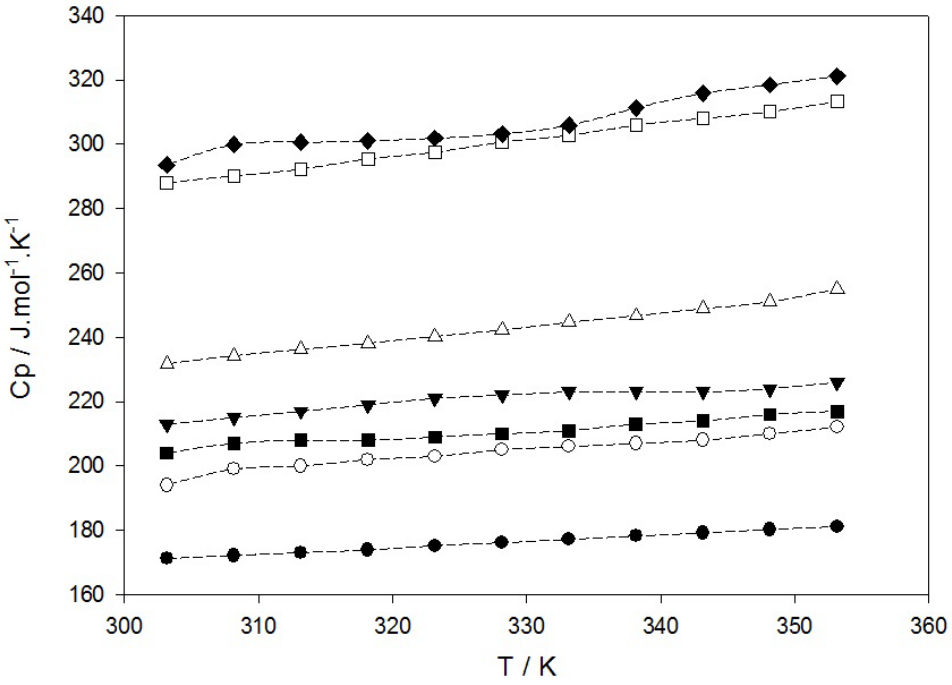

Figure 2.25. Comparison of heat capacities of the seven pure alkanolamines as a function of temperature: ●-, MEA; O-, MAE[40]; ▼-, DMAE[40]; △-, EAE; ■-, AP[40]; □-DEA[5]; ◆, BMOEA

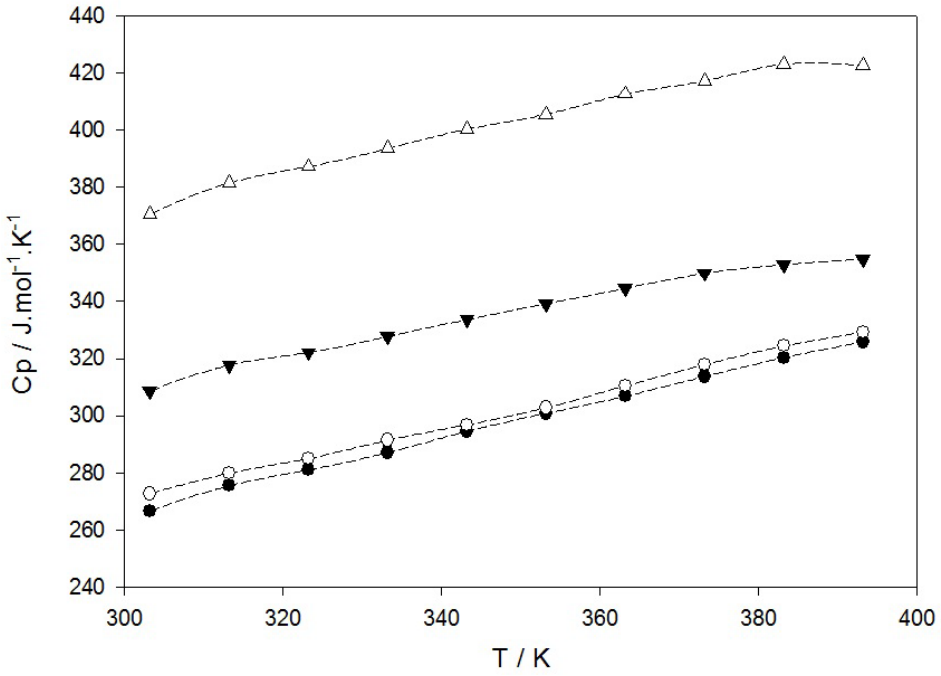

Figure 2.26. Comparison of heat capacities of the four pure alkanolamines as a function of temperature: ●-, DEA[30]; O-, MDEA[30]; ▼-, EDEA[30]; △-, N-BDEA[30]

"And He has set up on the earth mountains standing firm, lest it should shake with you...."

(Quran: 16:15)

3. HEATS OF MIXING

Molar heat of mixing is a vital thermodynamic property employed in numerous applications of chemical engineering such as distillation and heat exchanger design.[12] In addition, it is needed for the modeling multistage, multi-component equilibria in both absorption, and desorption columns.[4]

3.1. Literature review

Touhara et al.[63] published molar excess enthalpies for aqueous solutions of MEA, MMEA and DMEA at 298.15K. They pointed out that the hydrophobicity was observed in aqueous dilute solutions of alkanolamine, where the partial molar enthalpy frequently reduces to a limiting value at infinite dilution, and this tendency increased with the substitution of methyl groups with a hydrogen on the nitrogen of MEA.

Posey[64] measured the heat of mixing of DEA- and MDEA-water binary systems at two different temperatures (298.15 and 342.55K), and the MEA-water system at 342.55K. A portion of his data showed some scatter near the equimolar concentrations. Binary alkanolamine-water systems are extremely non-ideal since the heat of mixing is directly related to the activity coefficients which are dependent upon temperature. The sequence of heat of mixing from highest to lowest negative value was: MDEA>MEA>DEA.

Maham et al.[65] reported that the contribution in the excess enthalpy of amine is more dominant than the alcoholic group in the water-alkanolamine system. Also, alcohol and amine groups have the opposite effect on the excess enthalpies of aqueous binary mixtures. Furthermore, the alcoholic group gives an adverse effect upon the excess enthalpies of an aqueous binary mixture. When the number of alcoholic groups is increased, the excess enthalpy tends to be more positive. In other words, MEA has the most negative excess enthalpy and TEA the least negative enthalpy (MEA>DEA>TEA). Finally, the methyl group exhibited more negative excess enthalpy in the water-alkanolamine system. An alkyl group attached to a nitrogen atom plays a major role in influencing the molar excess enthalpy, as observed by Mathonat et al.[31] They concluded that the molar excess enthalpy of alkanolamine dominantly decreases with an addition of one or two methyl groups to the nitrogen atom; whereas, its excess enthalpy increased in the ethyl and propyl groups.

The molar excess enthalpies H^E for AEEA, AP, MAE, MIPA, and DMEA in water, at three different T = (298.15, 313.15, and 323.15K) and over the entire range of mole fractions, were reported by Mundhwa and Henni.[4] The measured molar excess enthalpy values were modelled using the following solution theory models: NRTL and UNIQUAC, and the modified functional group activity coefficient model (modified UNIFAC, Dortmund). Following a comparison of the magnitude of the MAE + water and DMEA + water systems, they concluded the addition of a methyl group increases the negative excess enthalpy. Poozesh[41] reported the molar excess enthalpies of cyclic amines of piperazine and morpholine derivatives at three different temperatures (298.15, 313.15 and 323.

15K) for the full range of mole fractions. He concluded that the addition of the $–CH_3$ group affected the excess enthalpy by elevating it by almost half, and shifted the minimum toward the water rich region. When the $–CH_3$ group was substituted with $–CH_2OH$, the excess enthalpies increased and had no effect on the position of the minimum. Also, if $–CH_2–NH_2$ was replaced with –OH and the –NH group in the central ring was substituted with the –O group, the excess enthalpies at three temperatures were increased by almost half.

Uddin[42] measured the molar excess enthalpy for the (amine + water) binary system of TMEDA, TMEDA-EO, 3DMA-1,2PD, 3DEA-1,2PD and 1, 3-Bis-DMA-2P at three temperatures (298.15, 313.15 and 333.15K) over the entire range of mole fractions. He concluded that the substitution of the methyl group on the nitrogen atom by an ethyl group or ethyl alcohol group resulted in a less negative on the molar excess enthalpies. Narayanaswamy[43] measured the molar excess enthalpies for 1DMAP, 3DMAP, DEEA, DETA, and EDA in water at three different temperatures (298.15, 313.15 and 323.15K) for the full range of mole fractions. He reported that an addition of a methyl group decreases H^E and hydroxyl groups increase the molar excess enthalpy.

3.2. Heats of mixing

The heat of mixing is the heat absorbed or liberated from one pure liquid into another upon mixing. Thus, the enthalpy change upon mixing is:[66]

$$\Delta H_{mixing} = H_{final} - H_{initial} \qquad (3.1)$$

Heat of mixing is dependent upon the concentration. Hence, the enthalpy value of the system, in its initial condition is expressed by a summation of the enthalpy values of each pure specie i as $\Sigma x_i H_i$ and the enthalpy in the final condition, H, is that of the mixture. The change of enthalpy in the mixing process can be then represented by:[12]

$$\Delta H = H - \sum_i x_i H_i \qquad (3.2)$$

The change of enthalpy of the mixing process at constant pressure and temperature to form one mole (or a unit mass) of solution, (ΔH), is also known as the "heat of mixing". It may be either negative, mixing is exothermic (or heat given off) because the mixture has a lower enthalpy than the pure species (positive), signifying endothermic mixing (or heat absorbed) because the mixture has a higher enthalpy than the pure species. Data for the heat of mixing are most commonly available in the literature for binary systems at few temperatures. They are somewhat similar, in several aspects, to heats of reaction.[12] A chemical reaction takes place due to differences in the forces of attraction of the solvent and solute molecules. The energy of the products is different from the energy of the reactants at the same temperature and pressure as a result of the chemical reorganization of the constituent atoms. Likewise, when a mixture is formed, a similar energy change takes place because the interactions between the force fields of like and unlike molecules are different. The signs and relative magnitudes of heats of mixing are useful for qualitative engineering purposes and to explain the molecular phenomena which are the basis for studying solution behaviour. Moreover, these quantities reflect the differences in the strengths of intermolecular attractions between pairs of unlike

substances on one side, and pairs of like substances on the other.[12] These energy changes are usually much smaller than those associated with chemical bonds; therefore heats of mixing are usually much smaller than heats of reaction.[12, 67]

3.2.1. Hydrogen bond

The most common chemical effect encountered in the thermodynamics of solutions, especially in aqueous solutions, is caused by the hydrogen bond. When two or more liquids are blended, breaking or formation of intermolecular hydrogen bonds between molecules in the liquids would cause an enthalpy change. They usually form between polar or polarized X – H bonds and electronegative atom A.[68] The resulting weak hydrogen bond, X – H ... A, is formed[69], where both X and A are highly electronegative atoms such as F, O, and N and it owns a significant electrostatic character. In the hydrogen bond X – H ... A, the group X – H is known as the "hydrogen - bond donor" (or proton donor) and A is known as the "hydrogen - bond acceptor" (or proton acceptor). Water, alcohols, and primary and secondary amines may function as both proton donors and proton acceptors; whereas tertiary amines, ethers, aldehydes, ketones and esters can serve only as proton acceptors.[12]

Hydrogen bonds, in comparison to covalent bonds, cover a wide range of bonding interactions, from the very strong to the very weak, when compared to van der Waals forces.[68] These bonds are extremely strong in directing intermolecular forces that keep the molecules together and the bond strength is powerfully dependent upon the solvent[70] in addition to the distance between interacting groups.[71] The bond strength

relies on its length and angle. The dependency upon bond length is very significant and the strength has been shown to exponentially decline with distance.[72]

Hydrogen bonding plays a vital role in investigating the structure and physical properties of various compounds and can be divided into two types.[73] The first is the intermolecular hydrogen bond developed between two different molecules. The second is the intramolecular hydrogen bond developed between two different atoms within the same molecule.

3.3. Excess molar enthalpy

An essential property in the field of chemical engineering thermodynamics is the molar excess enthalpy which is used to estimate heat duties during separation and mixing processes. The excess enthalpy of a solution is a measure of the difference between the enthalpy value of an actual and an ideal solution at the same temperature, composition, and pressure. This function indicates a deviation of the actual solution from the ideal. Mathematically, the molar excess enthalpy change is:[12]

$$\Delta H^E = \Delta H - \Delta H^{id} \tag{3.3}$$

In other words, it could be defined as the enthalpy change per mole of solution formed at constant temperature and pressure when the two pure liquid components mix physically and no chemical reaction occurs. According to the above definition, the molar excess enthalpy, H^E, is similar to the calorimetrically measured heats of mixing.[12]

$$\Delta H^E = \{H - \sum_{i=0}^{n} x_i H_i\} - \left\{H^{id} - \sum_{i=0}^{n} x_i H_i\right\} \tag{3.4}$$

where H, H^{id} and H_i are the enthalpies of the actual solution, ideal solution and the pure chemical species i, respectively. x_i is the mole fraction of the pure chemical species i. The enthalpy of an ideal solution, H^{id}, can be written as:

$$H^{id} = \sum_{i=0}^{n} x_i H_i \quad (3.5)$$

Substituting this value in the above equation means there is no change in molecular energies as a result of the formation of an ideal solution (i.e., $H^{id} = 0$). Hence, Equation 3.4 is reduced to:

$$\Delta H^E = H - \sum_{i=0}^{n} x_i H_i = \Delta H \quad (3.6)$$

According to the definition of an excess property ΔH^E can be reduced to H^E:

$$H^E = H - H^{id} = \Delta H^E \quad (3.7)$$

Equations 3.6 and 3.7 indicate that the enthalpy change of a mixing process (or heats of mixing) is identical to the molar excess enthalpy of the mixing process. [12, 13, 74]

3.4. Partial molar excess enthalpy

A partial molar property is a thermodynamic quantity which points out how an extensive property of a mixture or solution varies with changes in the molar composition of the mixture or solution at constant pressure and temperature. It is particularly beneficial when considering specific properties of pure chemical substances (that is, properties of one mole of pure chemical substance) and the properties of mixing. As for a binary mixture, the partial molar excess enthalpies of the alkanolamines

at infinite dilution in water ($x_1 = 0$) and of water in alkanolamines at infinite dilution ($x_2 = 0$ or $x_1 = 1$) are proposed by Maham et al.[65] and are as follows:

- for alkanolamines @$x_1 = 1$

$$H_1^0 - H_1^* = \Delta H_1^\infty = H^E - x_1 \left\{\frac{\partial H^E}{\partial x_1}\right\}_{P,T} = \sum_{i=0}^{n} a_i(-1)^{i-1} \qquad (3.8)$$

- for water @ $x_1 = 0$

$$H_2^0 - H_2^* = \Delta H_2^\infty = H^E - (1 - x_1) \left\{\frac{\partial H^E}{\partial x_1}\right\}_{P,T} = \sum_{i=0}^{n} a_i \qquad (3.9)$$

where a_i are the polynomial coefficients of Redlich-Kister equation, as obtained from the least squares regression method (which are the dependence of excess enthalpy on x_1 or x_2) and H_1^0 and H_2^0 represent the partial molar enthalpies of amine and water, while H_1^* and H_2^* represent the molar enthalpies of pure amine and water, respectively. ΔH_1^∞ and ΔH_2^∞ represent the molar enthalpy of a solution of the solvent at infinite dilution in water and of water at infinite dilution in solvent, respectively.

3.5. Molar excess enthalpy (H^E) measurements

The C80 heat flow calorimeter is a versatile instrument and also measures the heats of reaction, heats of mixing and heats of solution. In the experimental studies, the heats of mixing data were determined at three different temperatures of 298.15, 313.15, and 333.15K. A membrane mixing cell is used to perform the experiments. Two identical membrane mixing cells, one in the reference chamber and the second in the sample chamber of the calorimeter, are required.

With respect of the sample cell, both alkanolamine and water are placed into two sealed sections that are separated by an aluminum foil membrane. They are not mixed until the heat flow baseline and temperature baseline become horizontal and stable. The reason behind the use of a reference cell is to cancel the heat provided in order to maintain isothermal states and the negligible heat of stirring. Once the vessels have achieved the experimental temperature, the membrane is ruptured and the solutions are constantly stirred for one minute. Fluxmeters determine the deviation in heat flow between the vessels and the calorimetric block. The calorimetric block had a sufficient thermal mass to provide or obtain heat to or from the vessels without varying the temperature. A generated curve of differential heat flow against time, is presented in Figure 3.1. The area under the curve is measured using a baseline integration method to obtain the total heats of mixing of the sample solution. The experiments are carried out at three different temperatures (298.15, 313.15, and 333.15K) and atmospheric pressure.

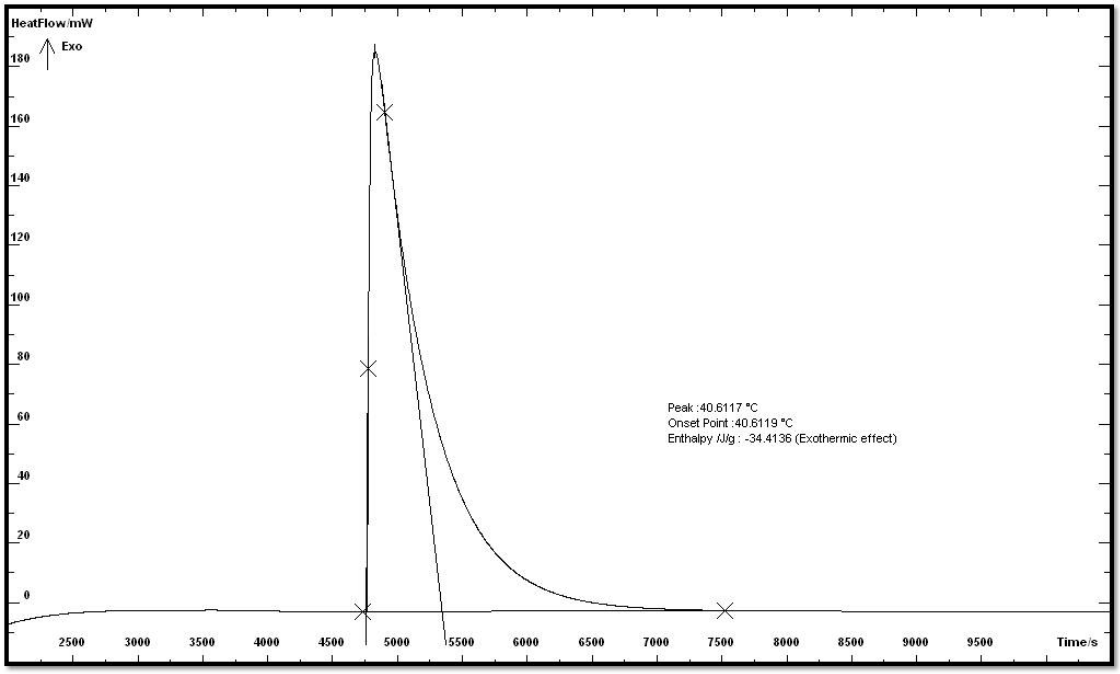

Figure 3.1. Molar excess enthalpy profile using SETSOFT-2000 software

3.5.1. Membrane mixing cell

The membrane mixing cell was utilized to study the mixing of two substances and measure the heats of interaction, as presented in Figure 3.2. It is made up of a stainless steel irregular body containing a shoulder in the center and fitted with two threaded ends. The volume of the upper compartment is 2ml and the lower compartment is 2.6ml and each contained one of the substances. The lower compartment of the cell is used to house a container into which one of the non-/reactive substances is placed. It is closed by a captive circular aluminum membrane between two Teflon sealing rings. They are fitted firmly into each other by clamping the membrane and closing the lower compartment. By screwing the upper compartment into the lower compartment of the body, the ring is pressed on top of the shoulder and allowed to seal the lower compartment of the cell.

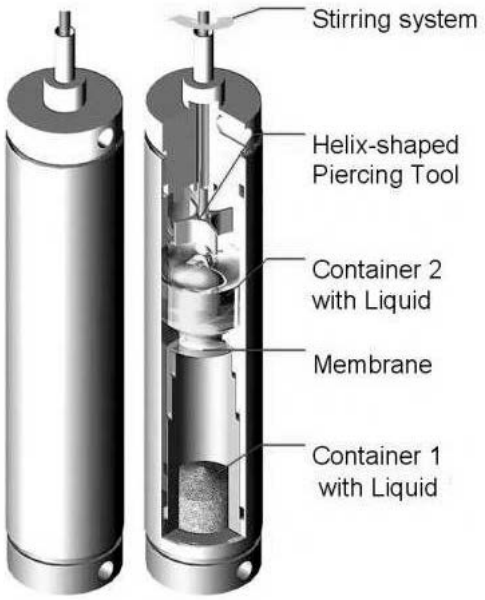

Figure 3.2. Membrane mixing cell for molar heats of mixing experiments (courtesy of SETARAM Co.)

In general, the membrane is made up of a 15µm thick aluminum disc. The upper compartment is used to house the second sample and is closed by a perforated lid, and threaded with a Teflon (O) ring. A moveable rod crosses the lid, which can be manually turned from outside the calorimeter, is screwed on to the top end of the rod and then enabled to be pressed into the cell through the membrane and turned. The bottom of the rod is threaded and is used to take a sharp-edged impeller which enables the membrane to tear and makes it possible to agitate the non-/reactive substances. By rupturing the membrane, the two substances are blended and mixing is performed by rotating the perforator.

3.6. Verification of the C80 heat flow calorimeter

3.6.1. Molar excess enthalpy measurements

To confirm the reliability the of C80 heat flow calorimeter for molar H^E measurements, two binary systems, monoethanolamine + water, and methyldiethanolamine + water, have been chosen to be investigated from the available literature. The molar excess enthalpy data of MEA + water binary system are in good agreement with those reported by Touhora et al.[63] at 298.15K, and the results for the MDEA + water binary system are

Table 3.1. Molar excess enthalpies of the MEA + water binary system at 298K

Touhora et al. [63]								This Study	
x_{MEA}	H^E/ J·mol^{-1}	x_{MEA}	H^E/ J·mol^{-1}	x_{MEA}	H^E/ J·mol^{-1}	x_{MEA}	H^E/ J·mol^{-1}	x_{MEA}	H^E/ J·mol^{-1}
0.0059	-72	0.1835	-1717	0.3738	-2373	0.6945	-1711	0.0993	-1046
0.0128	-151	0.2005	-1816	0.3970	-2390	0.7174	-1603	0.1995	-1780
0.0231	-269	0.2160	-1900	0.4200	-2395	0.7400	-1491	0.2995	-2173
0.0339	-381	0.2165	-1886	0.4443	-2385	0.7609	-1391	0.4000	-2340
0.0443	-498	0.2276	-1945	0.4694	-2362	0.7829	-1274	0.4985	-2278
0.0578	-633	0.2285	-1967	0.4945	-2327	0.8102	-1131	0.6007	-2039
0.0730	-784	0.2387	-2014	0.5224	-2277	0.8340	-1000	0.7013	-1657
0.0878	-945	0.2449	-2024	0.5475	-2219	0.8566	-866	0.8013	-1182
0.0998	-1057	0.2657	-2111	0.5715	-2148	0.8791	-734	0.9001	-633
0.1146	-1193	0.2867	-2186	0.5968	-2074	0.9025	-595		
0.1309	-1332	0.3077	-2249	0.6213	-1995	0.9342	-402		
0.1433	-1479	0.3302	-2307	0.6478	-1900	0.9591	-248		
0.1664	-1606	0.3527	-2349	0.6733	-1807	0.9808	-116		

Table 3.2. Molar excess enthalpies of the MDEA + water binary system at 313K

Maham et al. [65]		This Study	
x_{MDEA}	H^E/J·mol^{-1}	x_{MDEA}	H^E/J·mol^{-1}
0.0964	-1379	0.0497	-793
0.1413	-1762	0.1002	-1368
0.2238	-2178	0.2012	-2071
0.2703	-2327	0.3006	-2344
0.3468	-2326	0.4038	-2296
0.4274	-2252	0.5014	-2055
0.5151	-1942	0.6005	-1772
0.6360	-1609	0.7003	-1401
0.7412	-1143	0.8005	-970
0.8177	-838	0.8996	-497

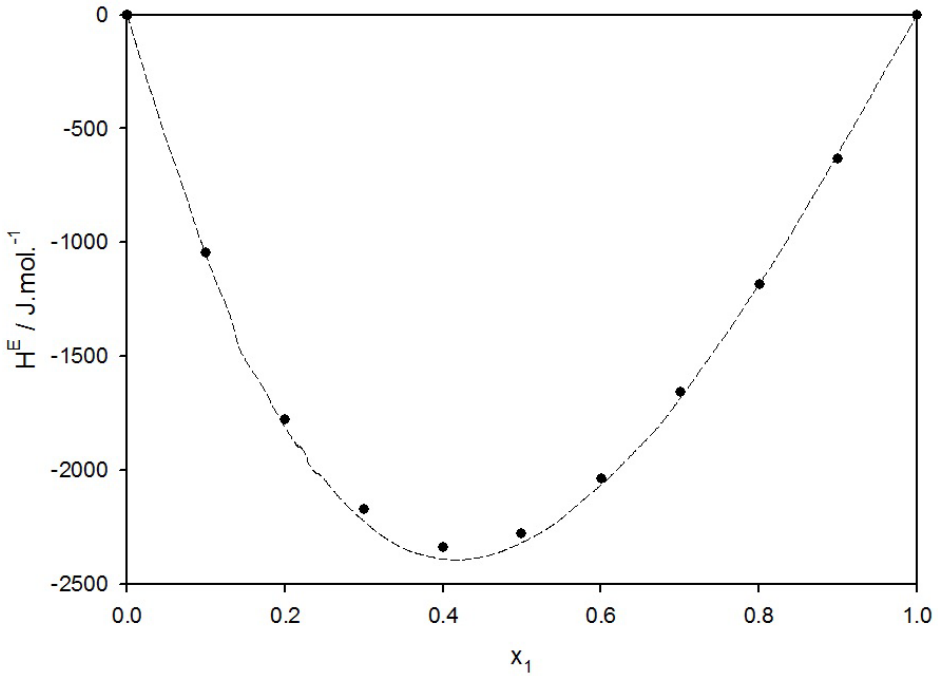

Figure 3.3. Molar excess enthalpies of the MEA (1) and Water (2) binary system at 298.15K: -, Touhora et al.[63]; ●, This Study

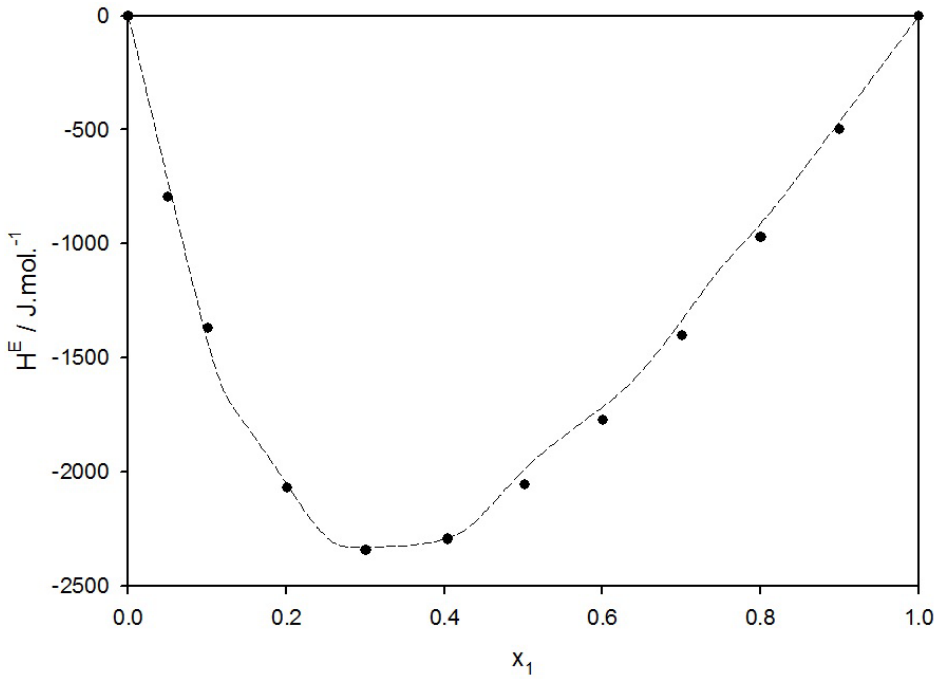

Figure 3.4. Molar excess enthalpies of the MDEA (1) and water (2) binary system at 313.15K: -, Maham et al.[65]; ●, This Study

also in good agreement with those published by Maham et al.[65] at 313.15K over the entire range of mole fractions, as represented in Tables 3.1 and 3.2, and Figures 3.3,and 3.4, respectively. The estimated uncertainty of the observed molar H^E data is 2% over the whole range of mole fractions.

3.7. Correlation and prediction approaches

The main purpose of the correlation is to provide appropriate and optimum usage of the experimental data. Due the complexities in the experimental measurement and the additional time required for extra components of a multi-component mixture, it is far more suitable to develop better approaches capable of estimating the physical and chemical properties of multi-component systems.[58] In the following sections, three different correlation and prediction methods are presented.

3.7.1. Empirical expressions

Empirical expressions are very helpful and desirable when dealing with data correlation and prediction. The parameters in the formulas are fitted to the measured data and a number of parameters can be determined according to the necessary accuracy.

3.7.1.1. Redlich-Kister equation

In this study, the experimental excess molar enthalpy data of the amine + water binary systems were correlated as a function of the amine mole fraction using the Redlich-Kister expression.[32] It is an excellent mixing rule form, which works similar to a convergent series with a finite number of terms. As for the binary system, this expression has the following polynomial form:

$$H^E/J.mole^{-1} = x_1 x_2 \sum_{i=0}^{n} a_i (x_1 - x_2)^i \qquad (3.10)$$

where, H^E is the excess molar enthalpy, x_1 and x_2 are the mole fractions of amine and water, respectively and a_i are the polynomial coefficients obtained from the least squares fitting of the dependence of H^E on x_1 or x_2; n is determined using the F-test.[59,60]

3.7.2. Solution theory methods

The most well-known solution theories are the regular theory, Quasi-Lattice theory, Two-Liquid theory, Associated Solution, and the Flory theory. The main purpose of the solution theory is to represent the behaviour of a solution in terms of its structure and intermolecular forces. This approach is useful with regard to understanding the solution behaviour even though it is at a semi empirical level. Wohl[75, 76] developed an expression derived from the standard solution theory, which is described as one in

which the components mix with no excess entropy, S^E, as long as the mixing has no volume change, i.e., $S^E = 0$ and $V^E = 0$. The major advantage of this expression is a certain amount of rough physical significance can be assigned to the expression parameters. Furthermore, it provided a better representation of the interactions of the molecules. Since all its parameters contribute to various groups of molecules, this expression is considered an empirical or semi-empirical expression. This means having more molecules in a group requires extra parameters.

Renon and Prausnitz implemented the Non-Random Two-Liquid (NRTL) model derived from the two-liquid theory.[77] As for a binary system in accordance to this model, the liquid has a structure composed of cells of molecules of '1' and '2' types, each surrounded by collections of the same molecules, with each of the surrounding molecules, consecutively, surrounded in a similar manner. The NRTL model has a similar accuracy as the Wilson expression for both correlation and prediction; however, for liquid-liquid immiscible systems, only the NRTL model can be used. The major drawback of this model, over the Wilson expression, is that it requires three parameters for each pair of constituents.

In adopting these local compositions and two-liquid model concepts, Abrams and Prausnitz implemented the UNIversal QUAsi-Chemical (UNIQUAC) equation which is frequently and for the most part used in today's chemical industry.[78] According to UNIQUAC, the expression of activity coefficients has two terms, one being the combinatorial term, which is due to dissimilarities in size and shape of the molecules

and the second being the residual term, as a result of energetic interactions. Furthermore, it was demonstrated that the Wohl, Wilson and NRTL expressions are special cases within the UNIQUAC expression when proper values of the parameters are assigned. The binary parameters, used in the UNIQUAC model, are regressed from experimental measurements. On the other hand, those parameters may be implemented in multi-component mixtures of three or more chemicals. The most important characteristics of the UNIQUAC expression are:

- Valid for multi-component mixtures in terms of binary parameters only
- Valid for liquid-liquid equilibria
- Temperature dependency is suitable over a moderate range
- Superior representation of mixtures of dissimilar molecular sizes

The major drawbacks of the UNIQUAC model are the algebraic complexity of the expression and very often, the representation of data is not as good as that of simpler expressions. The development of solution theories relies upon a molecular-based understanding of the solution. However, this model has demonstrated great potential and usefulness and also a promising future despite being less suitable in practice.

3.7.3. Group contribution methods

The group contribution method uses the principle that some simple aspects of the structures of chemical constituents, in many different molecules, are always the same. It is used to predict thermodynamic and other properties of mixtures and pure components by using group or atom properties. The components and their mixture

properties are required for synthesis, design, and optimization of thermal separation processes. In order to describe the experimental data, an approach derived from the group contribution method is used. This approach is based upon the hypothesis that an actual solution is composed of constituent groups of its components. This idea was proposed for the calculation of thermodynamic properties by Langmuir in 1925. One group contribution method, Analytical Solution of Groups (ASOG) was developed by Wilson and Deal[79], and was subsequently improved upon by Vera and Vidal[80] using an Analytical Group Solution method, referred to as "SImplified Group Method Analysis" (SIGMA). In 1975, another technique recognized as the UNIversal Functional Activity Coefficient (UNIFAC), has been suggested by Frendenslund et al.[81] This model is derived from the UNIQUAC method with the difference being in the residual term, which is contributed to by the interaction of groups in the UNIFAC method. By minimizing interactions between molecules to interactions between their functional groups, UNIFAC allows the representation of a huge variety of experimental data with a small set of parameters and the prediction, with reasonable confidence, regarding the behaviour of systems for which experimental observations are unavailable.

Another famous group contribution model is known as the "Dispersive-Quasi-Chemical" (DISQUAC) model which uses structure-dependent interaction parameters and applies a simple extension of the quasi-chemical theory.[82] Both polar and non-polar contacts were characterized by dispersive interchange energy and the polar contacts were further characterized by two extra parameters, the coordination number and the quasi-chemical interchange energy. This model proved to be useful for ternary systems having

polar compounds. Marongiu and co-workers[83, 84] successfully used the DISQUAC model to predict the excess enthalpies of two ternary mixtures Cyclohexane + Propanone + Tetrahydrofuran and Tetrahydrofuran + Cyclohexane + Butanenitrile. All group-contribution models simply required certain basic information regarding the constituent groups of each component but do require additional time and effort for their calculations.

Both the solution theory and group contribution models are superior as far as the representation of experimental H^E data.

3.8. Non-random two liquid (NRTL) model

As mentioned earlier, the Non-Random Two-Liquid model is derived from a local composition concept. Renon and Prausnitz[77, 85] improved the concept of local composition which was proposed by Wilson[86] for the two-fluid theory. The model supposes the mixing is not random and both local and bulk compositions are the same in case of random mixing. It is the difference in intermolecular forces that determines the nature of a non-random mixing. Thus, the nature of a non-random mixing is calculated by the difference in intermolecular forces and results in a dissimilarity between the local and the composition in the bulk. For an excess Gibbs energy, the NRTL model has the following original form:

$$\frac{g^E}{RT} = x_1 x_2 \left(\frac{\tau_{21} G_{21}}{x_1 + x_2 G_{21}} + \frac{\tau_{12} G_{12}}{x_2 + x_1 G_{12}} \right) \qquad (3.11)$$

where $\tau_{12} = a_{12} + \frac{b_{12}}{T}$, $\tau_{21} = a_{21} + \frac{b_{21}}{T}$, $G_{12} = exp(-\alpha_{12}\tau_{12})$, and $G_{21} = exp(-\alpha_{21}\tau_{21})$

To achieve more reliable and precise parameter values, the value of the non-randomness parameter, α, is regressed from 0 to 1. Subscripts 1 and 2 represent liquid components, alkanolamine and water, respectively. Five parameters, a_{12}, b_{12}, a_{21}, b_{21} and α, are used for a binary system, where the b terms represent temperature dependency. The Gibbs-Helmholtz relation can be utilized to specify the molar excess enthalpy, which points out the temperature dependence of the Gibbs free energy.

$$\frac{H^E}{R} = d\left(\frac{g^E}{RT}\right) \Big/ d\left(\frac{1}{T}\right) \tag{3.12}$$

The NRTL model can be obtained from Equations 3.11 and 3.12 for the molar excess enthalpy:

$$\frac{H^E}{R} = x_1 x_2 \left\{ \frac{G_{21} b_{21} (x_1 (1-\alpha_{21}\tau_{21}) + x_2 G_{21})}{(x_1 + x_2 G_{21})^2} + \frac{G_{12} b_{12} (x_2 (1-\alpha_{12}\tau_{12}) + x_1 G_{12})}{(x_2 + x_1 G_{12})^2} \right\} \tag{3.13}$$

3.9. Universal quasi-chemical (UNIQUAC) model

With respect to the NRTL equation, it is difficult to achieve precise and meaningful values for the three binary parameters as a result of a lack of binary experimental data. Abrams and Prausnitz[78] derived an expression that improves upon the quasi-chemical theory developed by Guggenheim[87] for non-random mixtures to solutions or mixtures of different molecular sizes. This improved theory is known as the "UNIversal QUAsi-Chemical" (UNIQUAC) theory.

The Universal Quasi Chemical model has two terms, Combinatorial and Residual. The combinatorial term describes combinatorial effects due to the differences in molecular size and shape and contains expressions of the mole fraction, average segment fraction, and average area fraction. The fraction expressions can be computed from the pure-component molecular structure constants (surface area and van der Waals volume of the molecule). Since the binary parameters are not present in this expression, empirical correlations or data are not required in order to calculate the combinatorial contribution.

The residual term is the contribution of the inter-molecular forces and is estimated from the area fractions, mole fractions and the energy of interactions between the components. Two parameters show the energy of the interactions which are not tabulated or measured, but must be determined empirically from liquid-liquid or vapor-liquid equilibrium data. The UNIQUAC expression is as follows:

$$\frac{g^E}{RT} = \left(\frac{g^E}{RT}\right)_{Combinatorial} + \left(\frac{g^E}{RT}\right)_{Residual} \tag{3.14}$$

For a binary mixture:

$$\left(\frac{g^E}{RT}\right)_{Combinatorial} = x_1 \ln\frac{\Phi_1^*}{x_1} + x_2 \ln\frac{\Phi_2^*}{x_2} + \frac{z}{2}\left(x_1 q_1 \ln\frac{\theta_1}{\Phi_1^*} + x_2 q_2 \ln\frac{\theta_2}{\Phi_2^*}\right) \tag{3.15}$$

$$\left(\frac{g^E}{RT}\right)_{Residual} = x_1 q_1' \ln\left(\theta_1' + \theta_2' \tau_{21}\right) - x_2 q_2' \ln\left(\theta_2' + \theta_1' \tau_{12}\right) \tag{3.16}$$

where the coordination number, z, and the segment fraction, Φ*, and the area fractions, θ and θ', are given by:

$$\Phi_1^* = \frac{x_1 r_1}{x_1 r_1 + x_2 r_2} \quad , \quad \Phi_2^* = \frac{x_2 r_2}{x_1 r_1 + x_2 r_2}$$

$$\theta_1 = \frac{x_1 q_1}{x_1 q_1 + x_2 q_2} \quad , \quad \theta_2 = \frac{x_2 q_2}{x_1 q_1 + x_2 q_2}$$

$$\theta_1^{'} = \frac{x_1 q_1^{'}}{x_1 q_1^{'} + x_2 q_2^{'}} \quad , \quad \theta_2^{'} = \frac{x_2 q_2^{'}}{x_1 q_1^{'} + x_2 q_2^{'}}$$

$$\tau_{12} = e^{a_{12} + \frac{b_{12}}{T}} \quad , \quad \tau_{21} = e^{a_{21} + \frac{b_{21}}{T}}$$

Parameters r, q, and q' are the pure-component molecular-structure constants and depend upon the molecular size and external surface areas, and τ_{12} and τ_{21} are two variable parameters. The molecular surface area and volume parameters of the chosen alkanolamines are given in Table 6.18 of Appendix 6.3. Equation 3.12 is used to obtain the expression of the UNIQUAC equation for the excess enthalpy. Only Equation 3.16, the residual term, is used to obtain the UNIQUAC equation for excess enthalpy as it has a temperature dependency term. The following form of the UNIQUAC equation is derived from Equations 3.12 and 3.16:

$$-\frac{H^E}{R} = q_1 x_1 \left(\frac{\theta_2 b_{21} \tau_{21}}{\theta_1 + \theta_2 \tau_{21}}\right) + q_2 x_2 \left(\frac{\theta_1 b_{12} \tau_{12}}{\theta_2 + \theta_1 \tau_{12}}\right) \qquad (3.17)$$

3.10. Modified UNIFAC (Dortmund) model

The Universal Functional Activity Coefficient (UNIFAC) method is derived from the quasi-chemical theory of liquid solutions, as introduced by Guggenheim.[87] Abrams and Prausnitz simplified this hypothesis[78] and Fredenslund et al.[81] applied it to functional groups inside the molecules. It was used earlier to successfully compute vapor-liquid[81], liquid-liquid[89], and solid-liquid[90] equilibria. It is also used in many areas to determine

activities in polymer solutions[91, 92], vapor pressures of pure components[93], flash points of solvent mixtures[94], the influence of solvent on the reaction rate[95] and the solubility of gas.[96, 97]

Weidlich et al.[58] pointed out that the results obtained from the UNIFAC method for the activity coefficient calculations at infinite dilution were unsatisfactory, in particular with regard to systems with dissimilar sizes of molecules. Furthermore, the original UNIFAC model was not capable of calculating the excess enthalpy and hence, was not able to accurately capture the temperature dependence of the Gibbs excess energy. Thus, Weidlich et al.[58] introduced several small modifications to the original UNIFAC expression so the vapor-liquid equilibria, excess enthalpy and activity coefficients at infinite dilution can be calculated with satisfactory accuracy using only one set of parameters.

The description of the original UNIFAC equation was presented by Fredenslund et al.[88] Only the residual term of the modified UNIFAC (Dortmund) equation is presented herein since the excess enthalpy results depend upon temperature. One of the major differences between the original UNIFAC and the modified UNIFAC (Dortmund) is the addition of temperature-dependent interaction parameters as follows:

Original UNIFAC: $$\Psi_{nm} = \exp\left(-\frac{a_{nm}}{T}\right) \quad (3.18)$$

Modified UNIFAC (Dortmund): $$\Psi_{nm} = \exp\left(-\frac{a_{nm}+b_{nm}T+c_{nm}T^2}{T}\right) \quad (3.19)$$

In order to find the equation of the modified UNIFAC (Dortmund) equation for excess enthalpy, the Gibbs-Helmholtz expression (Equation 3.12) is applied. The UNIFAC model breaks the activity coefficient into two terms for each constituent in the system - a combinatorial γ^C and a residual term γ^R. As for the i^{th} molecule, the model's equation is:

$$\frac{g^E}{RT} = \sum_i x_i\left(\ln \gamma_i^R + \ln \gamma_i^C\right) \tag{3.20}$$

Since the combinatorial term is temperature independent, only the residual term is used for the calculation of excess enthalpy:

$$\ln \gamma_i^R = \sum_k \nu_k^{(i)} \left(\ln \Gamma_k - \ln \Gamma_k^{(i)}\right) \tag{3.21}$$

$$\ln \Gamma_k = Q_k \left\{1 - \ln(\sum_m \theta_m \Psi_{\mathrm{mk}}) - \sum_m \frac{\theta_m \Psi_{\mathrm{km}}}{\sum_n \theta_n \Psi_{\mathrm{nm}}}\right\} \tag{3.22}$$

In view of Equations 3.12, 3.20, 3.21 and 3.22, the following relations could be obtained:

$$H^E = -RT \sum_i \sum_k x_i \nu_k^{(i)} \left\{T\left(\frac{\partial \ln \Gamma_k}{\partial T}\right)_{P,x} - T\left(\frac{\partial \ln \Gamma_{\mathrm{k}}^{(i)}}{\partial T}\right)_{P,x}\right\} \tag{3.23}$$

where Γ_k and $\Gamma_k^{(i)}$ are the group activity coefficient of group k in the mixture and pure substances, respectively.

$$T\left(\frac{\partial \ln \Gamma_k}{\partial T}\right)_{p,x} = Q_k \sum_m \theta_m \left[\frac{(b_{mk} + \ln \Psi_{mk} + 2c_{mk}T)\Psi_{mk}}{\sum_n \theta_n \Psi_{nk}} + \frac{\Psi_{km} \sum_n \theta_n \Psi_{nm}}{(\sum_n \theta_n \Psi_{nm})^2}\left\{b_{km} - b_{nm} + \ln\left(\frac{\Psi_{km}}{\Psi_{nm}}\right) + (c_{km} + c_{nm})2T\right\}\right] \tag{3.24}$$

where,

$$\Psi_{nm} = exp\left[-\frac{a_{nm} + b_{nm}T + c_{nm}T^2}{T}\right],\ \theta_m = \frac{Q_m X_m}{\sum_n Q_n X_n} \text{ and } X_m = \frac{\sum_j v_m^j x_j}{\sum_j \sum_n v_n^j x_j} \tag{3.25}$$

The van der Waals group parameters for the modified UNIFAC (Dortmund) method are given in Table 6.17 of Appendix 6.3.

3.11. Determination of the parameters

The parameters of the three selected models, NRTL, UNIQUAC and modified UNIFAC, are determined with the assistance of a Data Regression System from the ASPEN PLUS software, which includes algorithms for fitting the experimental results. ASPEN executes a nonlinear optimization by tuning the parameters for reducing the value of Q with the following objective function:

$$Q = \sum_k \left[\sum_j \left\{ \sum_i \left(\frac{Z_e - Z_m}{\sigma_Z} \right)^2 \right\}_j \right]_k \qquad (3.26)$$

where Q is the objective function to be reduced by data regression, z is variables, σ_z is the standard deviation of the designated data; whereas subscripts i, j, k, e, and m are the number of variables, number of data points, number of data sets, estimated data, and measured data, respectively.[4] Standard deviations are provided for every variable in each data set. In most cases, the standard deviations were set to 0.05 for temperature, 0.1% for mole fractions and 2% for the excess enthalpy data. Britt-Luecke's algorithm was selected to obtain the optimized values of the parameters.

3.12. Result and discussion of molar excess enthalpy measurements

The experimental molar excess enthalpies (or heats of mixing) of the 2-(Propylamino)ethanol (1) + water (2), 2-(Butylamino)ethanol (1) + water (2), 1-(2-Hydroxyethyl)piperidine (1) + water (2), Diglycolamine (1) + water (2), and Bis(2-

methoxyethyl)amine (1) + water (2)binary systems at three temperatures (298.15, 313.15, 333.15K) over the complete range of mole fractions are given in Tables 6.13, 6.14, 6.15, 6.16 and 6.17 of the Appendix 6.2, respectively. The experimentally observed data were then correlated as a function of mole fraction using the Redlich-Kister expression.[32] The molar enthalpies of alkanolamine and water at infinite dilution were also estimated using the method suggested by Maham et al.[65] The experimental data of molar excess enthalpies were modeled employing the "NRTL", "UNIQUAC" and modified functional groups activity coefficient "modified UNIFAC (Dortmund)" models. Finally, hydrogen bonding in water and aqueous solutions are also discussed in detail. As mentioned earlier, the uncertainty in the experimental H^E data was found to be 2%.

3.12.1. Hydrogen bonding in water

Water is a highly polar molecule. The hydrogen atom of a water molecule is covalently attached to the oxygen atom and can pose an extra attraction to a neighbouring oxygen atom of another water molecule. This additional attraction, known as hydrogen bonding, makes the water a structured liquid. The occurrence of a huge number of H-bonds in liquid water, however, has a significant cumulative effect on its physical and thermal properties.[73] As a result of hydrogen bonding, additional energy is needed to separate each water molecule from its neighbours and therefore, there is unusually high boiling point of water,[12] as shown in Figure 3.5. In addition, boiling point data show that H-bonds are stronger than van der Waal bonds and simple dipole-dipole bonds.[73] A molecule of water favours in a number of H-bond interactions from zero to four and can acts as both proton donor and proton acceptor.[98] The patterns of hydrogen

bonding are random in water; for any water molecule selected at random, there is an equal probability that the four H-bonds (i.e., the two proton donors and the two proton acceptors) are placed at any of the four sites surrounding the oxygen atom, 30% in three H-bonds and smaller fractions contribute in one and two H-bonds.[99] Water molecules enclosed by four H-bonds tend to clump together, forming clusters.[72] These clusters tend to have various H-bond frameworks at high temperature. In general, the temperature-entropy effect reduces the number of H-bond interactions. Particularly, the H-bond clusters with a slightly angled strain are affected by temperature.[100]

As water molecules are relatively well separated in an aqueous solution, there is ample room for bending and stretching of these H-bonds away from their favoured structures.[72] If hydrocarbon chains (or other polar substances) are present in water, H-bonds will still form between the water molecules surrounding these hydrocarbon chains, but the degree of freedom is reduced.[102] This indicates that the entropy is reduced or that the hydrocarbon chain is enclosed by structured water (iceberg theory). Hydrogen bonding is also significant in determining whether a molecular substance can dissolve in water.[103] Solutes which are unable to develop H-bonds, but reduce the number of H-bonds of water, tend to have low solubility. Therefore, substances capable of considerable hydrogen bonding should be quite soluble in water.[104]

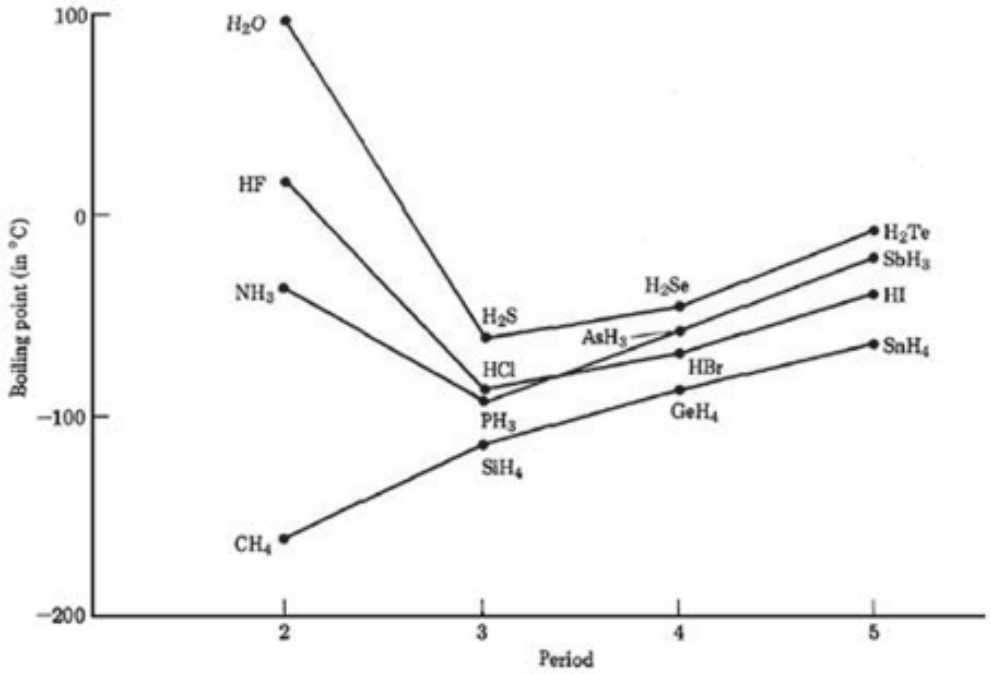

Figure 3.5. Comparison of boiling points in degrees (Celsius) of simple molecules MHx, versus the position of M in the periodic table [101]

3.12.2. Hydrogen bonding in alcohols

Alcohols are similar to water, except one of the hydrogen atoms of water is substituted by an alkyl group. If a methyl group is replaced for one of the hydrogen of water, methanol forms. Methanol is also a polar molecule because the hydroxyl-group leads to a high boiling point. On the other hand, methane is nonpolar and its boiling point is low due to weak intermolecular forces.[105] Alcohol boiling points are significantly higher than comparable molecular mass sized ethers (first two entries)[106], and that of alkanes. As a result of their hydroxyl group(s), alcohols are both a proton donor and proton acceptor and can participate in hydrogen bonding, while alkanes cannot.[107] Hydrogen bonding between alcohol molecules is similar to that which takes place between water molecules. Additional energy is required to overcome O:···HO H-bonds before alcohol molecules can enter the vapor phase. The boiling points of the straight chain alcohols

increase as the size of the alkyl groups in an alcohol increase. It receives extra energy to overcome the dispersion forces. There is a decrease in the boiling point for any given molecular mass when branching of alkyl groups occurs.[108]

The solubility of alcohols in water decrease as the size of the alkyl groups in alcohol increase.[105] The hydrophobic alkyl group has become a larger portion of the molecule, and properties associated with nonpolarity start to dominate. The hydroxyl group of the alcohol molecules interact via hydrogen bonding with water molecules.[107] The high solubility of the lower molecular mass alcohols such as methanol and ethanol in water can be attributed to hydrogen bonding between the hydroxyl group of the alcohol and water molecules. On the other hand, the hydrophobic alkyl group of the alcohol does not form hydrogen bonds with water in long-chain alcohols.[108] Methanol and ethanol are fully miscible in water, while 1-propanol and 1-butanol are moderately and fairly water-soluble, respectively. An extra -OH group attached to a hydrocarbon chain has an effect on water solubility. Two hydroxyl groups on a three-carbon chain, as in propylene glycol, convey full miscibility with water, in contrast to the restricted solubility of 1-propanol and 2-propanol. Thus, solubility in water relies on the number of alkyl groups (or carbon atoms) per hydroxyl group in the alcohol molecule. As a rule of thumb, one hydroxyl group can solubilise three to four carbon atoms per molecule.[109]

Wakisaka et al.[110] described the binary mixture of aqueous methanol. When a small amount of methanol is added to water, each hydroxyl group of methanol forms a H-bond with water (as a monomeric form) by substituting the hydrogen bonding network

of water. With a rising methanol concentration, the methanol molecules join each other to form larger methanol clusters. The interaction of methanol with water is robustly dependent upon the mixing ratio. Methanol mixes with water exothermically over the entire range of mole fractions. This indicates the interaction of methanol with water is energetically favourable and creates a stable structure (or cluster). The heats of mixing show a minimum around the alcohol mole fraction x_1 = 0.3, which may correspond to the maximum H-bonds formed between methanol and water molecules and thus, large methanol hydrate clusters were formed. In contrast, when a small quantity of water is added to methanol, the methanol-methanol interaction is stabilized due to the cooperative effect of the hydrophobic and the hydrogen-bonding interaction.

3.12.3. Hydrogen bonding in ether

Dimethyl ether and methyl ethyl ether are gases at ambient temperature. The boiling points of ethers, as compared to alkanes of similar molecular masses, are closer than to those of isomeric alcohols due to the inability of the ether molecules to form H-bonds with one another.[107] For example, the boiling point of diethyl ether (35°C, molecular mass 74) is very close to that of pentane (36°C, molecular mass 72) and significantly lower than that of its isomer n-butyl alcohol (117°C, molecular mass 74).[111] Intermolecular forces such as weak dipole-dipole exist in their liquid form.

On the other hand, the oxygen of an ether can contribute as the Lewis base partner of a H-bond. The solubility of alcohols and ether in water are quite similar. The low molecular mass of alcohols (methanol, ethanol) and ethers (dimethyl ether) are water

soluble. However, alcohols having four carbon and higher and ethers having three carbon or higher have a much lower water solubility. For example, the solubility of diethyl ether in water is 8.4g/100ml while that of n-butyl alcohol is 7.4g/100ml.[111] The higher solubility of ethers in water is due to the capability of their molecules to form an H-bond. This solubility decreases as the sizes of the alkyl groups increase and the relative increase in the hydrocarbon segment of the ether molecule reduces the tendency of H-bond formation.

3.12.4. Hydrogen bonding in amines

Mono-, di-, and tri-methylamines and ethylamines are gases at ambient temperature.[107] Primary and secondary amines are associated as a result of the formation of H-bonds. While tertiary amines do not associate because of the absence of a hydrogen atom capable of forming H-bonds.[112] Both trimethylamine and methylethylamine have the same chemical formula (C_3H_9N) although trimethylamine (4°C) has a lower boiling point than methylethylamine (37°C) because trimethylamine is a tertiary amine and it only has a proton acceptor group; whereas, methylethylamine is a secondary amine and it has both proton donor and proton acceptor groups and forms H-bonding between them.[103] The boiling points of amines are in the middle between those of similar molecular masses of alkanes and alcohols.[107] This indicates that the O:···HO H-bond is more polar than the N:···HN H-bond. Therefore, H-bonds in alcohols are stronger than H-bonds in amines.[113] The difference in H-bond strength results from differences in electronegativity (oxygen is more electronegative than nitrogen).[107]

Lower molecular masses of aliphatic amines are soluble in water. With an increase in molecular mass, their solubility in water declines (i.e., solubility of amine in water up to six carbon atoms). The solubility of lower members of amine in water is due to their capability to form H-bonds with water molecules.[114]

On the other hand, when an amine dissolves in water since it is a weak base (or Lewis base), it can react with water molecules. A proton is pulled off of the water molecule and shifted to the amine because it has a lone pair of electrons, changing it into a positively charged polyatomic ion known as a "quaternary ammonium ion".[112] The loss of a proton from a water molecule changes it into a hydroxide ion which makes the solution basic. The resulting aqueous amine solution will contain combined amine-water molecules with some amineH^+ and OH^- ions.[112] The dissolving in water is associated with H-bonding; whereas, dissociation of water to develop hydroxide ion is associated with the basic property of amines. Amines are stronger bases than oxygen-containing organic compounds such as alcohols and ethers since amines are stronger proton acceptors than the compounds.[107]

3.12.5. 2-(Propylamino)ethanol (PAE)

Molar heats of mixing for the (PAE (1) + Water (2)) binary system were experimentally measured at three different temperatures (298.15, 313.15, and 333.15K). The experimental data are given in Table 6.11, and shows mole fraction dependency at several temperatures (Figure 3.6.). The molar heats of mixing plots for the above three temperatures are negative with a minimum value of around x_1 = 0.45. As mentioned earlier, the negative sign and relative magnitude of the molar excess enthalpies indicate a mild exothermic mixing process between PAE and water. It also indicates that the interaction of PAE with water is energetically favourable and makes a stable structure (or cluster).[110] The exothermic mixing process between PAE and water is the result of a reaction between the amine group and water [112] and several groups interactions to form an H-bond such as -$NH^{\cdots}$:OH_2, -$OH^{\cdots}$:OH_2, -HO:$^{\cdots}$HOH and amineH^{+}-HO:$^{\cdots}$HOH. The molar heats of mixing are less negative at 333.15K compared to the values at 313.15K and 298.15K, as shown in Figure 3.6.

The coefficients of the Redlich-Kister relation and the percentages of relative deviation (%RD)[57] are listed in Table 3.3. The calculated molar heats of mixing for all three temperatures, using the Redlich-Kister equation[32], are plotted as dashed lines in Figure 3.6. The percentages of relative deviation (%RD)[57] were 0.82, 0.60, and 0.34% for 298.15, 313.15 and 333.15K, respectively.

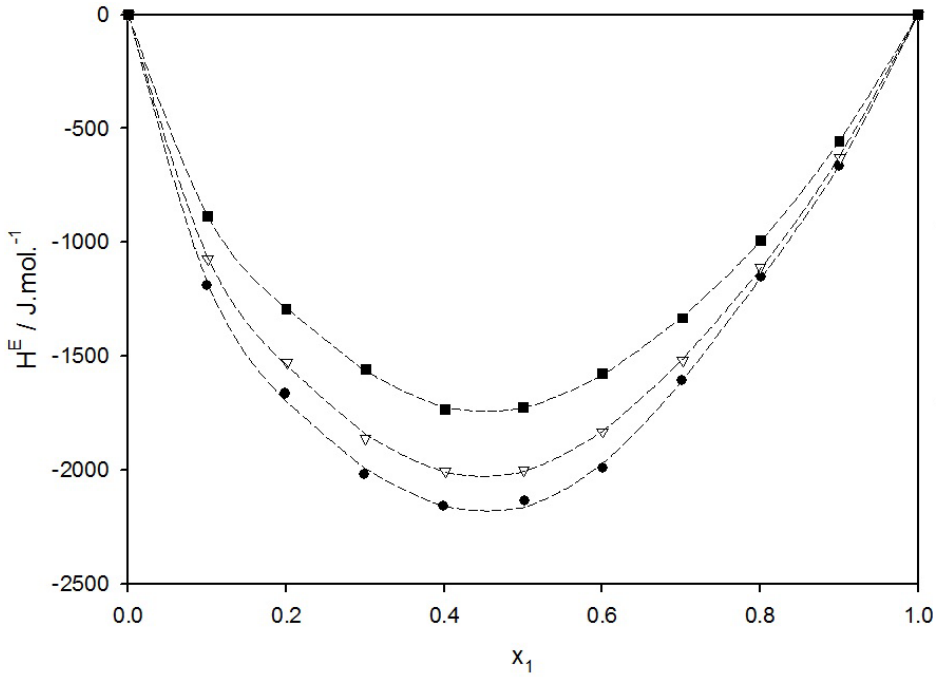

Figure 3.6. Molar excess enthalpy of a (PAE (1) + water (2)) binary system at three temperatures: ●,298.15 K; ▽, 313.15 K; ■, 333.15K and --, Redlich Kister

Table 3.3. Redlich-Kister coefficients for the molar excess enthalpies of a (PAE (1) + water (2)) binary system at three temperatures 298.15, 313.15 and 353.15K

T /K	Redlich Kister Coefficients						%RD
	a_0	a_1	a_2	a_3	a_4	a_5	
298.15	-8656.68	1839.24	1327.31	2706.82	-5862.63	---	0.82
313.15	-8029.68	1896.46	945.25	-326.34	-4793.07	3312.07	0.60
333.15	-6909.47	1530.97	690.85	-1503.03	-3737.95	4189.81	0.34

Table 3.4. Molar enthalpies of PAE at infinite dilution in water (ΔH_1^{∞}) and of water at infinite dilution in PAE (ΔH_2^{∞}) at three temperatures 298.15, 313.15 and 353.15K

T/K	ΔH_1^{∞} (KJ·mol^{-1})	ΔH_2^{∞} (KJ·mol^{-1})
298.15	-17.7	-8.6
313.15	-16.8	-7.0
333.15	-14.2	-5.7

Table 3.5. NRTL and UNIQUAC coefficients for the molar excess enthalpies of a (PAE (1) + water (2)) binary system at three temperatures (298.15, 313.15 and 353.15K)

NRTL			UNIQUAC		
Parameters	**Values**	**%RD**	**Parameters**	**Values**	**%RD**
a_{12}	1.73		a_{12}	50.00	
a_{21}	-4.46		a_{21}	0.11	
b_{12} / K	-687.50	4.94	b_{12} / K	27.51	6.74
b_{21} / K	-6.27		b_{21} / K	274.09	
α	0.80				

Table 3.6. UNIFAC coefficients for the molar excess enthalpies of a (PAE (1) + water (2)) binary system at three temperatures (298.15, 313.15 and 353.15K)

Groups (m) / (n)	**Parameters**	**CH_2**	**CH_2NH**	**OH**	**H_2O**	**%RD**
CH_2	a_{nm}/K	---	286.20	1235.30	-71.33	0.70
	b_{nm}	---	3.09	-2.38	-6.21	
	c_{nm}/K^{-1}	---	0.00	0.00	0.00	
CH_2NH	a_{nm}/K	-8.83	---	2869.34	-486.36	
	b_{nm}	-1.31	---	0.81	-0.73	
	c_{nm}/K^{-1}	0.00	---	-0.03	0.01	
OH	a_{nm}/K	1088.43	-1479.71	---	243.20	
	b_{nm}	0.11	-5.45	---	-0.25	
	c_{nm}/K^{-1}	-0.01	0.01	---	-0.01	
H_2O	a_{nm}/K	-28.42	-181.83	-158.05	---	
	b_{nm}	-2.04	-4.02	-1.22	---	
	c_{nm}/K^{-1}	0.00	0.00	0.00	---	

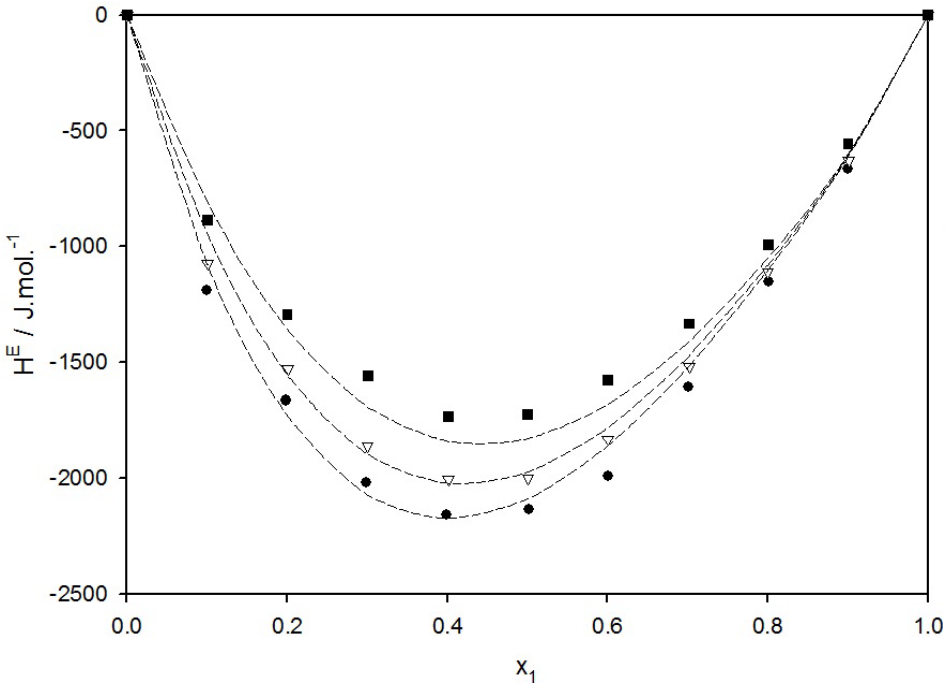

Figure 3.7. Molar excess enthalpy of a (PAE (1) + water (2)) binary system at three temperatures: ●, 298.15K; ▽, 313.15K; ■, 333.15K; --, NRTL

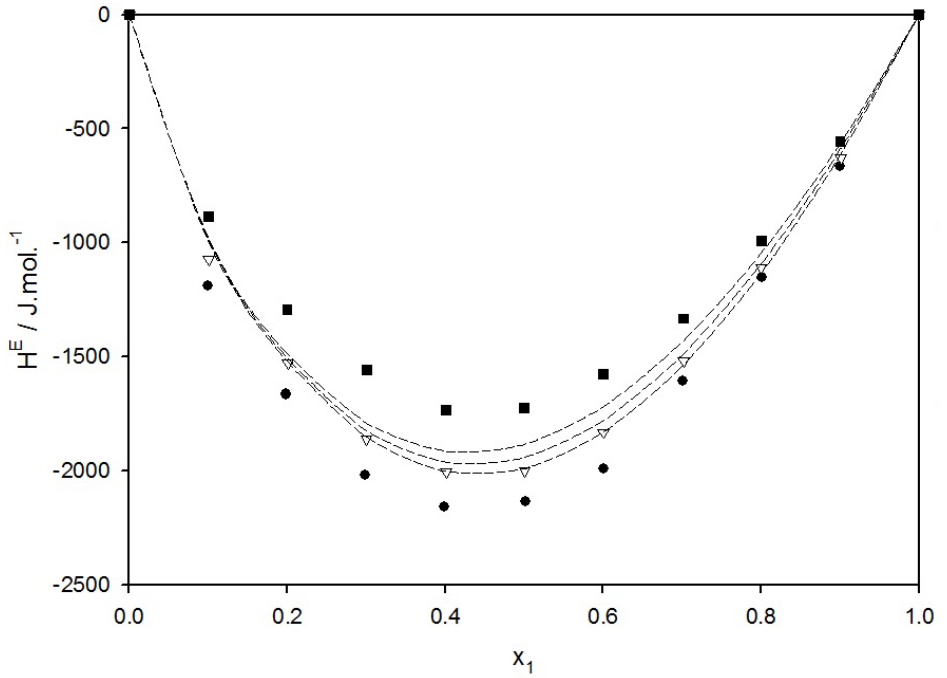

Figure 3.8. Molar excess enthalpy of a (PAE (1) + water (2)) binary system at three temperatures: ●,298.15K; ▽, 313.15K; ■, 333.15K; --, UNIQUAC

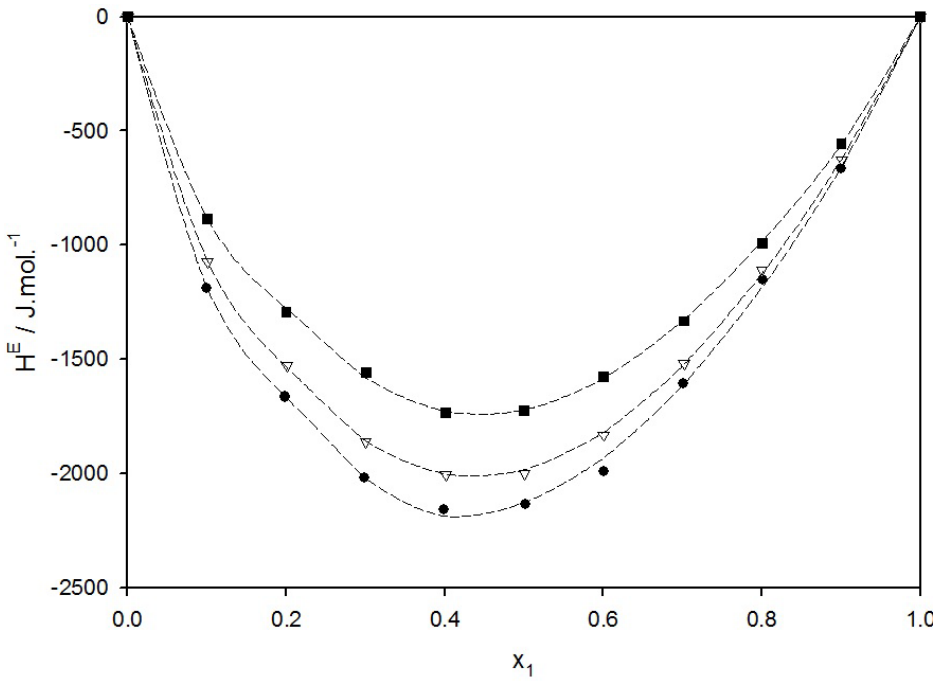

Figure 3.9. Molar excess enthalpy of a (PAE (1) + water (2)) binary system at three temperatures: ●,298.15K; ▽, 313.15K; ■, 333.15K; --, UNIFAC

Both the molar enthalpy of solution of PAE at infinite dilution (ΔH_1^{∞}) in water and water at infinite dilution (ΔH_2^{∞}) in PAE were derived using the method suggested by Maham et al.[65] Enthalpies at infinite dilution for PAE and water are presented in Table 3.4. Figures 3.7, 3.8, and 3.9 represent the experimental H^E of PAE + water binary system for three temperatures along with the fitted curves of NRTL, UNIQUAC and UNIFAC models, respectively. The built-in algorithm of ASPEN Plus software, also known as the "Data Regression System", (DRS) was used for the regression of the experimental molar heat of mixing data. Percentages of relative deviation (%RD)[57] between the experimental data and fitted data for the three models are 2.49, 6.75, and 0.70%, respectively, and parameters of the above models are presented in Tables 3.5 and 3.6. Among these models, UNIFAC furnished the best fitting to the experimental molar H^E data for this system.

3.12.6. 2-(Butylamino)ethanol (BAE)

Molar heats of mixing for a (BAE (1) + Water (2)) binary system were experimentally measured at three different temperatures (298.15, 313.15, and 333.15K). The experimental data are given in Table 6.12, and show the mole fractions dependency at several temperatures. The data is represented in Figure 3.10. The molar heats of mixing curves for the above three temperatures are negative with a minimum value of around x_1 = 0.50. A negative sign of molar heat of mixing and its magnitude indicate a mild exothermic mixing process between BAE and water, which further shows that the interaction is energetically favourable and forms a stable structure (or cluster).[110] The exothermic mixing process between 2-(Butylamino)ethanol and water is due to the reaction between the amine group and water[112] and a number of group interactions such as -$NH^{\cdots}$:OH_2, -$OH^{\cdots}$:OH_2, -HO:$^{\cdots}$HOH and amine$H^{+\cdots}$HO:$^{\cdots}$HOH and is recognized as the H-bond. The molar heat of mixing become less negative as the temperature rises, as presented in Figure 3.10.

The coefficients of the Redlich-Kister relation and percentages of relative deviation (%RD)[57] are listed in Table 3.7. The calculated molar heats of mixing for all three temperatures, employing the Redlich-Kister equation[32], are plotted as dashed lines in Figure 3.10. The percentages of relative deviation (%RD)[57] were 0.71, 0.94, and 1.40% for 298.15, 313.15 and 333.15K, respectively.

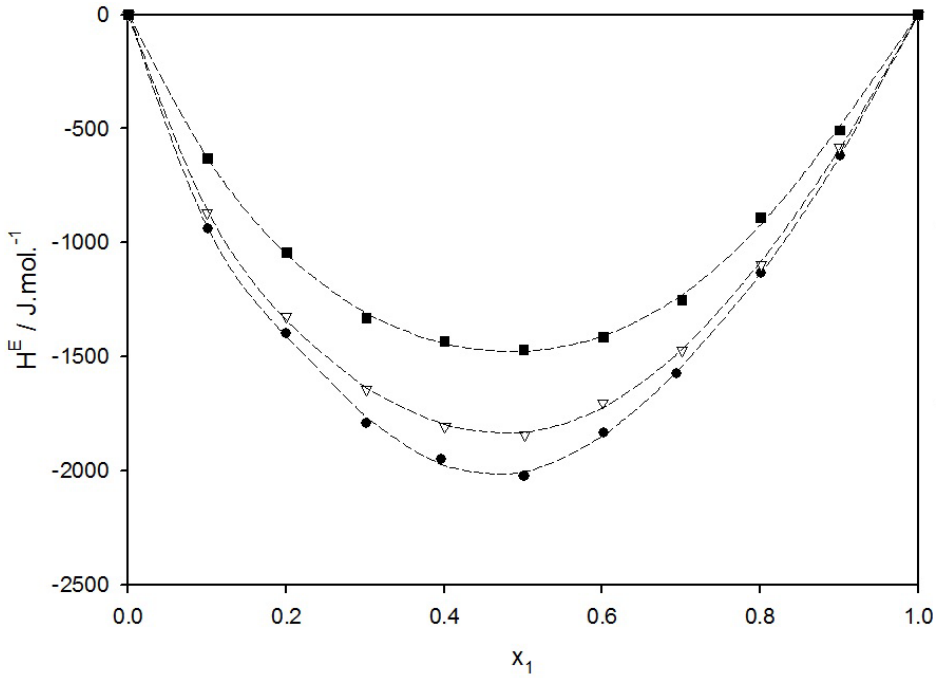

Figure 3.10. Molar excess enthalpy of a (BAE (1) + water (2)) binary system at three temperatures: ●,298.15K; ▽, 313.15K; ■, 333.15K; --, Redlich Kister

Table 3.7. Redlich-Kister coefficients for the molar excess enthalpies of a (BAE (1) + water (2)) binary system at three temperatures (298.15, 313.15 and 353.15K)

T /K	Redlich Kister Coefficients						%RD
	a_0	a_1	a_2	a_3	a_4	a_5	
298.15	-8030.71	1403.54	1616.21	-1381.55	-4048.02	4009.14	0.71
313.15	-7334.38	685.43	-138.40	1813.96	-1544.21	---	0.94
333.15	-5915.76	297.82	-932.53	1022.11	654.14	---	1.40

Table 3.8. Molar enthalpies of BAE at infinite dilution in water (ΔH_1^{∞}) and of water at infinite dilution in BAE (ΔH_2^{∞}) at three temperatures (298.15, 313.15 and 353.15K)

T/K	ΔH_1^{∞} (KJ·mol^{-1})	ΔH_2^{∞} (KJ·mol^{-1})
298.15	-14.5	-6.4
313.15	-11.5	-6.5
333.15	-7.5	-4.9

Table 3.9. NRTL and UNIQUAC coefficients for the molar excess enthalpies of a (BAE (1) + water (2)) binary system at three temperatures (298.15, 313.15 and 353.15K)

NRTL			UNIQUAC		
Parameters	**Values**	**%RD**	**Parameters**	**Values**	**%RD**
a_{12}	2.48		a_{12}	1.16	
a_{21}	3.00		a_{21}	-0.28	
b_{12} / K	-733.33	3.43	b_{12} / K	-736.09	3.90
b_{21} / K	-632.61		b_{21} / K	455.26	
α	0.80				

Table 3.10. UNIFAC coefficients for the molar excess enthalpies of a (BAE (1) + water (2)) binary system at three temperatures (298.15, 313.15 and 353.15K)

Groups (m) / (n)	**Parameters**	**CH_2**	**CH_2NH**	**OH**	**H_2O**	**%RD**
CH_2	a_{nm}/K	---	1575.90	-111.26	364.51	0.86
	b_{nm}	---	-4.22	0.03	-0.99	
	c_{nm}/K^{-1}	---	-0.01	0.00	0.00	
CH_2NH	a_{nm}/K	173.10	---	-557.43	198.80	
	b_{nm}	0.78	---	-4.97	0.13	
	c_{nm}/K^{-1}	0.01	---	0.01	-0.01	
OH	a_{nm}/K	309.59	861.55	---	-364.39	
	b_{nm}	2.11	-3.61	---	-0.10	
	c_{nm}/K^{-1}	0.01	-0.01	---	0.00	
H_2O	a_{nm}/K	-30.37	-271.88	-141.03	---	
	b_{nm}	3.98	-3.32	1.63	---	
	c_{nm}/K^{-1}	0.00	0.00	0.00	---	

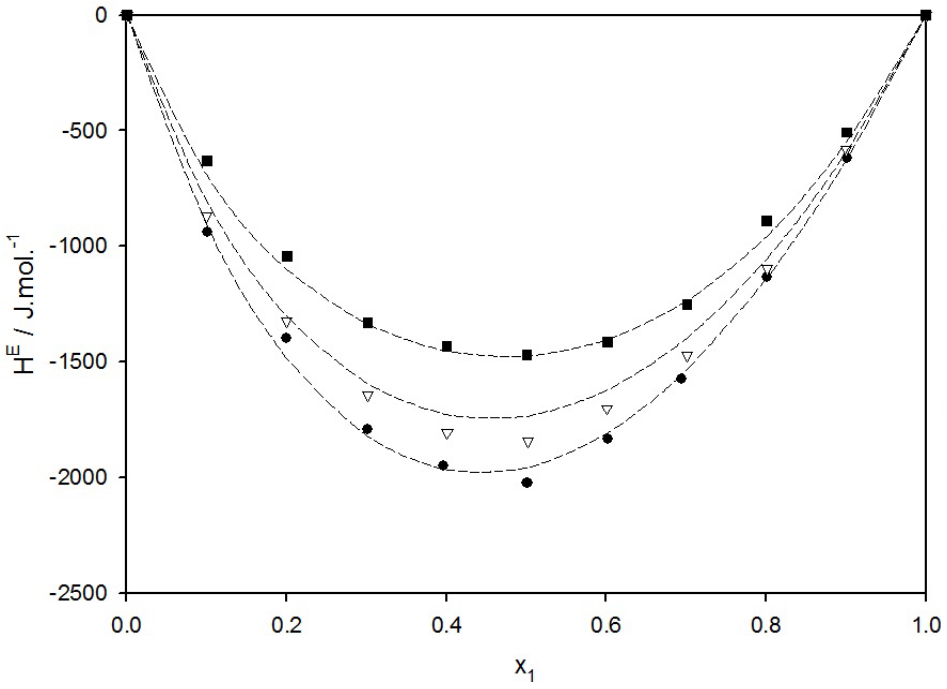

Figure 3.11. Molar excess enthalpy of a (BAE (1) + water (2)) binary system at three temperatures: ●,298.15K; ▽, 313.15K; ■, 333.15K; --, NRTL

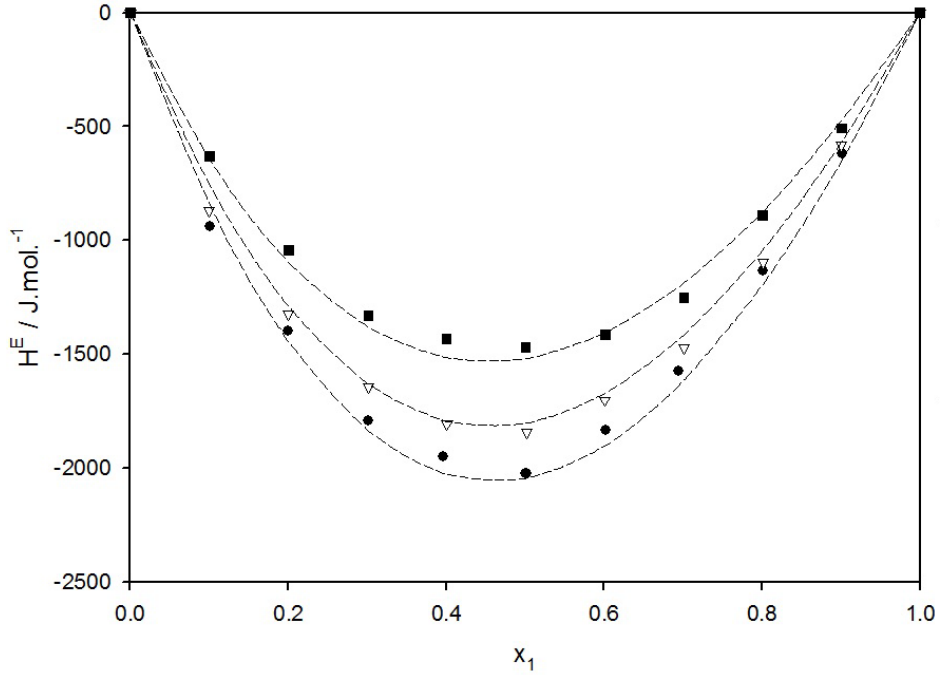

Figure 3.12. Molar excess enthalpy of a (BAE (1) + water (2)) binary system at three temperatures: ●,298.15K; ▽, 313.15K; ■, 333.15K; --, UNIQUAC

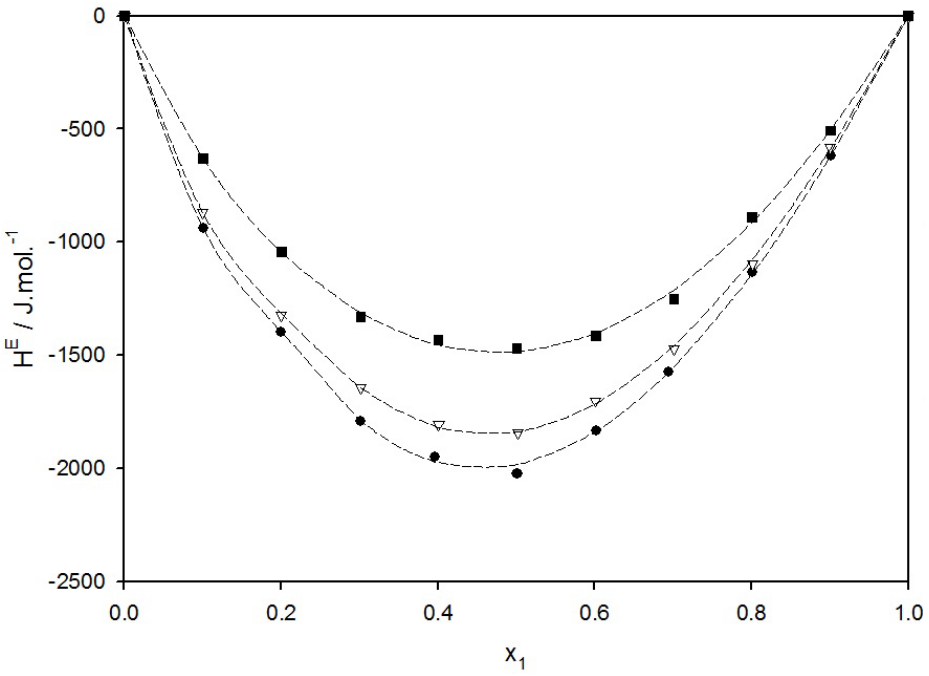

Figure 3.13. Molar excess enthalpy of a (BAE (1) + water (2)) binary system at three temperatures: ●, 298.15K; ▽, 313.15K; ■, 333.15K; --, UNIFAC

Both the molar enthalpy of solution of BAE at infinite dilution (ΔH_1^{∞}) in water and water at infinite dilution (ΔH_2^{∞}) in BAE were derived using the method suggested by Maham et al.[65] Enthalpies at infinite dilution for BAE and water are presented in Table 3.8. Figures 3.11, 3.12, and 3.13 present the experimental H^E of BAE + water binary system for three temperatures along with the fitted curves of NRTL, UNIQUAC and UNIFAC models, respectively. The built-in algorithm of ASPEN Plus software is also known as the "Data Regression System" (DRS) and was used for the regression of the experimental molar heat of mixing data. Percentages of relative deviation (%RD)[57] between the experimental data and fitted data for the three models are 3.02, 3.90, and 0.86%, respectively, and parameters of the above models are presented in Tables 3.9 and 3.10. Among these models, UNIFAC provided the best fitting to the experimental molar H^E data for this system.

3.12.7. 1-(2-Hydroxyethyl)piperidine (HEP)

Molar heats of mixing for the (HEP (1) + Water (2)) binary system were measured at three different temperatures (298.15, 313.15, and 333.15K). The experimental data are given in Table 6.13, showing the mole fraction dependency at several temperatures, and are represented in Figure 3.14. The molar excess enthalpy plots for the three temperatures were negative with a minimum value of around x_1 = 0.4. As previously mentioned, the negative sign of the molar excess enthalpies of HEP and water binary system and their relative magnitude indicate a mild exothermic mixing process, which is energetically favourable and forms a stable structure (or cluster).[110] The exothermic mixing process between HEP and water is due to the reaction between the amine group and water[112] and numerous group interactions to form H-bonds. The molar heats of mixing are less negative at temperatures 333.15K followed by 313.15K and 298.15K, as shown in Figure 3.14.

The coefficients of the Redlich-Kister relation and percentages of relative deviation (%RD)[57] are listed in Table 3.11. The calculated molar heats of mixing for all three temperatures, employing the Redlich-Kister equation[32], are plotted as dashed lines in Figure 3.14. The percentages of relative deviation (%RD)[57] were 0.21, 0.70, and 0.37% for 298.15, 313.15 and 333.15K, respectively.

Both the molar enthalpy of solution of HEP at infinite dilution (ΔH_1^{∞}) in water and water at infinite dilution (ΔH_2^{∞}) in HEP were derived using the method suggested by Maham et al.[65]

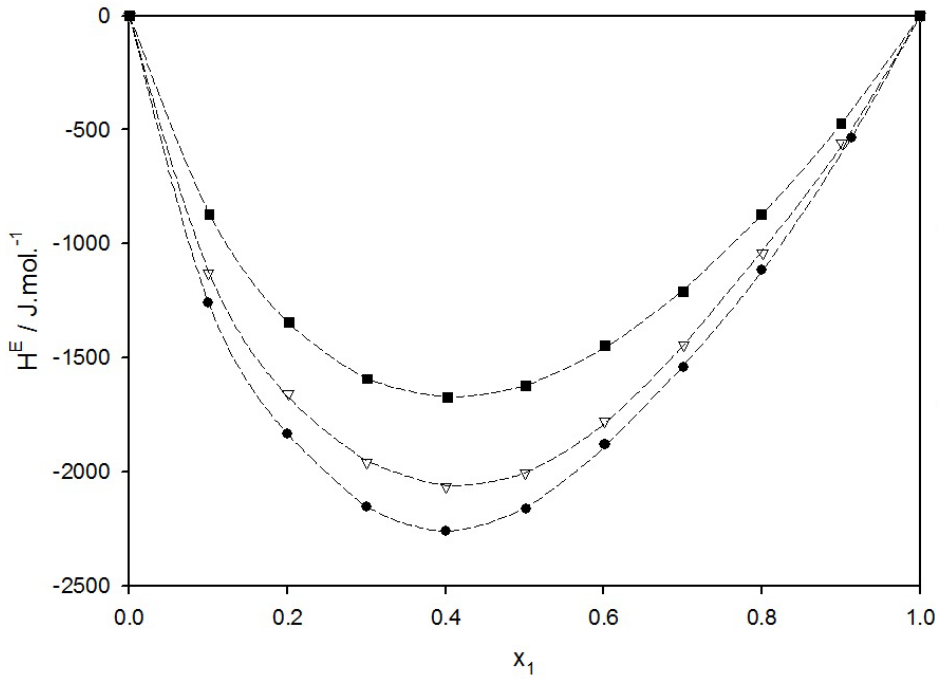

Figure 3.14. Molar excess enthalpy of a (HEP (1) + water (2)) binary system at three temperatures: ●,298.15K; ▽, 313.15K; ■, 333.15K; --, Redlich Kister

Table 3.11. Redlich-Kister coefficients for the molar excess enthalpies of a (HEP (1) + water (2)) binary system at three temperatures (298.15, 313.15 and 353.15K)

T /K	Redlich Kister Coefficients						%RD
	a_0	a_1	a_2	a_3	a_4	a_5	
298.15	-8635.39	3934.40	-362.50	-2398.62	-3695.54	5150.19	0.21
313.15	-8018.92	2743.90	87.17	1677.58	-3502.17	---	0.70
333.15	-6487.56	2186.40	-876.95	792.42	-911.78	---	0.37

Table 3.12. Molar enthalpies of HEP at infinite dilution in water (ΔH_1^{∞}) and of water at infinite dilution in HEP (ΔH_2^{∞}) at three temperatures (298.15, 313.15 and 353.15K)

T/K	ΔH_1^{∞} (KJ·mol^{-1})	ΔH_2^{∞} (KJ·mol^{-1})
298.15	-19.4	-6.0
313.15	-15.9	-7.0
333.15	-11.3	-5.3

Table 3.13. NRTL and UNIQUAC coefficients for the molar excess enthalpies of a (HEP (1) + water (2)) binary system at three temperatures (298.15, 313.15 and 353.15K)

NRTL			UNIQUAC		
Parameters	**Values**	**%RD**	**Parameters**	**Values**	**%RD**
a_{12}	2.01		a_{12}	0.93	
a_{21}	4.09		a_{21}	-1.27	
b_{12} / K	-666.61	2.63	b_{12} / K	-493.09	3.94
b_{21} / K	-925.62		b_{21} / K	604.67	
α	0.80				

Table 3.14. UNIFAC coefficients for the molar excess enthalpies of a (HEP (1) + water (2)) binary system at three temperatures (298.15, 313.15 and 353.15K)

Groups (m) / (n)	**Parameters**	**CH_2**	**CH_2N**	**OH**	**H_2O**	**%RD**
CH_2	a_{nm}/K	---	1098.89	1014.33	121.89	0.40
	b_{nm}	---	33.13	30.58	-8.16	
	c_{nm}/K^{-1}	---	-0.01	-0.01	0.00	
CH_2N	a_{nm}/K	-289.79	---	1489.00	-143.06	
	b_{nm}	-5.21	---	22.91	-0.31	
	c_{nm}/K^{-1}	0.00	---	-0.11	0.00	
OH	a_{nm}/K	594.27	-2449.09	---	465.68	
	b_{nm}	-2.58	-3.24	---	-0.36	
	c_{nm}/K^{-1}	-0.01	0.02	---	-0.01	
H_2O	a_{nm}/K	244.66	244.47	-73.37	---	
	b_{nm}	-4.97	-4.82	2.12	---	
	c_{nm}/K^{-1}	0.01	0.01	0.00	---	

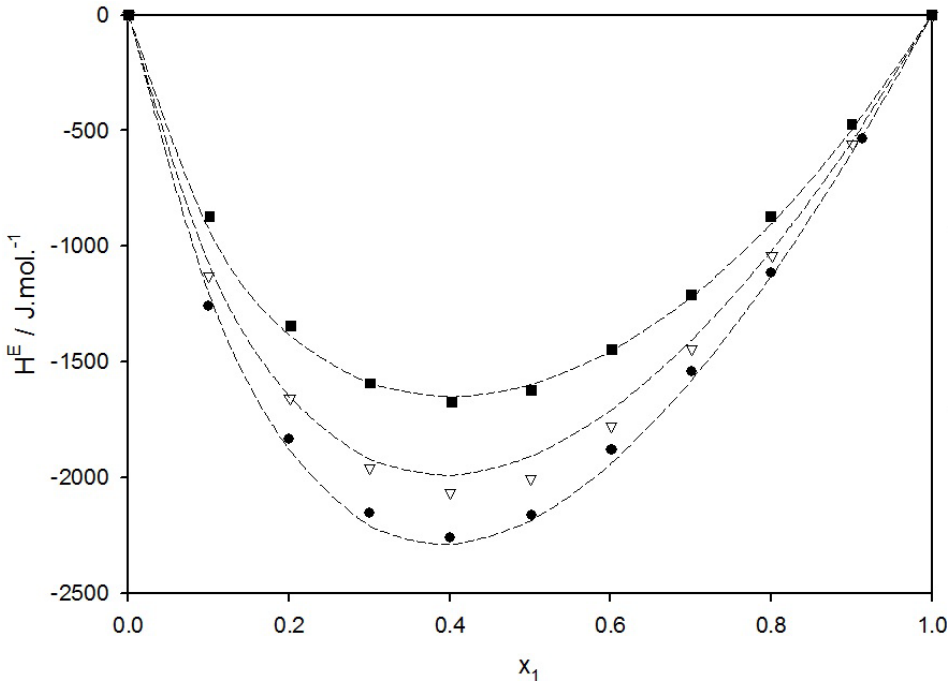

Figure 3.15. Molar excess enthalpy of a (HEP (1) + water (2)) binary system at three temperatures: ●,298.15K; ▽, 313.15K; ■, 333.15K; --, NRTL

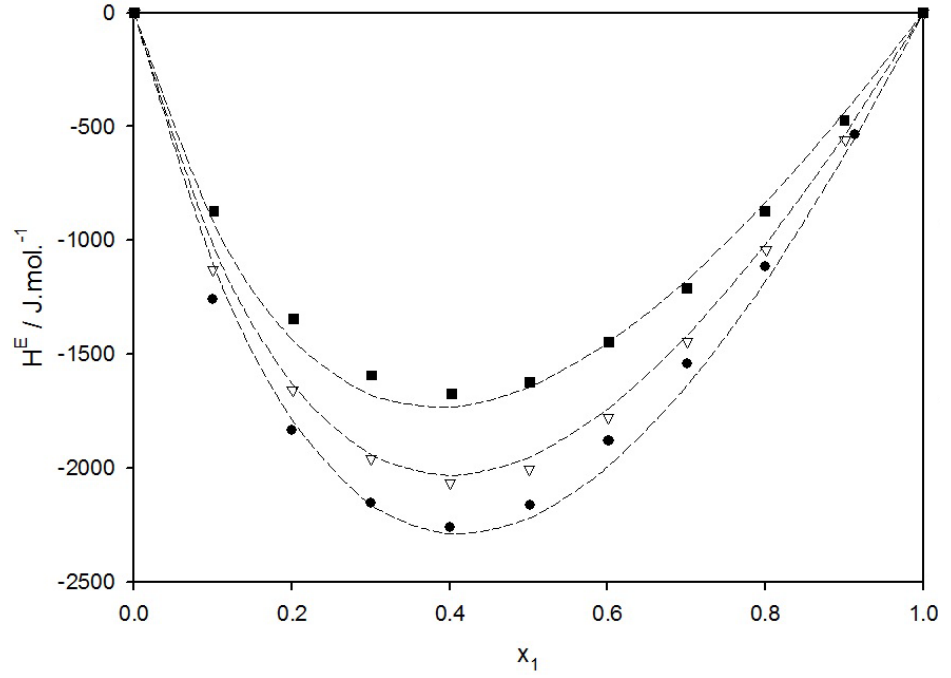

Figure 3.16. Molar excess enthalpy of a (HEP (1) + water (2)) binary system at three temperatures: ●,298.15K; ▽, 313.15K; ■, 333.15K; --, UNIQUAC

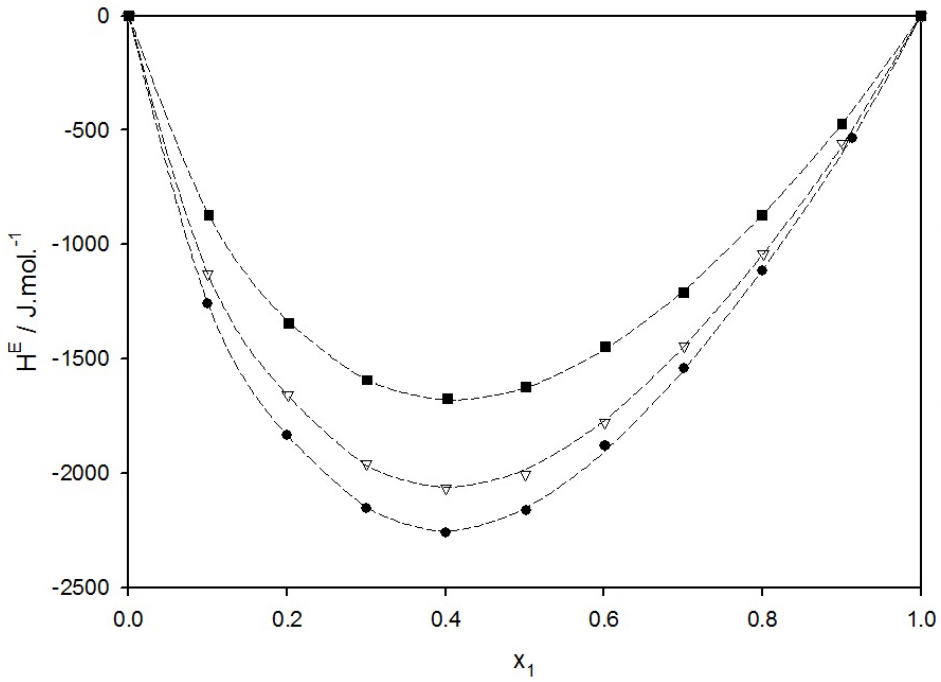

Figure 3.17. Molar excess enthalpy of a (HEP (1) + water (2)) binary system at three temperatures: ●,298.15K; ▽, 313.15K; ■, 333.15K; --, UNIFAC

The molar enthalpy of solution of HEP at infinite dilution (ΔH_1^{∞}) in water shows a linearity with temperature. Enthalpies at infinite dilution for HEP and water are presented in Table 3.12. Figures 3.15, 3.16, and 3.17 present the experimental H^E of HEP + water binary system for three temperatures along with the fitted curves of NRTL, UNIQUAC and UNIFAC models, respectively. The built-in algorithm of ASPEN Plus software, also known as the "Data Regression System" (DRS) was used for the regression of the experimental molar heat of mixing data. Percentages of relative deviation (%RD)[57] between the experimental data and the fitted data for the three models are 2.59, 3.94, and 0.40%, respectively, and the parameters of the above models are presented in Tables 3.13 and 3.14. Among these models, UNIFAC furnished the best fitting to the experimental molar H^E data for this system.

3.12.8. Diglycolamine (DGA)

Molar heats of mixing for the (DGA (1) + Water (2)) binary system were measured, experimentally, at three different temperatures (298.15, 313.15, and 333.15K). The experimental data are given in Table 6.14 showing the mole fractions dependency at several temperatures which are represented in Figure 3.18. The molar heats of mixing plots for the three temperatures were negative with a minimum value of around x_1 = 0.35. As mentioned earlier, the relative magnitude and the negative sign of the molar heat of mixing indicate a strong exothermic mixing process between DGA and water and this shows that the interaction is energetically favourable and forms a stable structure (or cluster).[110] The exothermic mixing process between DGA and water is the result of the amine-water reaction[112] and several group interactions to create H-bonds such as -NH$^{\cdots}$:OH_2, -OH$^{\cdots}$:OH_2, -HO:$^{\cdots}$HOH, >O:$^{\cdots}$HOH and amineH^{+-}HO:$^{\cdots}$HOH. The molar heats of mixing are more negative at temperatures of 298.15K, compared to values at 313.15K and 333.15K, as shown in Figure 3.18.

The coefficients of the Redlich-Kister relation and percentages of relative deviation (%RD)[57] are listed in Table 3.15. The calculated molar heats of mixing for all three temperatures, employing the Redlich-Kister equation[32], are plotted as dashed lines in Figure 3.18. The percentages of relative deviation (%RD)[57] were 0.38, 0.43, and 0.29% for 298.15, 313.15 and 333.15K, respectively.

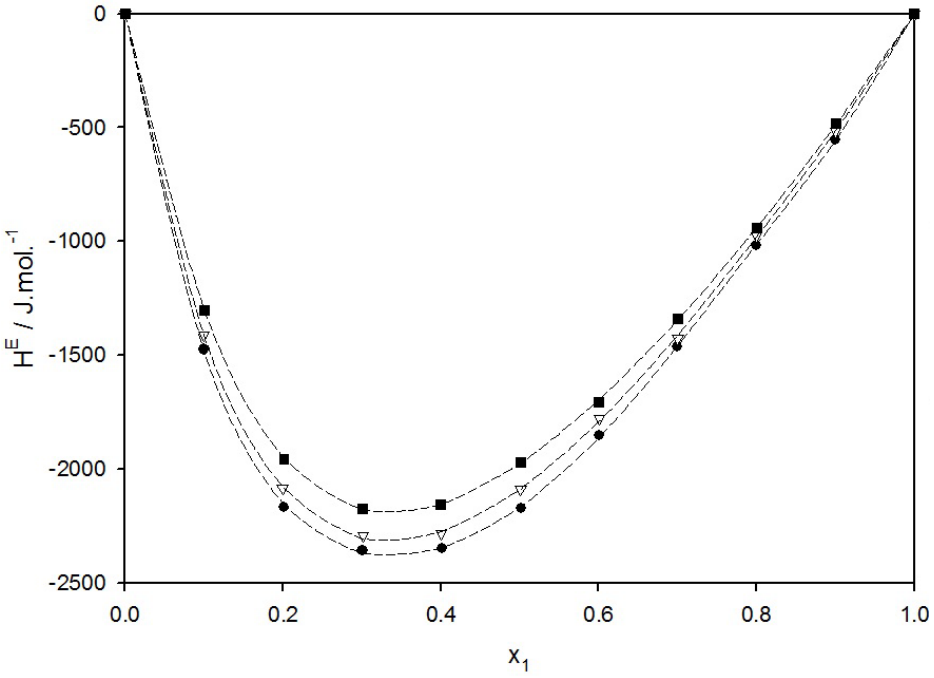

Figure 3.18. Molar excess enthalpy of a (DGA (1) + water (2)) binary system at three temperatures: ●,298.15K; ▽, 313.15K; ■, 333.15K; --, Redlich Kister

Table 3.15. Redlich-Kister coefficients for the molar excess enthalpies of a (DGA (1) + water (2)) binary system at three temperatures (298.15, 313.15 and 353.15K)

T /K	Redlich Kister Coefficients						%RD
	a_0	a_1	a_2	a_3	a_4	a_5	
298.15	-8673.45	4908.85	-2378.64	3413.32	-2773.52	-1618.27	0.38
313.15	-8359.02	4945.05	-2899.29	2383.20	-1278.53	-533.76	0.43
333.15	-7905.38	4720.54	-3014.22	1451.73	-262.09	---	0.29

Table 3.16. Molar enthalpies of DGA at infinite dilution in water (ΔH_1^{∞}) and of water at infinite dilution in DGA (ΔH_2^{∞}) at three temperatures (298.15, 313.15 and 353.15K)

T/K	ΔH_1^{∞} (KJ·mol^{-1})	ΔH_2^{∞} (KJ·mol^{-1})
298.15	-20.5	-7.1
313.15	-19.3	-5.7
333.15	-17.3	-5.0

Table 3.17. NRTL and UNIQUAC coefficients for the molar excess enthalpies of a (DGA (1) + water (2)) binary system at three temperatures (298.15, 313.15 and 353.15K)

NRTL			UNIQUAC		
Parameters	**Values**	**%RD**	**Parameters**	**Values**	**%RD**
a_{12}	-0.11		a_{12}	-1.22	
a_{21}	1.64		a_{21}	-1.77	
b_{12} / K	-356.09	1.05	b_{12} / K	280.68	1.02
b_{21} / K	-432.57		b_{21} / K	469.72	
α	0.80				

Table 3.18. UNIFAC coefficients for the molar excess enthalpies of a (DGA (1) + water (2)) binary system at three temperatures (298.15, 313.15 and 353.15K)

Groups (m) / (n)	Parameters	CH_2	CH_2O	CH_2NH	OH	H_2O	%RD
CH_2	a_{nm}/K	---	192.26	175.35	244.10	-53.63	
	b_{nm}	---	-0.56	-0.33	-2.24	0.04	
	c_{nm}/K^{-1}	---	0.00	0.00	0.00	0.00	
CH_2O	a_{nm}/K	192.56	---	207.95	270.01	-63.64	
	b_{nm}	-0.16	---	-0.29	-2.19	0.02	
	c_{nm}/K^{-1}	0.00	---	0.00	0.00	0.00	
CH_2NH	a_{nm}/K	175.36	209.86	---	256.14	-57.91	
	b_{nm}	-0.19	-0.56	---	-2.22	0.03	0.31
	c_{nm}/K^{-1}	0.00	0.00	---	0.00	0.00	
OH	a_{nm}/K	309.84	330.54	334.04	---	-97.33	
	b_{nm}	-0.66	-1.14	-0.88	---	0.04	
	c_{nm}/K^{-1}	0.00	0.00	0.00	---	0.00	
H_2O	a_{nm}/K	-36.86	-41.20	-39.22	-55.87	---	
	b_{nm}	-0.21	-0.12	-0.99	0.42	---	
	c_{nm}/K^{-1}	0.00	0.00	0.00	0.00	---	

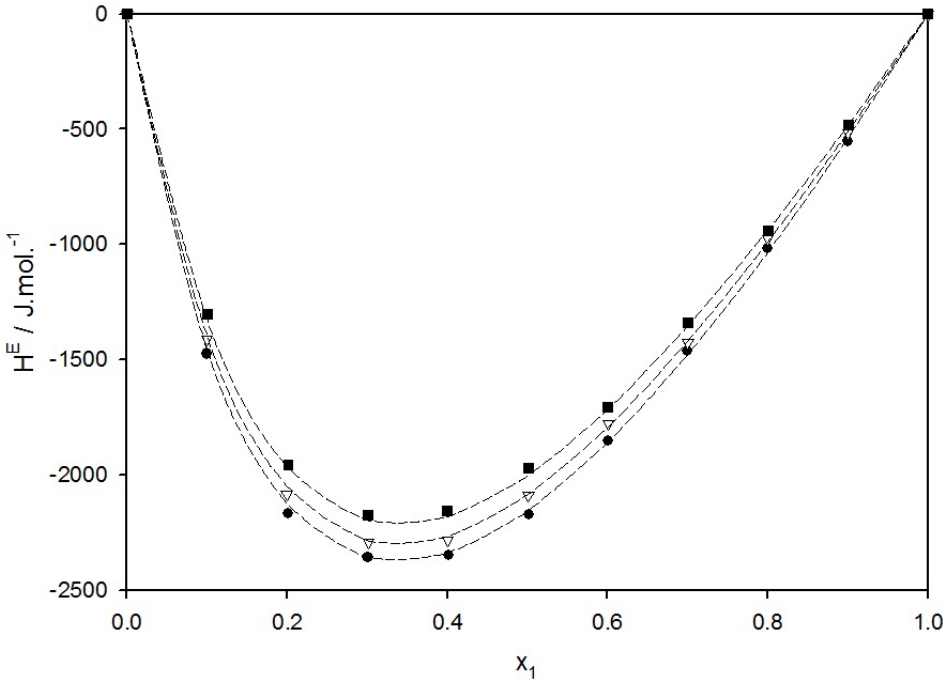

Figure 3.19. Molar excess enthalpy of a (DGA (1) + water (2)) binary system at three temperatures: ●,298.15K; ▽, 313.15K; ■, 333.15K; --, NRTL.

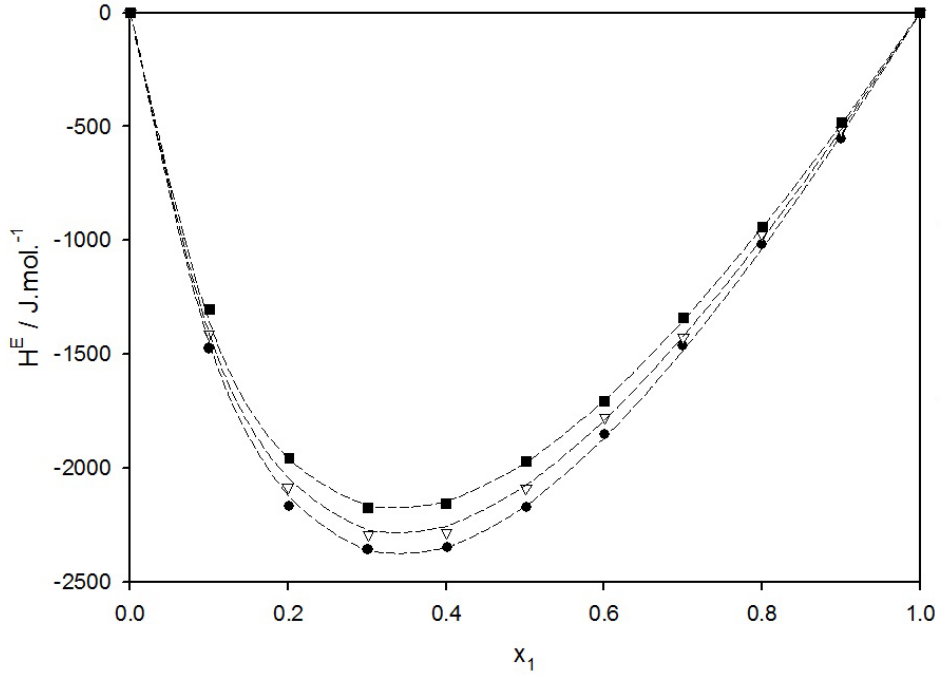

Figure 3.20. Molar excess enthalpy of a (DGA (1) + water (2)) binary system at three temperatures: ●,298.15K; ▽, 313.15K; ■, 333.15K; --, UNIQUAC

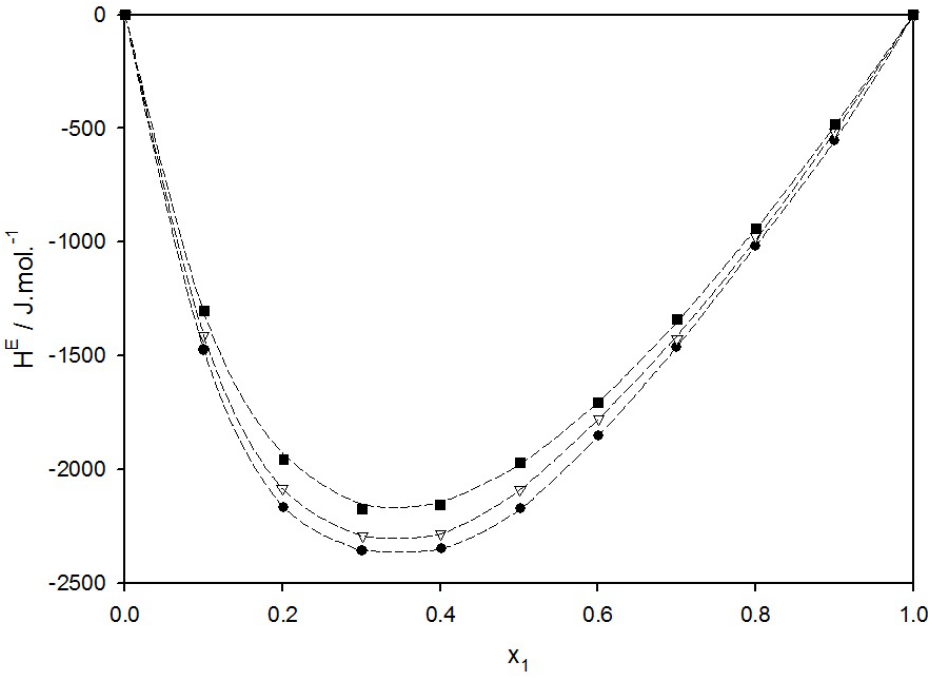

Figure 3.21. Molar excess enthalpy of a (DGA (1) + water (2)) binary system at three temperatures: ●, 298.15K; ▽, 313.15K; ■, 333.15K; --, UNIFAC

Both the molar enthalpy of solution of DGA at infinite dilution (ΔH_1^{∞}) in water and water at infinite dilution (ΔH_2^{∞}) in DGA were derived using the method suggested by Maham et al.[65]s The data shows that the molar enthalpy of solution of DGA at infinite dilution (ΔH_1^{∞}) in water varies linearly with temperature. Enthalpies at infinite dilution for DGA and water are presented in Table 3.16. Figures 3.19, 3.20, and 3.21 represent the experimental H^E of DGA + water binary system for the three temperatures along with the fitted curves of NRTL, UNIQUAC and UNIFAC models, respectively. Percentages of relative deviation (%RD)[57] between the experimental data and the fitted data for the three models are 0.79, 1.02, and 0.31, respectively. The parameters of the above models are presented in Tables 3.17 and 3.18. Among these models, UNIFAC allowed for the best fitting to the experimental molar H^E data for this system.

3.12.9. Bis(2-methoxyethyl)amine (BMOEA)

Molar heats of mixing for the (BMOEA (1) + Water (2)) binary system were measured at three different temperatures 298.15, 313.15, and 333.15K. The experimental data are given in Table 6.15 showing the mole fractions dependency at several temperatures and are represented in Figure 3.22. The molar heats of mixing plots for above three temperatures were negative with a minimum value of around x_1 = 0.30. Relative magnitude of molar heat of mixing and its negative sign indicate a strong exothermic mixing process between BMOEA and water, which shows that the interaction of BMOEA with water is energetically favourable and forms a stable structure (or cluster).[110] The exothermic mixing process between BMOEA and water is the result of a amine-water reaction[112] and several group interactions are discussed in DGA to form H-bonds. The molar heats of mixing are more negative at temperatures 298.15K compared to the values 313.15K and 333.15K, as shown in Figure 3.22.

The coefficients of the Redlich-Kister relation and percentages of relative deviation (%RD)[57] are listed in Table 3.19. The calculated molar heats of mixing for all three temperatures, employing the Redlich-Kister equation[32], are plotted as dashed lines in Figure 3.22. The percentages of relative deviation (%RD)[57] were 0.37, 0.42, and 0.98% for 298.15, 313.15 and 333.15K, respectively.

Both the molar enthalpy of solution of BMOEA at infinite dilution (ΔH_1^{∞}) in water and water at infinite dilution (ΔH_2^{∞}) in BMOEA were derived using the method suggested by Maham et al.[65]

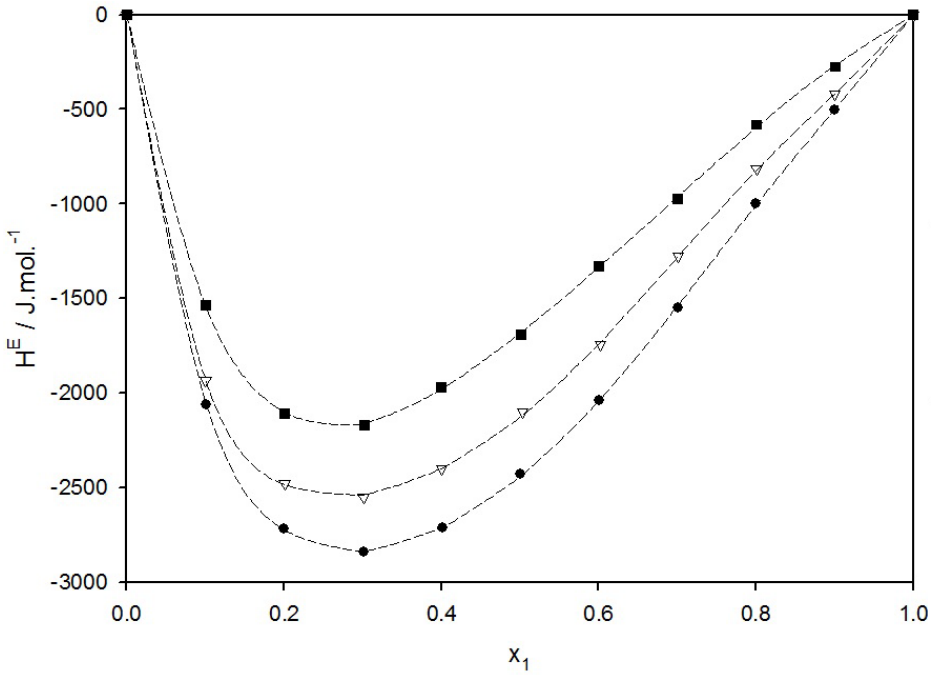

Figure 3.22. Molar excess enthalpy of a (BMOEA (1) + water (2)) binary system at three temperatures: ●,298.15K; ▽, 313.15K; ■, 333.15K; --, Redlich Kister

Table 3.19. Redlich-Kister coefficients for the molar excess enthalpies of a (BMOEA (1) + water (2)) binary system at three temperatures (298.15, 313.15 and 353.15K)

T /K	Redlich Kister Coefficients						%RD
	a_0	a_1	a_2	a_3	a_4	a_5	
298.15	-9766.43	6736.14	-3235.81	6051.84	-5697.07	387.69	0.37
313.15	-8511.58	6665.33	-2543.52	4946.00	-7092.29	1681.69	0.42
333.15	-6740.03	6595.47	-4159.96	3507.57	-1567.76	---	0.98

Table 3.20. Molar enthalpies of BMOEA at infinite dilution in water (ΔH_1^{∞}) and of water at infinite dilution in BMOEA (ΔH_2^{∞}) at three temperatures (298.15, 313.15 and 353.15K)

T/K	ΔH_1^{∞} (KJ·mol^{-1})	ΔH_2^{∞} (KJ·mol^{-1})
298.15	-31.9	-5.5
313.15	-31.4	-4.8
333.15	-22.6	-2.4

Table 3.21. NRTL and UNIQUAC coefficients for the molar excess enthalpies of (BMOEA (1) + water (2)) binary system at three temperatures (298.15, 313.15 and 353.15K)

NRTL			UNIQUAC		
Parameters	**Values**	**% RD**	**Parameters**	**Values**	**%RD**
a_{12}	-0.17		a_{12}	24.07	
a_{21}	5.38		a_{21}	-4.75	
b_{12} / K	-337.44	2.68	b_{12} / K	-48.51	5.29
b_{21} / K	-1368.52		b_{21} / K	1243.20	
α	0.8				

Table 3.22. UNIFAC coefficients for the molar excess enthalpies of a (BMOEA (1) + water (2)) binary system at three temperatures (298.15, 313.15 and 353.15K)

Groups (m) / (n)	**Parameters**	**CH_2**	**CH_2O**	**CH_2N**	**H_2O**	**%RD**
CH_2	a_{nm}/K	---	97.95	17.24	50.05	1.03
	b_{nm}	---	0.55	-13.58	2.62	
	c_{nm}/K^{-1}	---	0.00	0.01	0.00	
CH_2O	a_{nm}/K	-723.49	---	695.86	-98.59	
	b_{nm}	0.00	---	-6.19	-0.43	
	c_{nm}/K^{-1}	0.01	---	0.00	0.00	
CH_2N	a_{nm}/K	1815.42	-666.61	---	-1025.75	
	b_{nm}	0.01	-3.73	---	-1.11	
	c_{nm}/K^{-1}	-0.03	0.01	---	0.02	
H_2O	a_{nm}/K	-87.03	-57.97	-30.14	---	
	b_{nm}	7.22	8.39	-3.00	---	
	c_{nm}/K^{-1}	0.00	0.00	0.00	---	

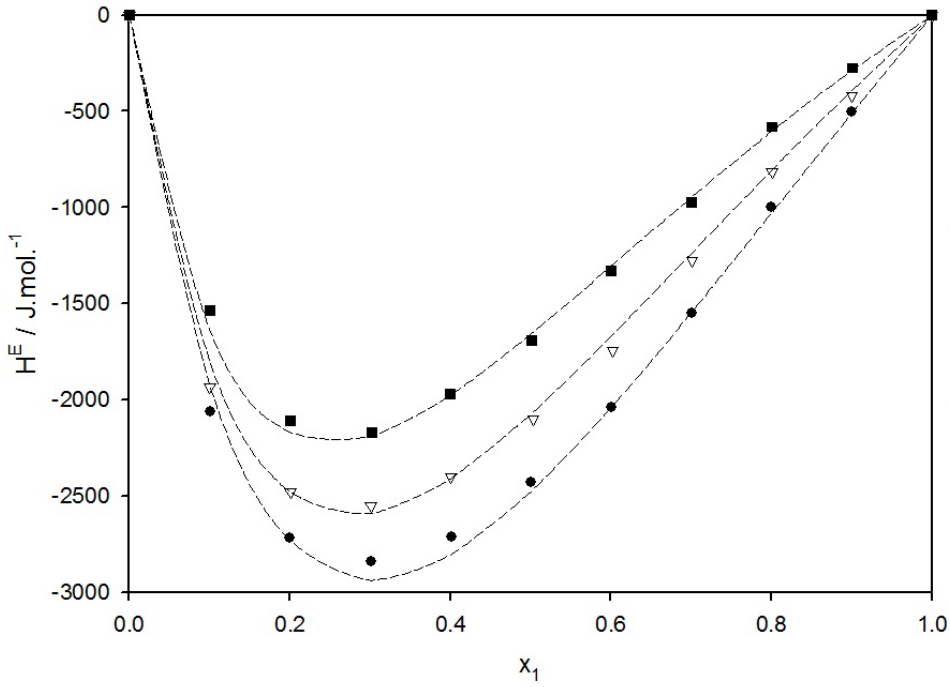

Figure 3.23. Molar excess enthalpy of a (BMOEA (1) + water (2)) binary system at three temperatures: ●,298.15K; ▽, 313.15K; ■, 333.15K; --, NRTL

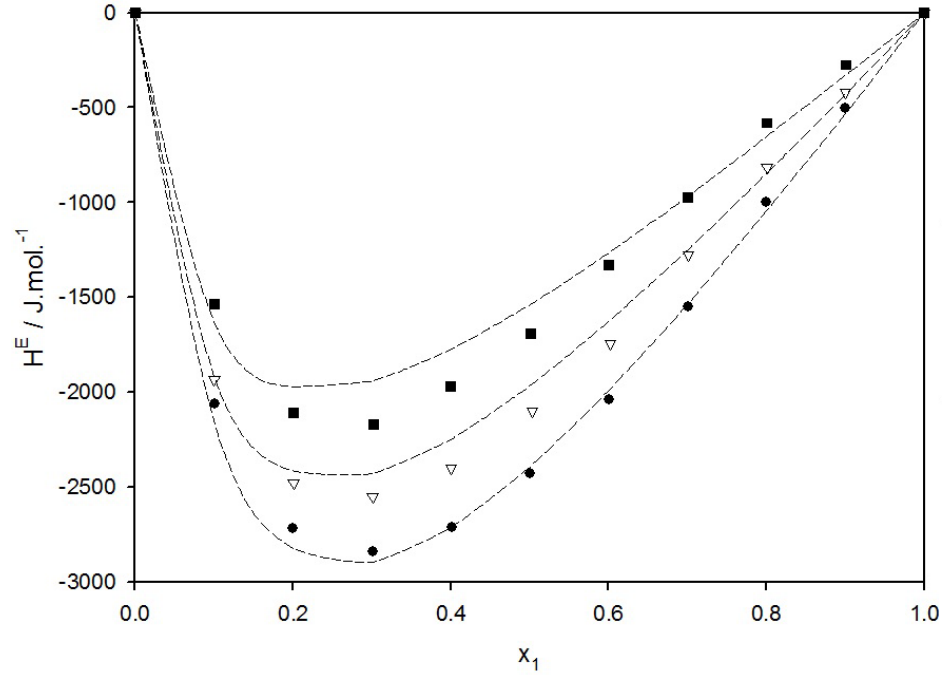

Figure 3.24. Molar excess enthalpy of a (BMOEA (1) + water (2)) binary system at three temperatures: ●, 298.15K; ▽, 313.15K; ■, 333.15K; --, UNIQUAC

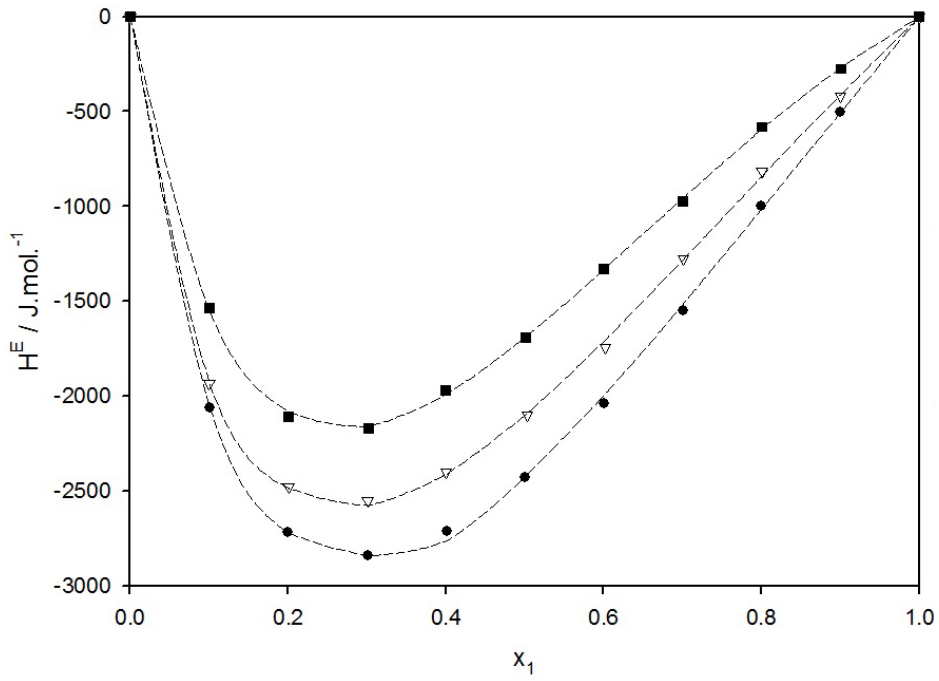

Figure 3.25. Molar excess enthalpy of a (BMOEA (1) + water (2)) binary system at three temperatures: ●, 298.15K; ▽, 313.15K; ■, 333.15K; --, UNIFAC

The molar enthalpy of solution of water at infinite dilution (ΔH_2^{∞}) in BMOEA shows a linear dependency with temperature. Enthalpies at infinite dilution for BMOEA and water are presented in Table 3.20. Figures 3.23, 3.24, and 3.25 represent the experimental H^E of BMOEA + water binary systems for three temperatures along with the fitted curves of NRTL, UNIQUAC and UNIFAC models, respectively. The percentages of relative deviation (%RD)[57] between the experimental data and the fitted data for the three models are 2.68, 5.29, and 1.03%, respectively, and the parameters of the above models are presented in Tables 3.21 and 3.22. Among these models, UNIFAC had the best fitting to the experimental molar H^E data for this system.

3.13. Comparison of the excess molar enthalpy data of different alkanolamines

A comparison among the five molar excess enthalpies is shown in Figures 3.26, 3.27 and 3.28. Among the five amine-water binary systems, BMOEA + water system exhibited the lowest values of molar excess enthalpy at 298.15K followed by DGA + water, HEP + water, PAE + water and BAE + water. The minimum molar excess enthalpy values for all five amines occurred in the water region near 0.3 to 0.45 mole fraction, except for BAE which occurred near 0.5 mole fraction. It is at this mixing ratio (minimum H^E) value that the enthalpy is the most exothermic which corresponds to the maximum number of interactions (H-bonds) between the alkanolamine and water molecules. The interaction of alkanolamines with water are strongly dependent on the mixing ratio.[110]

Alkanolamines are multifunctional compounds with amine, alcohol, ether and alkyl groups. In general, they are soluble in water and form H-bonds due to the hydroxyl, ether and amino groups. Considering the molecular structures of ethanol and monoethanolamine (MEA), one hydrogen of the methyl ($–CH_3$) group of ethanol (EtOH)[116] is substituted by an amine ($–NH_2$) group to form monoethanolamine (MEA). As a result of this substitution, it was experimentally observed that a large amount of heat was released or in other words, the molar excess enthalpy decreased, as shown in Figure 3.29. This is due to the interaction between the nitrogen of an amine group with the water molecule and during this reaction, a dissociation of water molecules occurs.

A comparison between alkylaminoethanols is presented in Figure 3.29. Methylaminoethanol (MAE)[4] exhibited the lowest molar excess enthalpy at 298.15K followed by ethylaminoethanol (EAE)[31], PAE and BAE. This indicates the molar excess

enthalpies of alkylaminoethanol increase with an increase in the size of the carbon chain, in agreement with Mathonat et al.[31]. As previously mentioned, the molar heat of mixing became more positive as the temperature rose. In general, the effects of hydrogen-bonding decrease at higher temperatures where the kinetic energy of the molecules is enough to break these loose bonds.[115] In addition, similar contribution of alkyl- groups, observed at higher temperatures, are presented in Figures 3.30 and 3.31. The order of H^E for alkylaminoethanol is:

BAE > PAE > EAE> MAE

or Butyl > Propyl > Ethyl > Methyl (3.27)

2,3-Diethylaminoethanol (DEEA)[43] and 2-Butylaminoethanol (BAE) have the same chemical formula ($C_6H_{15}NO$) while BAE (secondary amine with butyl and one ethanol groups) has a higher molar excess enthalpy than DEEA (tertiary amine with two ethyl and one ethanol groups), as presented in Figure 3.34. 3-Amino-1-propanol (AP)[40] and Methylaminoethanol (MAE)[4] are both isomers and their chemical formula is C_3H_9NO. AP (primary amine with one propanol group) has a higher molar excess enthalpy than MAE (secondary amine with one methyl and one ethanol groups), as shown in Figure 3.34. The order of the H^E for amines is therefore:

primary amine > secondary amine > tertiary amine (3.28)

As well known in CO_2-amine kinetics, primary and secondary amines show faster reaction with CO_2 when compared to tertiary amine. The presence of hydrogen in primary and secondary amines allows for the reaction with CO_2, whereas for tertiary

amines, the absence of hydrogen makes the reaction in water quite slow as to appear to be only a physical absorption.

HEP has lower excess enthalpy as compared to PAE and BAE, whereas all have an ethanolamine group, HEP is a cyclic alkylethanolamine with a tertiary amine, while PAE and BAE are straight chain alkylethanolamines with secondary amines (Figure 3.26). Primary and secondary amines are associated with water with the hydrogen forming an H-bond. HEP is a tertiary amine and tertiary amines do not associate with water as a result of the absence of a hydrogen atom capable of forming H-bonds.[112]

In addition, considering the molecular structure of a diamine 1-(2-hydroxyethyl) piperazine (1, 2-HEPZ)[41], 4-(2-Hydroxyethyl) morpholine (4, 2-HEMO)[41]and HEP. HEP is a cyclic compound and has a higher excess molar enthalpy because the alkyl- group does not form hydrogen bonding. In contrast, the ether group of the 4, 2-HEMO forms H-bonding with water molecules, whereas the amine group reacts with water to form quaternary ammonium ion as well as it forms H-bonding with water and has the lowest excess molar enthalpy as presented in Figure 3.32. In adding a second amine group to form 2-HEPZ from HEP, the excess molar enthalpy is greatly increase (negative sense). In general, the molar excess enthalpies of aqueous alkanolamines increased with the increase in temperature and more or less each group contribution appeared with its own molar excess enthalpy increment pattern. Figures 3.27 and 3.28 show that the excess molar enthalpy of HEP increased abruptly at higher temperatures, and the contributions of both the cyclic alkyl- group and tertiary amine were observed.

When considering the molecular structures of Diethanolamine (DEA)[65] and Bis(2-methoxyethyl)amine (BMOEA), it is obvious that each hydrogen of the hydroxyl (-OH) group of DEA is substituted with a methyl ($–CH_3$) group. Figure 3.33 shows, that as a result of these substitutions, a decrease in the molar excess enthalpy occurs. The H-bond between an ether group and a water molecule is stronger than a hydroxyl group and a water molecule.

Furthermore, by comparing the molecular structures of MEA and DGA, it is as if in the middle of the MEA molecule, a dimethylether group was introduced. It was experimentally discovered that despite this, the molar excess enthalpy has observed a less drastic change than that anticipated at 298.15K. In the case of DGA, the ether group releases large amounts of heat and the size of the alkyl chain increases, as observed in the case of BMOEA and alkylaminoethanols. The ether group is known to form an H-bond with water that is stronger than the one formed with a hydroxyl group.

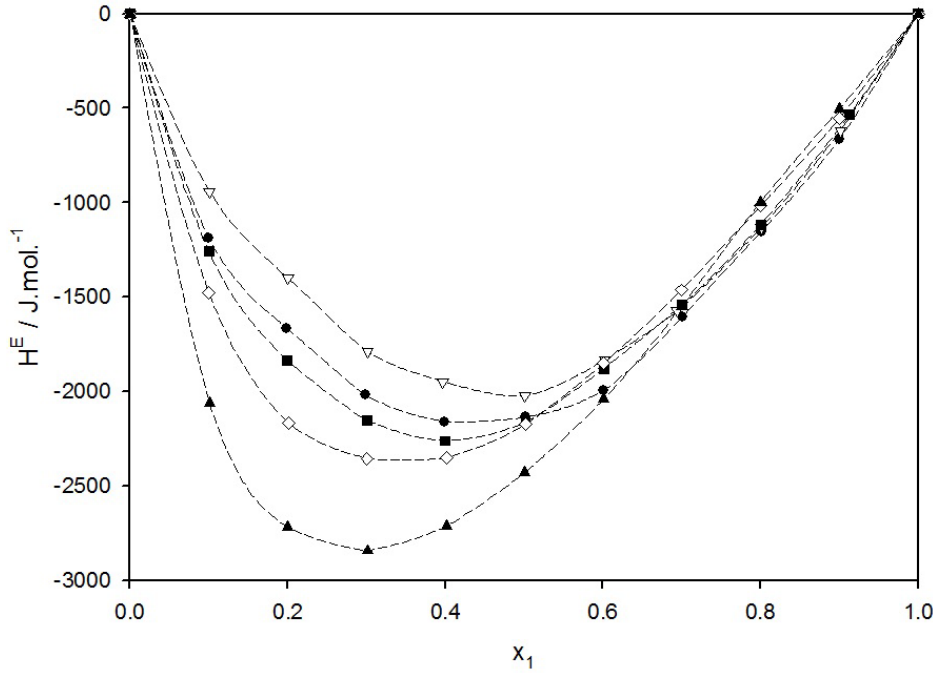

Figure 3.26. Comparison of measured excess molar enthalpies of the five selected (alkanolamines (1) + water (2)) binary systems at 298.15K: ●-, PAE; ▽-, BAE; ■-, HEP; ◇-, DGA; ▲-, BMOEA

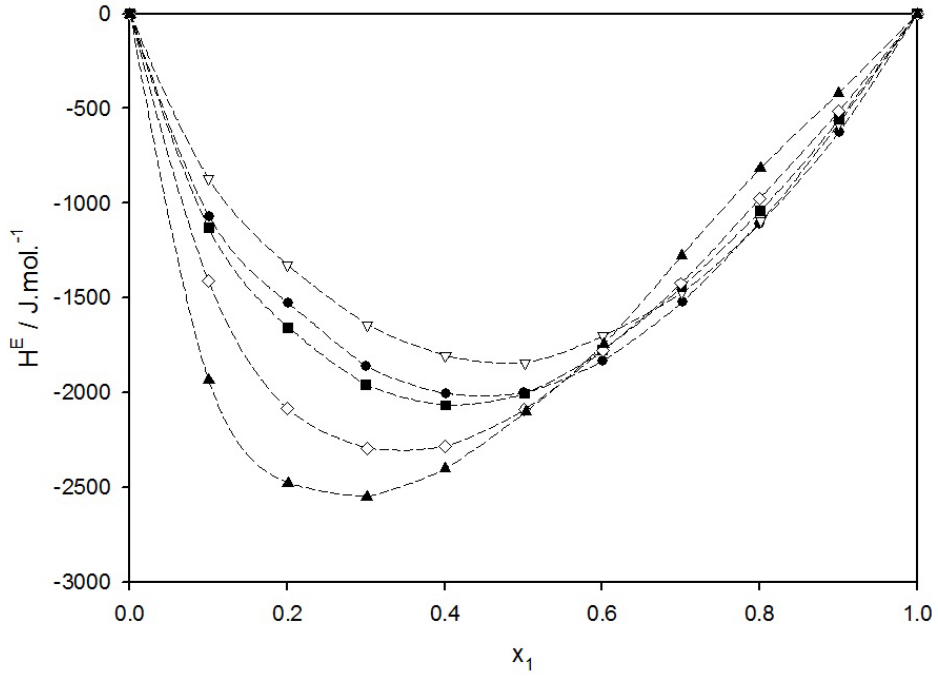

Figure 3.27. Comparison of measured excess molar enthalpies of the five selected (alkanolamines (1) + water (2)) binary systems at 313.15K: ●-, PAE; ▽-, BAE; ■-, HEP; ◇-, DGA; ▲-, BMOEA

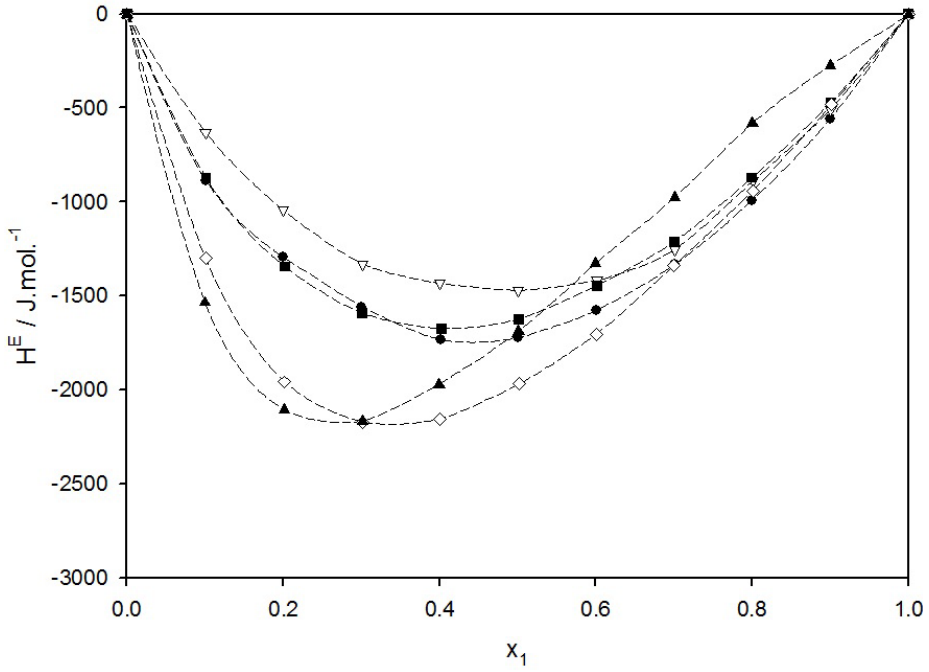

Figure 3.28. Comparison of measured excess molar enthalpies of the five selected (alkanolamines (1) + water (2)) binary systems at 333.15K: ●-, PAE; ▽-, BAE; ■-, HEP; ◇-, DGA; ▲-, BMOEA

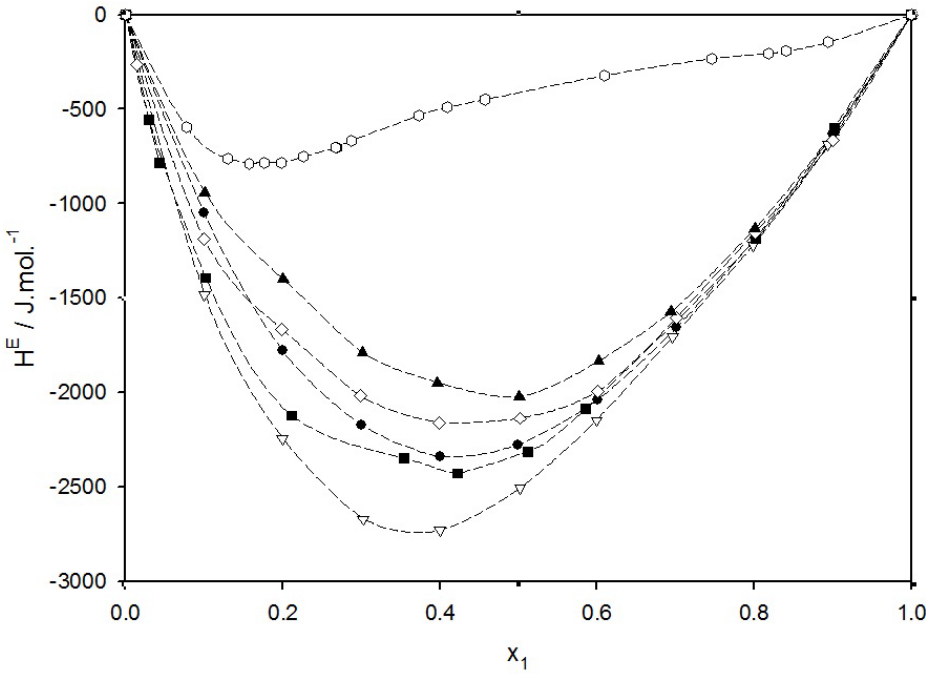

Figure 3.29. Comparison of measured excess molar enthalpies of solvent (1) + water (2) binary systems at 298.15K: ○-, EtOH[116]; ●-, MEA; ▽-, MAE[4]; ■-, EAE[31]; ◇-, PAE; ▲-, BAE

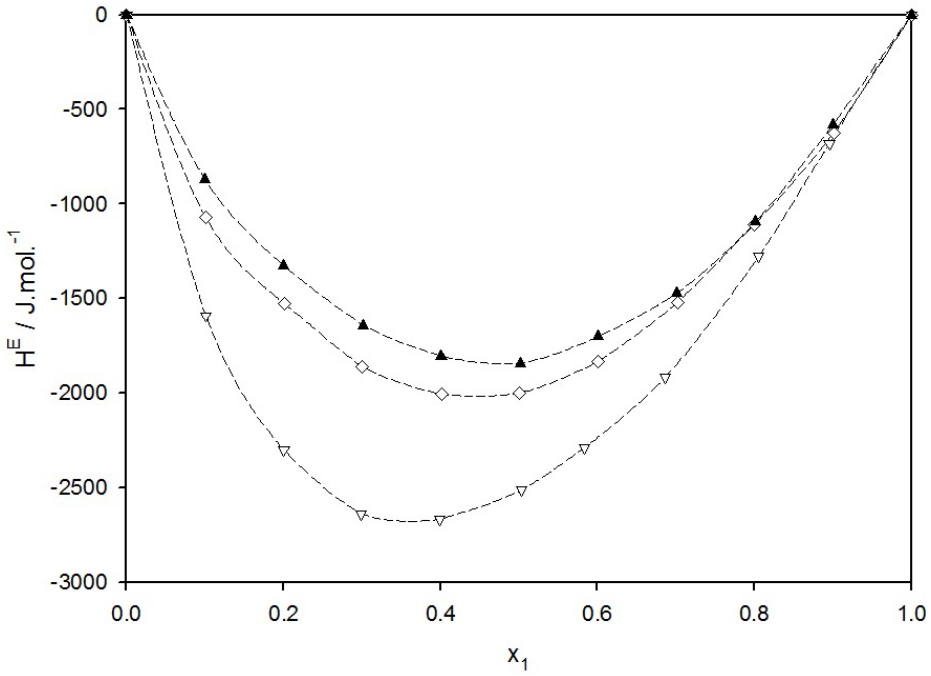

Figure 3.30. Comparison of measured excess molar enthalpies of alkylaminoethanol (1) + water (2) binary systems at 313.15K: ▽-, MAE[4]; ◇-, PAE; ▲-, BAE

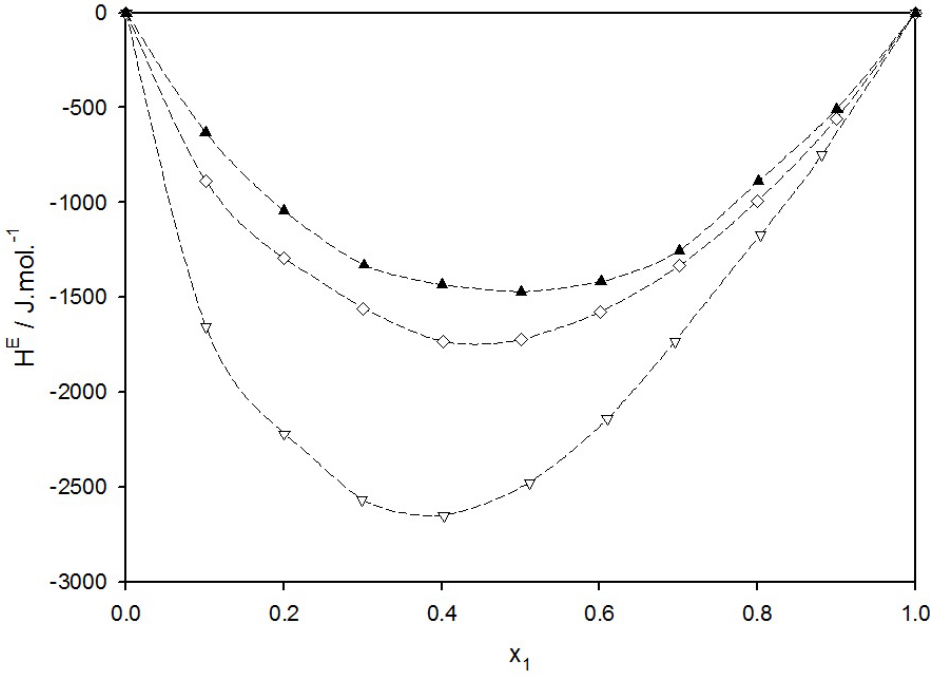

Figure 3.31. Comparison of measured excess molar enthalpies of alkylaminoethanol (1) + water (2) binary systems at 333.15K: ▽-, MAE[4]; ◇-, PAE; -▲-, BAE

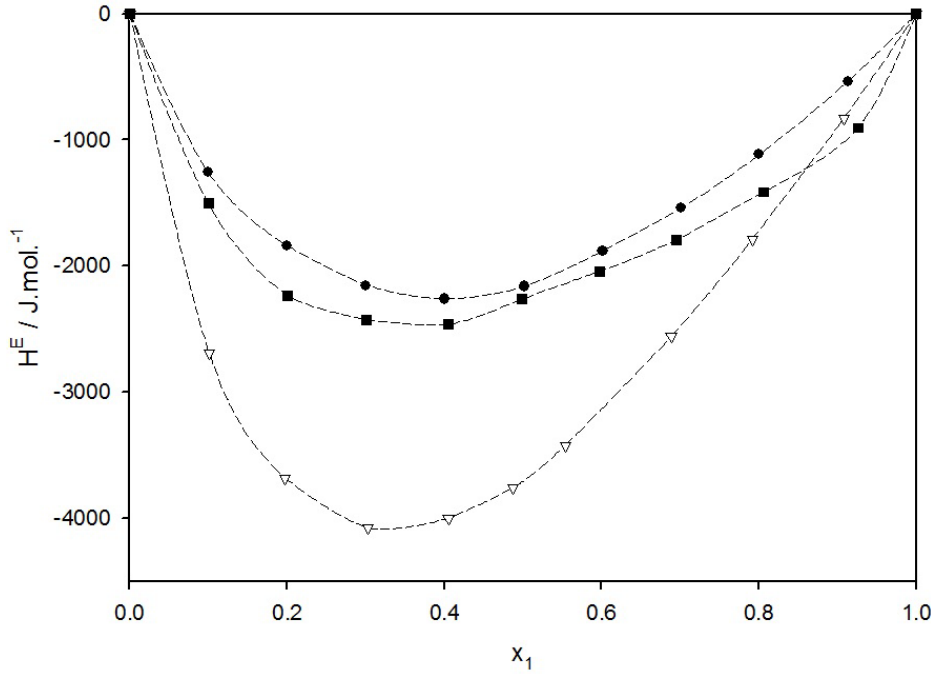

Figure 3.32. Comparison of measured excess molar enthalpies of alkanolamine (1) + water (2) binary systems at 298.15K: ●-, HEP; ▽-, 1, 2-HEPZ[41]; ■-, 4, 2-HEMO[41]

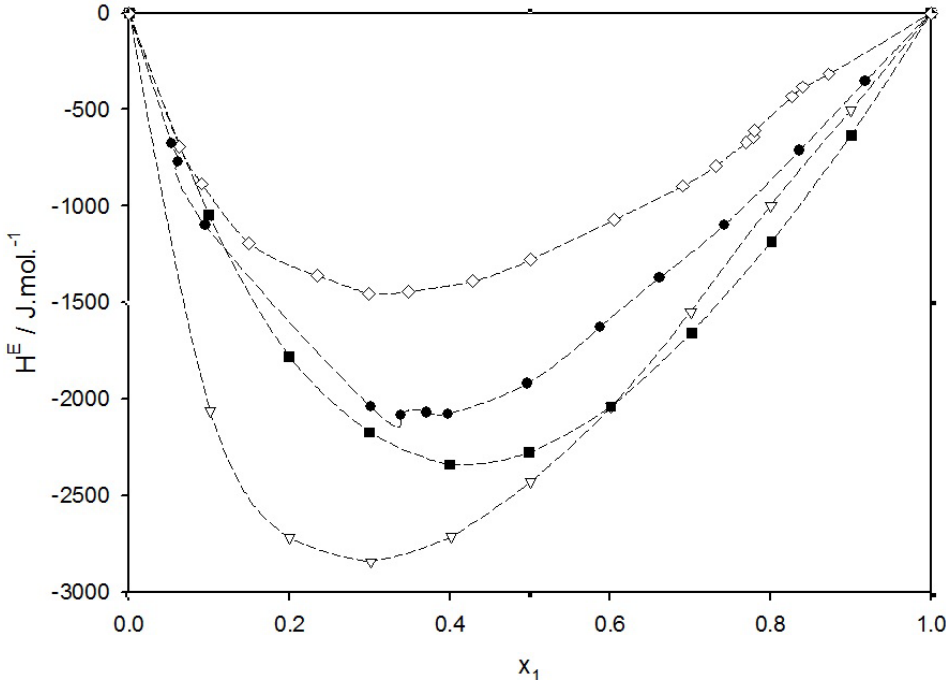

Figure 3.33. Comparison of measured excess molar enthalpies of alkanolamine (1) + water (2) binary systems at 298.15K: ■-, MEA; ●-, DEA[65] ; ◇-, TEA[65]; ▽-, BMOEA

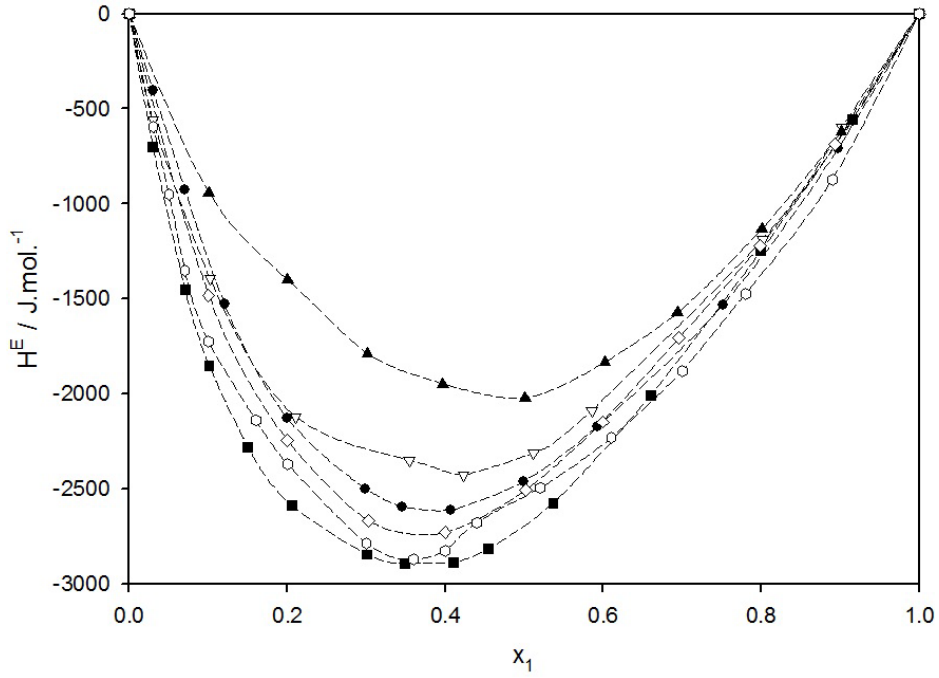

Figure 3.34. Comparison of measured excess molar enthalpies of alkanolamine (1) + water (2) binary systems at 298.15K: ●-, AP[4]; ▽-, EAE[31]; ■-, DMAE[4]; ◇-, MAE[4]; ▲-, BAE; ○-, DEEA[43]

"And certainly did We create man from an extract of clay. Then We placed him as a sperm-drop in a firm lodging [i.e., the womb]. Then We made the sperm-drop into a clinging clot, and We made the clot into a lump [of flesh], and We made [from] the lump, bones, and We covered the bones with flesh; then We developed him into another creation. So blessed is Allah, the best of creators".

(Quran: 23:12-14)

4. CONCLUSION AND FUTURE WORK

4.1. Conclusion

Molar heat capacities of aqueous EAE, PAE, BAE, HEP, and BMOEA solutions were measured at eleven temperatures ranging from 303.15 to 353.15K for the entire range of mole fractions. Both BMOEA and BAE exhibited the maximum Cp values whereas, EAE had the lowest values. Cp increased with an increase in the size of the alkyl group. Primary amines where associated with the lowest values, followed by secondary and tertiary amines. Cyclic alkyl groups (excluding aromatic amines) were associated with values lower than straight chains, and the ether group contributed to a higher heat capacity than the hydroxyl group.

Derived molar excess heat capacity (Cp^E) values were positive at all temperatures and mole fractions. The data were correlated as a function of x_1 using the Redlich-Kister expression. The shape of all curves for Cp^E and reduced Cp^E, were of the general case (compounds with differences in polarity and size) as categorized by Desnoyers and Perron. [47] Partial molar excess quantities of amines did not show any particular trend

associated with temperature. Percentages of relative deviation of all predicted Cp data for GAA and MCA were found to be 1.83 and 2.64%, respectively.

Alkanolamines are usually water soluble and form H-bonds due to the presence of hydroxyl, ether and amine groups. Amine groups acting as strong bases react with water molecule. BMOEA exhibited the lowest values for H^E at 298.15K, followed by DGA, HEP, PAE and BAE. The excess enthalpies increased with an increase in the size of the carbon chain, in agreement with the conclusion of Mathonat et al.[31] H^E becomes more positive as the temperature increases. Cyclic amines (not including aromatic amines) had lower values than straight chain amines. Tertiary amines exhibited the lowest values, followed by secondary, then primary amines. In general, the ether group formed stronger H-bonding with water than the hydroxyl group.

The Redlich–Kister expression was used to correlate the experimentally measured H^E data as a function of x_1. Molar enthalpies at infinite dilution were calculated from the coefficients of Redlich–Kister. Data were regressed using NRTL, UNIQUAC and the modified UNIFAC (Dortmund) model. The modified UNIFAC correlated with the lowest %RD for all systems.

4.2. Future work

The folowing work is suggested:

- The measurement of molar heat capacity and the molar excess enthalpy for binary mixtures of alkanolamines at higher temperatures and for ternary mixtures of alkanolamines at different temperatures.
- Determination of molar heat capacity and molar excess enthalpy for CO_2 and H_2S loaded alkanolamines at a wide range of temperatures and pressures.
- Improvement to the Group Additivity Analysis (GAA) in order to gain the ablilty to predict the heat capacity of alkanolamines in a case where the alcoholic group is 1^o, 2^o, 3^o (based on the position of OH on the carbon atom i.e. -CH_2-OH, >CH-OH, →C-OH), cyclic-CH_2 and straight chain-CH_2 group.
- Further investigation into the heat of mixing using computational chemistry is recommended.

5. REFERENCES

1. Chhetri, A.B. and Islam, M.R. (2008). *Inherently-Sustainable Technology Development*. Nova Science Publishers, Inc., New York.
2. Islam, M.R.; Chhetri, A.B. and Khan, M.M. (2010). *The Greening of Petroleum Operations: The Science of Sustainable Energy Production*. Wiley-Scrivener Publishing LLC, Canada.
3. Karim, G.A. (2010). *Handbook of Combustion* (Vol. 5). Wiley-VCH Verlag GmbH & Co. KGaA..
4. Mundhawa, M. and Henni, A. (2007). *Molar Excess Enthalpy for Various {Alkanolamine (1) + Water (2)}Systems at T = (298.15, 313.15 and 323.15) K*. Journal of Chemical Thermodynamics, 39, 1439-1451.
5. Chiu, L.F.; Liu, H.F. and Li, M.H. (1999). Heat Capacity of Alkanolamines by Differential Scanning Calorimetry. Journal of Chemical and Engineering Data, 44 (3), 631-636.
6. Chowdhury, F.A.; Okabe, H.; Shimizu, S.; Onoda, M. and Fujioka, Y. (2009). *Development of Novel Tertiary Amine Absorbent for CO_2 Capture*. Engineering Procedia-1, GHGT-9, 1241-1248.
7. Sakwattanapong, R.; Aroonwilas, A. and Veawab, A. (2005). *Behavior of Reboiler Heat Duty for CO_2 Capture Plants Using Regenerable Single and Blended Alkanolamines*. Industrial and Engineering Chemistry Research, 44, 4465-4473.
8. Erga, O.; Juliussen, O. and Lidal, H. (1995). *Carbon Dioxide Recovery by Means of Aqueous Amines*. Energy Conversion Management, 36 (6-9), 387–392.
9. Rochelle, G.; Goff, G.S.; Cullininane, T. and Freguira, S. (2002). *Research Results for CO_2 Capture from Flue Gas by Aqueous Absorption/Stripping*. In Proceedings of Lawrence Reid Gas Conditioning Conference, Norman, OK, February 25-27.
10. Czichos, H.; Saito, T. and Smith, L. (2006). *Handbook of Materials Measurement Methods*, Springer.
11. Sandler, S.I. (1999). *Chemical and Engineering Thermodynamics* (3rd ed.). John Wiley and Sons, New York, NY.

12. Smith, J.M.; Van Ness, H.C. and Abbott, M.M. (2001). *Introduction to Chemical Engineering Thermodynamics* (6th ed.). McGraw-Hill Companies Inc., New York, NY 10020, USA.

13. Larkin, J.A.; McGlashan, M.L. (1961). *A New Calorimeter for Heat of Mixing. The Heat of Mixing of Benzene with Carbon Tetrachloride*. Journal of the Chemical Society, , 3425-3432.

14. Armitage, D.A. and Morcom, K.W. (1969). *Thermodynamic Behavior of Mixture of Hexafluorobenzene with Amines. Part1 - Enthalpies of Mixing*. Transactions of the Faraday Society, 65,688-695.

15. Hill, R.J. and Swinton, F.L. (1980*). The Thermodynamic Properties of Binary Mixtures Containing Carbon Disulphide. II Excess Enthalpies*. The Journal of Chemical Thermodynamics, 12(4), 383-385.

16. van Miltenburg, J.C.; van den Berg, G.J.K. and van Bommel, M.J. (1987). *Construction of an Adiabatic Calorimeter. Measurements of Molar Heat Capacity of Synthetic Sapphire and of n-Heptane*. The Journal of Chemical Thermodynamics, 19, 1129-1137.

17. Goodwin, A.R.H.; Marsh, K.N. and Wakeham, W.A. (2003). *Measurement of the Thermodynamic Properties of Single Phases*(Vol.4). Elsevier Science, Amsterdam, The Netherlands.

18. Alonso, R.; Guerrero, R. and Corrales, J.A. (1987). *Excess Molar Enthalpies of (Methylcyclohexane+ Alkanol) at 323.15K. I. Results for n-Butanol, n-Pentanol, and n-Hexanol*. The Journal of Chemical Thermodynamics,19, 1271-1273.

19. Lim, K.H.; Whiting, W.B. and Smith, D.H. (1994). *Excess Enthalpies and Liquid-Liquid Equilibrium Phase Composition of the Nonionic Amphiphile 2-Butoxyethanol and Water*. Journal of Chemical and Engineering Data, 39, 399-403.

20. Marsh, K.N. (1978). *Chemical Thermodynamics; Specialist Periodical Reports*. The Chemical Society: London.

21. Mann, W.B. (1954). *Use of Callendar's Radio Balance for the Energy Emission from Radioactive Sources*. Journal of Research of the National Bureau of Standards, 52, 177-184.

22. Rossini, F.D. (1956). *Experimental Thermochemistry* (Vol.1). Interscience, New York, 239-297.

23. Mundhawa, M. *Calorimetric Measurements of the Molar Heat Capacity and The Molar Excess Enthalpy for Various Alkanolamines in Aqueous Solutions*. Master's Thesis, University of Regina, Regina, Canada, 2007.

24. Savini, C.G.; Winterhalter, D.R.; Kovach, L.H. and Van Ness, H.C. (1966). *Endothermic Heats of Mixing by Isothermal Dilution Calorimetry*. Journal of Chemical and Engineering Data, 11 (1), 40-43.

25. Winterhalter, D.R. and Van Ness, H.C. (1966). *An Isothermal Dilution Calorimeter for Exothermic Heats of Mixing*. Journal of Chemical and Engineering Data, 11 (2), 189-192.

26. Rowlinson, J.S. and Swinton, F.L. (1982). *Liquid and Liquid Mixtures* (3rd ed.). Butterworths.

27. Calvet, E.; Part, H. and Skinner, H.A. (1963). *Recent Progress in Microcalorimetry*. Pergamon Press, New York.

28. SETARAM Instrumentation (Caluire, France). URL: "http://www.setaram.com/C80.htm"

29. SETARAM Instrumentation. SETSOFT 2000 User's Manual.

30. Rayer, A.V.; Henni, A. and Tontiwachwuthikul, P. (2011). *Molar Heat Capacities of Solvents Used in CO_2 Capture: A Group Additivity and Molecular Connectivity Analysis*. The Canadian Journal of Chemical Engineering, 90(2), 367-376.

31. Mathonat, C.; Maham, Y.; Mather, A.E. and Hepler, L.G. (1997). *Excess Molar Enthalpies of (Water + Monoalkanolamine) Mixtures at 298.15 K and 308.15 K*. Journal of Chemical and Engineering Data, 42, 993-995.

32. Redlich, O. and Kister, A.T. (1948). *Algebraic Representation of Thermodynamic Properties and the Classification of Solutions*. Industrial and Engineering Chemistry Research, 40, 345-348.

33. Hayden, T.A.; Smith T.G.A. and Mather, A.E. (1983). *Heat Capacity of Aqueous Methyldiethanolamine Solutions*. Journal of Chemical and Engineering Data, 28, 196-197.

34. Riddick, J.A.; Bunger, W.B. and Sakano, T.K. (1986). *Organic Solvents* (4th ed.). Wiley-Interscience, New York.

35. Lee, L.L. (1994). *Thermodynamic Models for Natural Gas Sweetening Fluids, Annual report to Gas Research Institute*. University of Oklahoma, Norman, OK.

36. Lide, D. R. (1995). *Handbook of Organic Solvents*. CRC Press: Boca Raton, FL.

37. Maham, Y.; Hepler, L.G.; Mather, A.E.; Hakin, A.W. and Marriott, R.A. (1997). *Molar Heat Capacities of Alkanolamines from 299.1 to 397.8 K Group Additivity and Molecular Connectivity Analyses*. Journal of the Chemical Society, Faraday Transactions, 93, 1747-1750.

38. Chiu, L.F.; Liu, H.F. and Li, M.H. (1999). *Heat Capacity of Alkanolamines by Differential Scanning Calorimetry*. Journal of Chemical and Engineering Data, 44 (4), 631-636.

39. Chiu, L.F. and Li, M.H. (1999). *Heat Capacity of Alkanolamine Aqueous Solutions*. Journal of Chemical and Engineering Data, 44 (6), 1396-1401.

40. Mundhwa, M. and Henni, A. (2007). *Molar Heat Capacity of Various Aqueous Alkanolamine Solutions from 303.15 K to 353.15 K*. Journal of Chemical and Engineering Data, 52 (2), 491-498.

41. Poozesh S. *Molar Heat Capacity and Molar Excess Enthalpy Measurements in Aqueous Amine Solutions*. Master's Thesis, University of Regina, Regina, Saskatchewan, December 2009.

42. Uddin S.M. *Molar Heat Capacity and Molar Excess Enthalpy of Aqueous Solutions of Tertiary Amines*. Master's Thesis, University of Regina, Regina, Saskatchewan, January 2011.

43. Narayanaswamy K. *Molar Heat Capacity and Molar Excess Enthalpy Measurements of Various Aqueous Tertiary and Diamine Solutions*. Master's Thesis, University of Regina, Regina, Saskatchewan, June 2011.

44. Lide, D.R. and Kehiaian, H.V. (1994). *CRC Handbook of Thermophysical and Thermochemical Data*. CRC Press, Boca Raton, FL.

45. Osborne, N.S.; Stimson, H.F. and Ginnings, D.C. (1939). *Measurements of Heat Capacity and Heat of Vaporization of Water in the Range 0°C to 100°C*. *Journal of Research of the National Bureau of Standards*, 23, 197-260.

46. Andreoli-Ball, L.; Sun, S.J.; Trejo, L.M.; Costas, M. and Patterson, D. (1990). *Thermodynamics and Structure in non-Electrolyte Solutions*. Pure and Applied Chemistry, 62(11), 2097-2106.

47. Desnoyers, J.E. and Perron, G. (1997). *Treatment of Excess Thermodynamic Quantities for Liquid Mixtures. Journal of Solution Chemistry*. 26, 749-755.

48. Davis, M.I. (1993). *Thermodynamic and Related Studies of Amphiphile + Water Systems*. Chemical Society Reviews, 22, 127-134.

49. Maham, Y.; Teng, T.T.; Hepler, L.G. and Mather, A.E. (1994). *Densities, excess molar volumes, and partial molar volumes for binary mixtures of water with monoethanolamine, diethanolamine, and triethanolamine from 25 to 80 °C*. Journal of Solution Chemistry, 23, 195-205.

50. Maham, Y.; Teng, T.T.; Mather, A.E. and Hepler, L.G. (1995). *Volumetric properties of (water + diethanolamine) systems*. Canadian Journal of Chemistry, 73, 1514−1519.

51. The International Confederation for Thermal Analysis and Calorimetry (ICTAC) URL: "http://www.ictac.org/"

52. Becker, L.; Aufderhaar, O. and Gmehling, J. (2000). *Measurement of Heat Capacities for Nine Organic Substances by Tian-Calvet Calorimetry*. Journal of Chemical and Engineering Data, 45, 661-664.

53. Becker, L. and Gmehling, J. (2001). *Measurement of Heat Capacities for 12 Organic Substances by Tian-Calvet Calorimetry*. Journal of Chemical and Engineering Data, 46, 1638-1642.

54. Hohne, G.; Hemminger, W. and Flammersheimer, H.-J. (1996). *Differential Scanning Calorimetry, An Introduction for Practitioners*. Springer-Verlag: Berlin Heidelberg, New York.

55. Ditmars, D.A.; Bernstein, G.; Chang, S.S.; Ishihara, S. and West, E. D. (1982). *Enthalpy and Heat-Capacity Standard Reference Material − Synthetic Sapphire (α-Al_2O_3) from 10 to 2250 K*. Journal of Research of the National Bureau of Standards, 87, 159−163.

56. Chen, Y.-J.; Shih, T.-W.; Li, M.-H. (2001). *Heat Capacity of Aqueous Mixtures of Monoethanolamine with N-Methyldiethanolamine*. Journal of Chemical and Engineering Data, 46, 51−55.

57. Checoni, R.F. and Francesconi, A.Z. (2009). *Measurements of Excess Molar Enthalpy and Excess Molar Heat Capacity of (1-Heptanol or 1-Octanol) + (Diethyamine or s-Butylamine) Mixtures at 298.15 K and 0.1 MPa*. Journal of Thermal Analysis and Calorimetry. 97(2), 747–753.

58. Weidlich, U. and Gmehling, J. (1987). *A Modified UNIFAC Model. 1. Prediction of VLE, H^E, and γ^∞ (gamma Infinite)*. Industrial and Engineering Chemistry Research, 26, 1372-1381.

59. Shoemaker, D.P.; Garland, C.W. and Nibler, J.W. (1989). *Experiments in Physical Chemistry* (5^{th} ed.). McGraw Hill, New York.

60. Harris, D.C. (1991). *Quantitative Chemical Analysis* (3^{rd} ed.). W.H. Freeman & Company: New York.

61. Randic, M. (1975). *Characterization of Molecular Branching*. Journal of the American Chemical Society, 97, 6609–6615.

62. Kier, L.B. and Hall, L. H. (1986). *Molecular Connectivity in Structure-Activity Analysis*. Wiley, Research Study Press, Letchworth.

63. Touhara, H.; Okazaki, S.; Okino, F.; Tanaka, H.; Ikari, K. and Nakanishi, K. (1982). *Thermodynamic properties of aqueous mixtures of hydrophillic compounds. 2. Aminoethanol and its methyl derivatives*. Journal of Chemical Thermodynamics, 14, 145-156.

64. Posey M.L. *Thermodynamic Model for Acid Gas Loaded Aqueous Alkanolamine Solutions*. Ph.D. Thesis, University of Texas at Austin, 1996.

65. Maham, Y.; Mather, A.E.; Hepler, L.G. (1997). *Excess Molar Enthalpies of (Water + Alkanolamine) Systems and Some Thermodynamic Calculations*. Journal of Chemical and Engineering Data, 42(5), 988-992.

66. Klotz, I.M. and Rosenberg, R.M. (2008). *Chemical Thermodynamics - Basic Concepts and Methods* (7th ed.). John Wiley & Sons, Inc., New Jersy, USA.

67. Himmelblau, D.M. and Riggs, J.B. (1989). *Basic Principles and Calculations in Chemical Engineering* (5th ed.). Prentice Hall International Series, Englewood Cliffs, New Jersey, USA.

68. Jeffrey , G.A. (1997). *An Introduction of Hydrogen Bonding*. Oxford University Press , Oxford.

69. Steiner, T. (2002). *The Hydrogen Bond in the Solid State*. Angewandte Chemie International Edition, 41 , 48-76.

70. Pihko, P.M. (2009). *Hydrogen Bonding in Organic Synthesis*. WILEY-VCH Verlag GmbH & Co. KGaA, Weinheim.

71. Gupta P.K. (2009). *Cell and Molecular Biology*. Rastogi Publications, New Delhi, India.

72. Hemat, R.A.S. (2004). *Principles of Orthomolecularism*. Urotext.

73. Webber, H.D.; Bilings, G.R. and Hill, R.A. (1970). *Chemistry a search for understanding*. Holt, Rinehart and Winston of Canada, Ltd.

74. Perry, R.H.; Green, D.W. and Maloney, J.O. (1999) *Perry's Chemical Engineers's Handbook* (7th ed.). McGraw-Hill, USA.

75. Wohl, K. (1946). *Thermodynamic Evaluation of Binary and Ternary Liquid Systems*. Transactions of the American Institute of Chemical Engineers, 42, 215-249.

76. Wohl, K. (1953). *Thermodynamic Evaluation of Binary and Ternary Liquid Systems*. Chemical Engineering Progress, 49*,* 218-219.

77. Renon, H. and Prausnitz, J.M. (1968). *Local Compositions in Thermodynamic Excess Functions for Liquid Mixtures*. AIChE Journal, 14, 135-144.

78. Abrams, D.S. and Prausnitz, J.M. (1975). *Statistical Thermodynamics of Liquid Mixtures: A New Expression for the Excess Gibbs Energy of Partly or Completely Miscible Systems*. AIChE Journal, 21(1), 116–128.

79. Wilson G.M. and Deal, C.H. (1962). *Activity Coefficients and Molecular Structure. Activity Coefficients in Changing Environments-Solutions of Groups*. Industrial and Engineering Chemistry Fundamentals, 1*,* 20-23.

80. Vera, J.H.; Vidal, J. (1984). *An Improved Group Method for Hydrocarbon-Hydrocarbon Systems Arising from a Comparative Study of ASOG and UNIFAC*. Chemical Engineering Science, 39*,* 651-661.

81. Fredenslund, A.; Jones, R.L. and Prausnitz, J.M. (1975). *Group-Contribution Estimation of Activity Coefficients in Nonideal Mixtures*. AIChE Journal, 21(6), 1086-1099.

82. Kehiaian, H.V.; Grolier, J.P.E. and Benson, G.C. (1978). *Thermodynamics of Organic Mixtures. A Generalized Quasichemical Theory in Terms of Group Surface Interactions*. Journal of Chemical Physics, 75*,* 1031-1048.

83. Marongiu, B.; Delitala, C.; Pittau, B. and Porcedda, S. (1995). *DISQUAC Predictions on Excess Enthalpies of the Ternary Mixture: Cyclohexane + Propanone + Tetrahydrofuran*. Fluid Phase Equilibria, 109 (1), 67-81.

84. Fanni, A.M.; Marongiu, B.; Pittau, B. and Porcedda, S. (1996). *DISQUAC Predictions of Excess Enthalpies of The Ternary Mixture: Tetrahydrofuran + Cyclohexane + Butanenitrile*. Fluid Phase Equilibria, 126 (2), 163-175.

85. Renon, H.; Prausnitz, J.M. (1969). *Estimation of Parameters for the NRTL Equation for Excess Gibbs Energies of Strongly Nonideal Liquid Mixtures*. Industrial and Engineering Chemistry Research, 8*,* 413-419.

86. Wilson, G.M. (1964). A New Expression for Excess Free Energy of Mixing. Journal of the American Chemical Society, 86(2), 127-130.

87. Guggenheim, E.A. (1952). *Mixtures: The Theory of the Equilibrium Properties of Some Simple Classes of Mixtures, Solutions and Alloys*. Oxford University Press, Oxford.

88. Fredenslund, A.; Gmehling, J. and Rasmussen, P. (1977). *Vapor-Liquid Equilibria Using UNIFAC*. Elsevier, Amsterdam.

89. Magnussen, T.; Rasmussen, P. and Fredenslund, A. (1981). *UNIFAC Parameter Table for Prediction of Liquid-Liquid Equilibriums*. Industrial and Engineering Chemistry Process Design and Development, 20*,* 331-339.

90. Gmehling, J.G.; Anderson, T.F. and Prausnitz, J.M. (1978). *Solid-Liquid Equilibria Using UNIFAC*. Industrial and Engineering Chemistry Fundamentals, 17*,* 269-273.

91. Oishi, T. and Prausnitz, J.M. (1978). *Estimation of Solvent Activities in Polymer Solutions Using a Group-Contribution Method*. Industrial and Engineering Chemistry Research, 17*,* 333-339.

92. Gottlieb, M.; Herskowitz, M. (1981). *Estimation of the X Parameter for Poly(dimethylsiloxane) Solutions by the UNIFAC Group Contribution Method*. Macromolecules, 14*,* 1468-1471.

93. Jensen, T.; Fredenslund, A. and Rasmussen, P. (1981). *Pure-Component Vapor Pressures Using UNIFAC Group Contribution*. Industrial and Engineering Chemistry Fundamentals, 20*,* 239-246.

94. Gmehling, J.G. and Rasmussen, P. (1982). *Flash Points of Flammable Liquid Mixtures Using UNIFAC*. Industrial and Engineering Chemistry Fundamentals, 21*,* 186-188.

95. Lo, H.S and Paulaitis, M.E. (1981). *Estimation of Solvent Effects on Chemical Reaction Rates Using UNIFAC Group Contribution*. AIChE Journal, 27*,* 842-844.

96. Nocon, G.; Weidlich, U.; Gmehling, J.; Menke, J. and Onken, U. (1983). *Prediction of Gas Solubilities by a Modified UNIFAC Equation*. Fluid Phase Equilibria, 13*,* 381-392.

97. Sander, B.; Skjold-Jørgensen, S. and Rasmussen, P. (1983). Gas Solubility Calculations. I. UNIFAC. Fluid Phase Equilibria, 11, 105-126.

98. Dill, K.A.; Bromberg, S. and Stigter, D. (2003) *Molecular Driving Forces Statistical Thermodynamics in Chemistry amp Biology*. Garland Science, a member of the Taylor and Francis Group, New York, USA.

99. Ladanyi, B.M. and Skaf, M.S. (1993). *Computer simulation of hydrogen-bonding liquids*. Annual Review of Physical Chemistry, 44, 335-368.

100. Leszczynski, J. (2006). *Hydrogen Bonding-New Insights: Challenges and Advances in Computational Chemistry and Physics*(Vol. 3). Springer, Dordrecht, The Netherlands.

101. Pauling, L. (1960). *The Nature of the Chemical Bond and the Structure of Molecules and Crystals: An Introduction to Modern Structural Chemistry*. Cornell University Press.

102. Tanford, C. (1980). *The Hydrophobic Effect: Formation of Micelles Biological Membranes*. Wiley, New York.

103. Armstrong, J. and Hollyman, K. and R. N. (CON) (2012). *General, Organic, and Biochemistry: An Applied Approach*. Brooks/Cole Cengage Learning, Belmont CA, USA.

104. Fanun, M. (2011). *Colloids in Biotechnology*. CRC Press, Taylor & Francis Group, Boca Raton, FL USA.

105. Kotz, J.C.; Treichel, P. and Townsend, J.R. (2009). *Chemistry and Chemical Reactivity* (Vol. 2) (7th ed.). Cengage Learning Inc., Belmont, CA, USA.

106. Brady, J.E.; *Russell, J.W.* and Holum, J.R. (2000). *Chemistry:* the *Study of Matter and its Changes* (3rd ed.). Wiley, John and Sons, Incorporated.

107. Stoker H.S. (2011). *General, Organic and Biological Chemistry* (6th ed.). Brooks/Cole, Cengage Learning, Belmont USA.

108. Cheremisinoff, N.P. (2003). *Industrial Solvents Handbook* (2nd ed.).Marcel Dekker, Inc. CRC Press, New York, USA.

109. Seager, S.L. and Slabaugh, M.R. (2011). *Chemistry for Today: General, Organic, and Biochemistry*. Brooks/Cole Cengage Learning, Belmont, USA.

110. Wakisaka, A.; Abdoul-Carime, H.; Yamamoto, Y. and Kiyozumi, Y. (1998). *Non-ideality of Binary Mixtures Water-Methanol and Water-Acetonitrile from the Viewpoint of Clustering Structure*. Journal of the Chemical Society, Faraday Transactions, 94(3), 369-374.

111. Hornback, J.M. (2006). *Organic Chemistry* (2nd ed.). Thomson Brooks/Cole USA.

112. Chandra, S. (2004). *Comprehensive Inorganic Chemistry*. New Age International (P) Ltd., New Delhi.

113. Tuteja, A. (2007). *Fundamentals of Physical Chemistry*. Discovery Publishing House, New Delhi, India.

114. Johnson, A.W. (1999). *Invitation to Organic Chemistry*. Jones and Bartlett Learning, Mississauga, Canada.

115. Prausnitz, J.M.; Lichtenthaler, R.N. and de Azevedo, E.G. (1999). *Molecular Thermodynamics of Fluid-Phase Equilibria* (3rd ed.). Prentice Hall, Inc. New Jersey, USA.

116. Boyne, J.A. and Williamson, A.G. (1967). *Enthalpies of Mixture of Ethanol and Water at 25 degree C*. Journal of Chemical and Engineering Data, 12 (3), 318-318.

117. Missopolinou, D.; Tsivintzelis, I. and Panayiotou, C. (2006). *Excess enthalpies of binary mixtures of 2-ethoxyethanol with four hydrocarbons at 298.15, 308.15, and 318.15K An experimental and theoretical study*. Fluid Phase Equilibria 245, 89-101.

6. APPENDICES

6.1. Appendix 1 - molar heat capacity

Molar heat capacities of the aqueous EAE, PAE, BAE, HEP, and BMOEA solutions were measured at eleven temperatures ranging from 303.15 to 353.15K and over the entire range of mole fractions. The calculated molar excess heat capacity data for above five studied aqueous amine solution are reported in this section.

Table 6.1. Experimental molar heat capacity of aqueous 2-(Ethylamino)ethanol (EAE) solution at several temperatures from 303.15 to 353.15K

T/K	Mole Fraction of 2-(Ethylamino)ethanol (x_1)								
	0.1002	0.2004	0.2998	0.4010	0.5009	0.6007	0.7019	0.8007	0.9005
	Molar Heat Capacity Cp / J·mol^{-1}·K^{-1}								
303.15	104	119	132	148	161	175	190	204	218
308.15	106	122	136	152	165	179	193	207	221
313.15	106	123	138	154	168	182	196	210	223
318.15	107	125	141	156	171	185	199	212	225
323.15	109	127	143	159	174	188	202	215	228
328.15	110	130	146	163	178	192	205	218	230
333.15	112	133	150	166	182	195	209	222	233
338.15	115	137	154	170	186	200	212	225	236
343.15	118	141	159	175	191	204	215	229	239
348.15	123	147	165	182	198	210	220	233	241
353.15	128	153	172	188	204	215	226	238	246

Table 6.2. Experimental molar heat capacity of aqueous 2-(Propylamino)ethanol (PAE) solution at several temperatures from 303.15 to 353.15K

T/K	Mole Fraction of 2-(Propylamino)ethanol (x_1)								
	0.1002	0.2002	0.3000	0.3999	0.4998	0.5996	0.7003	0.7999	0.9003
	Molar Heat Capacity Cp / $J \cdot mol^{-1} \cdot K^{-1}$								
303.15	107	126	145	163	181	199	215	232	248
308.15	109	128	148	167	185	203	220	236	252
313.15	109	130	150	170	188	206	224	240	256
318.15	110	132	153	173	191	209	227	243	258
323.15	112	134	157	176	194	213	230	247	261
328.15	113	137	160	180	198	217	234	250	264
333.15	115	140	164	185	203	221	238	253	267
338.15	117	144	168	190	208	227	243	258	270
343.15	120	149	174	196	214	232	248	261	273
348.15	123	155	180	203	221	238	253	267	277
353.15	126	161	188	210	228	244	260	272	282

Table 6.3. Experimental molar heat capacity of aqueous 2-(Butylamino)ethanol (BAE) solution at several temperatures from 303.15 to 353.15K

T/K	Mole Fraction of 2-(Butylamino)ethanol (x_1)								
	0.1002	0.2008	0.3012	0.4006	0.5006	0.6000	0.7012	0.8003	0.9007
	Molar Heat Capacity Cp / $J \cdot mol^{-1} \cdot K^{-1}$								
303.15	108	132	154	176	196	215	235	254	272
308.15	111	136	159	181	204	222	243	261	280
313.15	112	138	162	185	208	227	246	265	283
318.15	114	142	167	189	212	231	250	268	286
323.15	117	146	172	194	216	235	254	272	289
328.15	120	151	178	200	222	240	258	276	291
333.15	124	156	185	208	229	247	264	280	294
338.15	129	163	192	216	237	255	270	286	298
343.15	135	171	201	224	246	264	280	294	306
348.15	144	182	212	235	256	273	287	301	312
353.15	156	195	225	247	264	281	294	307	318

Table 6.4. Experimental molar heat capacity of aqueous 1-(2-Hydroxyethyl)piperidine (HEP) solution at several temperatures from 303.15 to 353.15K

T/K	Mole Fraction of 1-(2-Hydroxyethyl)piperidine (x_1)								
	0.1000	0.2006	0.3005	0.4008	0.4997	0.6010	0.7016	0.8006	0.9000
	Molar Heat Capacity Cp / $J \cdot mol^{-1} \cdot K^{-1}$								
303.15	108	130	151	170	188	207	224	240	255
308.15	110	133	154	175	194	212	231	247	262
313.15	111	135	157	178	198	216	235	250	265
318.15	112	137	161	182	203	221	238	254	269
323.15	113	139	165	187	208	226	243	258	273
328.15	115	142	169	192	213	232	248	262	277
333.15	117	145	173	198	219	238	252	267	281
338.15	119	148	177	202	225	243	256	270	285
343.15	121	152	181	207	231	248	263	275	289
348.15	124	156	187	213	236	255	268	280	293
353.15	125	159	190	218	242	260	274	285	297

Table 6.5. Experimental molar heat capacity of aqueous Bis(2-methoxyethyl)amine (BMOEA) solution at several temperatures from 303.15 to 353.15K

T/K	Mole Fraction of Bis(2-methoxyethyl)amine (x_1)								
	0.0998	0.2002	0.3007	0.4008	0.5008	0.6006	0.7002	0.8003	0.9002
	Molar Heat Capacity Cp / $J \cdot mol^{-1} \cdot K^{-1}$								
303.15	109	135	161	185	207	228	246	264	279
308.15	112	139	165	191	213	234	252	270	285
313.15	113	141	168	193	215	237	255	273	287
318.15	115	144	171	197	218	240	258	274	288
323.15	118	147	175	201	222	244	261	277	289
328.15	120	151	180	205	229	248	265	280	291
333.15	122	156	186	212	234	254	271	284	295
338.15	127	162	193	221	243	262	278	291	302
343.15	131	170	202	228	251	270	285	297	308
348.15	138	180	214	241	263	279	294	305	313
353.15	148	191	226	254	276	290	302	311	318

Table 6.6. Calculated molar excess heat capacity of aqueous 2-(Ethylamino)ethanol (EAE) solution at several temperatures from 303.15 to 353.15K

T/K	Mole Fraction of 2-(Ethylamino)ethanol (x_1)								
	0.1002	0.2004	0.2998	0.4010	0.5009	0.6007	0.7019	0.8007	0.9005
	Molar Excess Heat Capacity Cp^E / $J \cdot mol^{-1} \cdot K^{-1}$								
303.15	12.6	12.1	10.2	9.6	7.4	5.9	4.8	3.2	2.0
308.15	14.3	14.5	12.8	12.6	10.0	8.3	6.5	4.5	2.3
313.15	14.9	15.8	14.5	14.4	11.9	9.8	7.9	5.4	2.9
318.15	15.7	17.3	16.4	15.8	14.1	11.7	9.5	6.6	3.4
323.15	16.7	19.1	18.5	17.6	16.2	13.6	11.0	7.6	3.8
328.15	18.0	21.2	20.9	20.4	18.9	15.9	12.8	9.2	4.7
333.15	19.9	24.0	23.5	23.2	21.7	18.2	14.6	10.8	5.4
338.15	22.3	27.3	26.8	26.3	25.0	21.2	16.6	12.8	6.2
343.15	25.2	31.2	31.2	30.1	28.9	23.9	18.3	14.7	7.0
348.15	29.5	36.1	36.8	35.9	34.4	28.9	21.3	16.7	7.5
353.15	34.7	41.7	42.4	40.5	38.5	31.6	24.1	19.1	8.4

Table 6.7. Calculated molar excess heat capacity of aqueous 2-(Propylamino)ethanol (PAE) solution at several temperatures from 303.15 to 353.15K

T/K	Mole Fraction of 2-(Propylamino)ethanol (x_1)								
	0.1002	0.2002	0.3000	0.3999	0.4998	0.5996	0.7003	0.7999	0.9003
	Molar Excess Heat Capacity Cp^E / $J \cdot mol^{-1} \cdot K^{-1}$								
303.15	12.8	13.3	12.9	12.5	11.3	10.1	7.6	5.6	3.3
308.15	13.9	14.6	15.1	14.8	13.7	12.2	9.8	7.1	4.1
313.15	14.4	15.7	16.7	16.8	15.7	14.0	12.2	9.4	5.5
318.15	15.3	17.3	18.7	19.3	17.8	16.2	14.2	10.8	6.3
323.15	16.4	19.3	21.7	21.8	20.0	18.7	16.4	12.7	7.4
328.15	17.7	21.6	24.6	24.8	22.7	21.1	18.3	14.2	7.9
333.15	19.5	24.5	27.8	28.6	26.4	23.8	20.9	15.7	9.3
338.15	21.5	27.9	31.7	33.1	30.7	29.0	24.8	19.1	10.7
343.15	24.0	32.0	36.2	38.3	35.6	33.1	28.4	21.4	12.2
348.15	26.7	37.3	41.7	43.5	40.4	37.0	31.2	23.4	12.9
353.15	29.2	42.6	48.2	49.4	46.1	40.9	35.1	26.6	14.6

Table 6.8. Calculated molar excess heat capacity of aqueous 2-(Butylamino)ethanol (BAE) solution at several temperatures from 303.15 to 353.15K

T/K	Mole Fraction of 2-(Butylamino)ethanol (x_1)								
	0.1002	0.2008	0.3012	0.4006	0.5006	0.6000	0.7012	0.8003	0.9007
	Molar Excess Heat Capacity Cp^E / $J \cdot mol^{-1} \cdot K^{-1}$								
303.15	11.4	13.6	14.1	15.0	14.1	11.3	9.5	7.2	4.0
308.15	13.1	16.2	17.3	17.5	17.6	14.2	12.1	8.5	5.2
313.15	14.5	18.2	19.7	19.9	20.1	17.0	13.9	10.1	5.8
318.15	16.3	21.3	23.1	22.8	23.5	20.0	16.3	12.1	6.7
323.15	18.6	24.8	28.0	26.9	26.9	23.1	18.8	14.4	7.9
328.15	21.5	29.2	33.0	32.8	31.0	26.7	21.5	16.2	8.9
333.15	25.3	34.0	39.8	40.0	37.7	32.5	26.0	19.1	9.7
338.15	30.0	40.1	45.7	46.4	44.4	38.8	30.7	22.9	11.7
343.15	35.9	47.1	53.1	52.9	50.5	45.1	36.8	26.8	14.4
348.15	44.1	57.0	63.4	61.7	58.0	51.1	40.9	30.3	16.9
353.15	55.3	69.6	75.0	72.1	65.3	56.9	45.5	34.0	19.8

Table 6.9. Calculated molar excess heat capacity of aqueous 1-(2-Hydroxyethyl)piperidine (HEP) solution at several temperatures from 303.15 to 353.15K

T/K	Mole Fraction of 1-(2-Hydroxyethyl)piperidine (x_1)								
	0.1000	0.2006	0.3005	0.4008	0.4997	0.6010	0.7016	0.8006	0.9000
	Molar Excess Heat Capacity Cp^E / $J \cdot mol^{-1} \cdot K^{-1}$								
303.15	13.0	15.3	16.6	15.9	15.0	13.7	11.3	8.3	4.0
308.15	14.6	16.9	18.1	18.5	17.6	15.3	13.6	9.6	4.3
313.15	15.0	18.1	20.4	20.5	20.1	17.7	15.6	10.5	5.1
318.15	15.8	19.6	22.9	23.6	23.0	20.5	16.9	11.8	6.1
323.15	16.8	21.3	25.9	27.2	26.7	23.9	18.9	13.1	7.2
328.15	17.9	23.5	29.5	31.0	30.7	27.7	22.1	14.7	8.4
333.15	19.3	25.8	32.4	35.2	35.3	32.0	24.0	17.2	9.5
338.15	21.0	28.7	35.0	37.8	39.3	34.8	26.3	18.5	10.9
343.15	23.3	31.9	39.0	42.2	43.7	38.6	30.9	20.9	12.8
348.15	25.6	35.1	43.2	46.6	47.9	43.6	34.0	23.8	14.6
353.15	26.3	38.2	45.7	51.5	52.8	47.4	38.8	27.1	16.6

Table 6.10. Calculated molar excess heat capacity of aqueous Bis(2-methoxyethyl)amine (BMOEA) solution at several temperatures from 303.15 to 353.15K

T/K	Mole Fraction of Bis(2-methoxyethyl)amine(x_1)								
	0.0998	0.2002	0.3007	0.4008	0.5008	0.6006	0.7002	0.8003	0.9002
	Molar Excess Heat Capacity Cp^E / $J \cdot mol^{-1} \cdot K^{-1}$								
303.15	11.8	16.0	19.9	22.6	22.8	21.6	17.9	13.5	7.1
308.15	14.3	18.9	22.2	25.5	25.2	23.9	19.5	15.1	7.8
313.15	15.6	20.7	24.5	27.7	27.1	26.2	22.1	16.9	8.5
318.15	17.5	23.0	27.5	30.7	29.9	28.7	24.4	17.8	9.5
323.15	19.9	25.9	31.1	34.7	33.5	32.3	27.2	20.7	10.1
328.15	21.7	30.4	35.8	38.3	39.0	35.9	30.1	22.0	10.7
333.15	23.9	34.5	41.1	44.1	43.5	40.4	33.8	24.4	11.8
338.15	28.3	39.1	46.4	50.6	49.3	44.4	37.2	26.6	14.0
343.15	31.7	46.4	54.4	56.6	55.5	50.2	41.6	29.3	15.7
348.15	37.8	56.0	65.3	68.5	65.4	57.9	48.4	34.6	18.4
353.15	47.6	66.3	76.6	80.0	76.9	66.9	53.9	38.7	21.2

6.2. Appendix 2 - molar excess enthapy

The experimental molar excess enthalpies of (Amine (1) + Water (2)) binary systems for PAE, BAE, HEP, DGA, and BMOEA were measured at three temperatures 298.15, 313.15 and 323.15K and over the entire range of mole fractions are also included in this section.

Table 6.11. Molar excess enthalpies of (PAE (1) + water (2)) binary system at 298.15, 313.15 and 353.15K

Temperature T/K					
298.15		**313.15**		**333.15**	
x_1	H^E/ J·mol^{-1}	x_1	H^E/ J·mol^{-1}	x_1	H^E/ J·mol^{-1}
0.1000	-1188	0.1003	-1072	0.1004	-886
0.1979	-1665	0.2006	-1529	0.1997	-1293
0.2985	-2020	0.3001	-1861	0.3005	-1559
0.3993	-2159	0.4009	-2005	0.4012	-1734
0.5013	-2137	0.5001	-2001	0.5000	-1723
0.6012	-1994	0.6002	-1832	0.6004	-1578
0.7009	-1605	0.7018	-1519	0.7013	-1333
0.8009	-1152	0.7997	-1109	0.8001	-991
0.9001	-664	0.9007	-626	0.9000	-557

Table 6.12. Molar excess enthalpies of (BAE (1) + water (2)) binary system at 298.15, 313.15 and 353.15K

Temperature T/K					
298.15		313.15		333.15	
x_1	H^E/ J·mol^{-1}	x_1	H^E/ J·mol^{-1}	x_1	H^E/ J·mol^{-1}
0.1002	-940	0.0999	-868	0.1003	-632
0.2002	-1400	0.1998	-1325	0.2002	-1044
0.3015	-1791	0.3013	-1642	0.3011	-1330
0.3967	-1948	0.4008	-1805	0.4002	-1433
0.5010	-2024	0.5016	-1843	0.5003	-1470
0.6021	-1834	0.6010	-1702	0.6016	-1415
0.6938	-1574	0.7005	-1473	0.7010	-1252
0.8007	-1133	0.8012	-1095	0.8007	-888
0.9012	-618	0.9001	-580	0.9006	-507

Table 6.13. Molar excess enthalpies of (HEP (1) + water (2)) binary system at 298.15, 313.15 and 353.15K

Temperature T/K					
298.15		313.15		333.15	
x_1	H^E/ J·mol^{-1}	x_1	H^E/ J·mol^{-1}	x_1	H^E/ J·mol^{-1}
0.1000	-1258	0.0998	-1129	0.1009	-872
0.1992	-1836	0.2005	-1657	0.2014	-1344
0.3003	-2153	0.2998	-1959	0.3002	-1593
0.3998	-2262	0.4005	-2067	0.4019	-1675
0.5016	-2161	0.5006	-2006	0.5012	-1624
0.6013	-1880	0.6005	-1777	0.6011	-1445
0.7005	-1542	0.7009	-1442	0.7007	-1210
0.8002	-1116	0.8006	-1040	0.7997	-870
0.9131	-534	0.9009	-557	0.9000	-473

Table 6.14. Molar excess enthalpies of (DGA (1) + water (2)) binary system at 298.15, 313.15 and 353.15K

Temperature T/K					
298.15		313.15		333.15	
x_1	H^E/ J·mol^{-1}	x_1	H^E/ J·mol^{-1}	x_1	H^E/ J·mol^{-1}
0.0996	-1475	0.0996	-1410	0.1003	-1301
0.2013	-2169	0.1992	-2086	0.2011	-1959
0.3006	-2356	0.3014	-2295	0.3010	-2175
0.4011	-2351	0.4004	-2284	0.3998	-2157
0.5012	-2175	0.5010	-2091	0.5015	-1969
0.6007	-1851	0.6008	-1777	0.6006	-1705
0.7000	-1463	0.7001	-1424	0.6997	-1340
0.7998	-1017	0.7998	-977	0.8006	-941
0.9005	-553	0.9004	-515	0.9011	-483

Table 6.15. Molar excess enthalpies of (BMOEA (1) + water (2)) binary system at 298.15, 313.15 and 353.15K.

Temperature T/K					
298.15		313.15		333.15	
x_1	H^E/J·mol^{-1}	x_1	H^E/ J·mol^{-1}	x_1	H^E/ J·mol^{-1}
0.1007	-2062	0.1000	-1936	0.0997	-1535
0.1998	-2720	0.2005	-2479	0.2008	-2108
0.3011	-2844	0.3008	-2549	0.3017	-2170
0.4011	-2714	0.3999	-2403	0.3993	-1972
0.5001	-2431	0.5029	-2103	0.5010	-1690
0.6008	-2042	0.6018	-1745	0.5998	-1327
0.7003	-1548	0.7007	-1278	0.7007	-974
0.8003	-997	0.8007	-816	0.8004	-580
0.9000	-504	0.9001	-419	0.9001	-274

6.3. Appendix 3 - miscellaneous

6.3.1. Materials

Alkanolamines used in this study were purchased from Sigma-Aldrich with a mass purity of 99.5% for Monoethanolamine, ≥99% for N-Methyldiethanolamine, ≥98% for 2-(Ethylamino)ethanol, ≥99% for 2-(Propylamino)ethanol, ≥98% for 2-(Butylamino)ethanol, 99% for 1-(2-Hydroxyethyl)piperidine, and 98% for Diglycolamine, and 98% for Bis(2-methoxyethyl)amine were used without any further purification. A standard reference material synthetic sapphire 99.99% pure by mass (chemical name: Al_2O_3,) was purchased from the National Institute of Standards and Technology, Gaithersburg.

6.3.2. Solution preparation

All solutions were prepared on the basis of mole fractions and an analytical balance Ohaus (Model AP250D, Florham Park, NJ) was used to prepare the binary mixtures of alkanolamine and deionized water with a precision of ±0.1mg. Amount of water needed for the specific mole fractions of solvent was calculated as:

$$MoleFraction(x_i) = \frac{molesofcomponenti}{totalmolesofsolution} \tag{6.1}$$

$$MoleFraction(x) = \frac{\frac{M_{solvent}}{M.Wt._{solvent}}}{\frac{M_{solvent}}{M.Wt._{solvent}} + \frac{M_{water}}{M.Wt._{water}}} \tag{6.2}$$

or

$$x = \frac{N_{solvent}}{N_{solvent} + N_{water}} \tag{6.3}$$

where $N_{solvent} = \frac{M_{solvent}}{M.Wt._{solvent}}$ and $N_{water} = \frac{M_{water}}{M.Wt._{water}}$

$$N_{solvent} = x(N_{solvent} + N_{water}) \quad (6.4)$$

or

$$N_{water} = \left\{\frac{N_{solvent}}{x}\right\} - N_{solvent} \quad (6.5)$$

$$N_{water} = N_{solvent}\left\{\frac{1}{x} - 1\right\} \quad (6.6)$$

$$\frac{M_{water}}{M.Wt._{water}} = \frac{M_{solvent}}{M.Wt._{solvent}}\left\{\frac{1}{x} - 1\right\} \quad (6.7)$$

$$M_{water} = M.Wt._{water} \times \frac{M_{solvent}}{M.Wt._{solvent}}\left\{\frac{1}{x} - 1\right\} \quad (6.8)$$

where *x* is the mole fraction of alkanolamine, M and M.Wt. are the mass and molecular weight, respectively. For a known amount of solvent, Equation 6.8 was used to calculate the required amount of water at a specific mole fraction (*x*) .

6.3.3. Sources of error

During the experimental study, there are several sources of indeterminate errors: (a) solvent may get stuck in the cell walls and may never blend with the whole solution; (b) absorption of carbon dioxide throughout the weighing process of the solvents and generation of the heats of reaction/mixing of the two components; (c) cell not being properly cleaned and dried.

6.3.4. Error estimations

There is a significant amount of new experimental data involved in this study. Generally these values can be represented by differential mathematical expressions. A number of these mathematical equations have certain physical meanings. The formula described in these equations varies from simple linear, to polynomial, and much more complex forms. Deviation with different definitions points out the quality of data representations with different emphases. In this study, three types of formulae of deviation were used. They are:

The percentage of relative deviation (%RD) or average absolute deviation (%AAD):[57]

$$\% RD = \frac{100}{n}\sum_{i=1}^{n}\left|\frac{Exp_i - Calc_i}{Exp_i}\right| \quad (6.9)$$

The standard deviation (SD), or the root mean square deviation (RMSD):[116]

$$SD = \left\{\frac{1}{n-p}\sum_{i=1}^{n}(Exp_i - Calc_i)^2\right\}^{1/2} \quad (6.10)$$

where, n and p are the number of experimental data points and the number of parameters that were adjusted, respectively.

6.3.5. Molecular area and volume parameters

This section contains pure-component molecular-structure constants depending on the molecular size and the external surface areas. Table 6.18 lists the molecular surface area and volume parameters for the UNIQUAC model. Table 6.19 displays the functional group area (Q) and volume (R) parameters for the Modified UNIFAC (Dortmund) Model.

The parameters in both Tables 6.18 and 6.19 were retrieved from the ASPEN PLUS Data Regression Tool.

Table 6.16. Molecular surface area and volume parameters for UNIQUAC model

Amines	Surface Area Parameters		Volume Parameter
	q	q'	R
2-(Propylamino)ethanol	3.988	3.988	4.661
2-(Butylamino)ethanol	4.528	4.528	5.336
1-(2-Hydroxyethyl)piperidine	4.456	4.456	5.536
Diglycolamine	3.680	3.680	4.166
Bis(2-methoxyethyl)amine	4.732	4.732	5.520
Water	1.400	1.000	0.920

Table 6.17. Main groups, subgroups and the corresponding van der Waals quantities for the modified UNIFAC (Dortmund) model

Main Group	Subgroup	R	Q
CH_2	**CH_3**	0.901	0.848
CH_2	**CH_2**	0.674	0.540
CNH_2	**CH_2NH_2**	1.369	1.236
$(C)_2NH$	**CH_2NH**	1.207	0.936
$(C)_3N$	**CH_2N**	0.960	0.632
$(C)_2O$	**CH_2O**	0.918	0.780
OH	**OH (1^o)**	0.530	0.584
H_2O	**H_2O**	1.733	2.456

6.3.5. Chemical names and their structures

This section contains chemical names and their molecular-structures discussed in our results and discussion section.

Table 6.18. Chemical names and their structures.

Chemical Name	Molecular Structure	Chemical Name	Molecular Structure
3-Amino-1-propanol [AP]	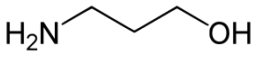	N-Butyldiethanol-amine [BDEA]	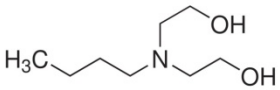
Diethanolamine [DEA]	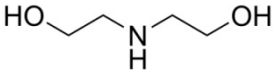	2-(Diethylamino)-ethanol [DEEA]	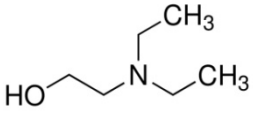
1, 4-dimethylpiperazine [1,4-DMPZ]	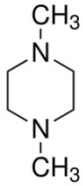	2-Dimethylamino-ethanol [DMAE]	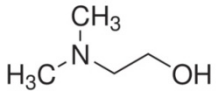
N-Ethyldiethanolamine [EDEA]	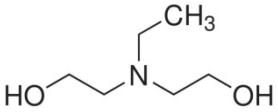	Ethanol [EtOH]	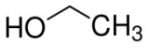
4-(2-Hydroxyethyl)-morpholine [4, 2-HEMO]	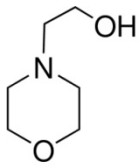	1-(2-Hydroxyethyl)-piperazine [1, 2-HEPZ]	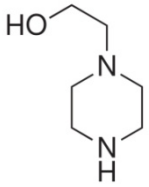
1-Methylpiperazine [1-MPZ]	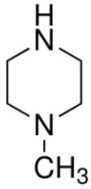	2-(Methylamino)-ethanol [MAE]	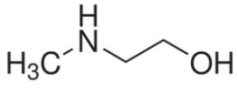
N-Methyldiethanol-amine [MDEA]	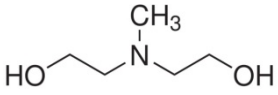	Monoethanolamine [MEA]	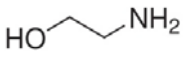
Triethanolamine [TEA]	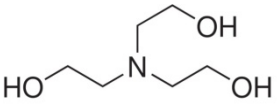	Water	H_2O